Role of Histones in DNA Double-Strand Break Repair in *Dictyostelium*

A thesis submitted to the Board of the faculty of Biological Sciences, University of Oxford in partial fulfillment of the requirements for the degree of Doctor of Philosophy

Alina Rakhimova

Word count: 33,114

University College Trinity Term, 2015

Role of Histones in DNA Double-Strand Break Repair in *Dictyostelium*

Alina Rakhimova – University College

Submitted for the degree of Doctor of Philosophy, Trinity Term, 2015

Correct repair of DNA double-strand breaks is crucial for maintenance of genome integrity. Despite data showing the importance of histones variants and histone post-translational modifications in the cellular response to DNA damage, there is still a lack of knowledge concerning the role of histone H3 and its variants as well as histone ADP-ribosylation in such processes. In this work *Dictyostelium discoideum* was employed as genetically tractable model organism to address the role of histone H3 variants and histone ADP-ribosylation in DNA double-strand break (DSB) repair. Vegetative cells lacking two out of three histone H3 variants – H3b and H3c, were shown not to be sensitive to DNA DSB. No evidence for altered DSB repair was found as phosphorylation of histone H2AX (a marker of DSB) and one of the pathways of DSB repair, non-homologous end joining, were not altered. Altogether, this work demonstrates that H3b and c variants are not required for overall DNA DSB repair in *Dictyostelium*. Among the core histones histone H2B was discovered to be the major acceptor of ADP-ribosylation by major ADP-ribosyl transferase involved in DSB repair, Adprt1a, *in vitro*. ADP-ribosylation *in vitro* was shown to occur on glutamate E18 with E19 being a potential regulator of this modification. Using an epitope-tagged overexpressed H2B, *in vivo* H2B ADP-ribosylation in response to DSBs was observed in *Dictyostelium* for the first time. Decreased ADP-ribosylation of epitope-tagged H2B mutated in both E18 and E19 residues was demonstrated. Overall, this work demonstrates the presence of the ADP-ribosylation of H2B in *Dictyostelium* in response to DSBs and identifies the major site of this modification.

Publications during D.Phil

Couto, C.A., Hsu, D.W., Teo, R., **Rakhimova, A.**, Lempidaki, S., Pears, C.J., and Lakin, N.D. (2013). Nonhomologous end-joining promotes resistance to DNA damage in the absence of an ADP-ribosyltransferase that signals DNA single strand breaks. J Cell Sci *126*, 3452-3461.

Acknowledgements

Firstly, I would like to thank my supervisor, Dr. Catherine Pears, for endless support and encouragement, for teaching me a new way of scientific thinking and making this thesis possible. I would also like to thank my second supervisor, Dr. Nicholas Lakin, for advises and guidance during my DPhil.

Next, I would like to thank all members of Pears and Lakin labs, past and present, for a great time during my DPhil. In particular, I want to thank Dr. Duen-Wei Hsu for his help in both experimental and theoretical parts of the project, Dr. Anne-Marie Couto and Dr. Hong Yu Wang for their help and support and Dr. Peggy Paschke for being the best labmate of all times.

I would also like to thank our collaborators, Prof. Keith Caldecott and members of his laboratory, for performing mass-spectrometry analysis and advising on experimental procedures. Additionally, I would like to thank Prof. Wolfgang Nellen and members of his laboratory for providing expression vectors used in this project.

Additionally, this thesis would be impossible without Clarendon Fund and University College that sponsored my DPhil, and I would like to thank them for both financial and administrative support.

And finally, I would like to thank my family and especially my mother – the only person who always supported all my endeavors and made my studies possible.

Abbreviations

ALC1	Amplified in liver cancer 1
Alt-NHEJ	Alternative non-homologous end joining
APLF	Aprataxin and PNKP like factor
ARH	ADP-ribosyl hydrolase
ART	ADP-ribosyl transferase
ATM	Ataxia-telangiectasia mutated
BLM	Bloom syndrome protein
BSR	Blasticidin resistance
BRCA1	Breast cancer 1
BRCA2	Breast cancer 2
BRCT	BRCA1 C terminus
CDK	Cyclin-dependent kinases
CHD	Chromodomain-Helicase-DNA binding
CtIP	CtBP-interacting protein
DDR	DNA damage response
DNA-PKcs	DNA-dependent protein kinase catalytic subunit
DSB	double-strand break
GFP	green fluorescent protein
FHA	Forkhead-associated
HDAC	Histone deacetylases
HP1	Heterochromatin protein 1
HR	Homologous recombination
IR	Ionising radioation

MAR	Mono-ADP-ribose
MDC1	Mediator of DNA damage checkpoint protein 1
MMS	Methyl methanesulfonate
MOF	Male absent on the first
MRN	Mre11/Rad50/Nbs1
NAD^+	Nicotinamide adenine dinucleotide
NHEJ	Non-homologous end joining
PAR	Poly-ADP-ribose
PARG	Poly-ADP-ribose glycohydrolase
PARP	Poly-ADP-ribose polymerase
PBM	PAR-binding motif
PBZ	PAR-binding Zinc-finger
PIK	Phosphatidylinositol kinase
PNKP	Polynucleotide kinase 3'-phosphatase
REMI	Restriction enzyme mediated integration
RNF	Ring finger protein
RPA	Replication protein A
SDS-PAGE	Sodium dodecyl sulphate polyacrylamide gel electrophoresis
SSB	Single-strand break
TRRAP	Transformation/Transcription Domain-Associated Protein
UV	Ultraviolet
WRN	Werner syndrome ATP-dependent helicase
XRCC	X-ray repair cross complementing
53BP1	p53-binding protein 1

Table of contents

1 Introduction

1.1 DNA double-strand break repair

Maintenance of genome integrity is crucial for the normal functioning and survival of all organisms. Any aberrations in the genome could lead to developmental defects and increased risk of diseases such as cancer (Jackson and Bartek, 2009; Kasparek and Humphrey, 2011). Although the genome is exposed to frequent environmental and endogenous damaging agents, there are number of mechanisms by which cells can repair the damage and prevent alteration of the genomic material (Hoeijmakers, 2007). One of the most toxic lesions that occur in cells on a daily basis is the DNA double-strand break (DSB) (Hoeijmakers, 2009; Lieber, 2010). DSBs can be caused by both endogenous mechanisms such as stalled or collapsed replication forks, incorrect function of topoisomerases or reactive oxygen species arising from metabolic processes as well as by exogenous agents such as ionizing radiation (IR), various chemicals and even ultraviolet light (Adachi et al., 2003; Dahle and Kvam, 2003; De Bont and van Larebeke, 2004). Cellular responses to DNA DSBs are comprised of two major repair pathways: homologous recombination and non-homologous end joining.

Homologous recombination (HR) is the most accurate way to repair the double-strand break as it utilizes sequences homologous to the damaged region on sister chromatids or homologous chromosomes and restores the original sequence with no deletions or rearrangements (Jasin and Rothstein, 2013). In mammalian cells the initial step of the HR pathway is the recognition of the DSB ends by the MRN complex that includes Mre11, Rad50 and NBS1 factors. The complex possesses endo- and exonuclease activity and initiates the 5’ to 3’ end resection process by creating a short 3’-overhanging single strand

at the end (Fig. 1.1 A) (Lamarche et al., 2010; Shibata et al., 2014). Additionally, MRN loading triggers the recruitment of CtIP that further promotes MRN nuclease activity (Sartori et al., 2007). The CtIP-mediated end resection is further facilitated by breast cancer type 1 susceptibility protein (BRCA1) (Cruz-Garcia et al., 2014). Next the initial 3'-overhangs are subjected to extensive resection by the Exo1 endonuclease either with or without DNA2 nuclease creating long single-stranded fragments (Nimonkar et al., 2011; Tomimatsu et al., 2012). In order to stabilise the resulting single stranded DNA, RPA binds to covers the whole length of the overhanging fragment (Chen et al., 2013). Extensive end resection and RPA binding is followed by the displacement of the latter by the RAD51 ATPase that forms nucleoprotein filaments and catalyses the strand invasion of the homologous template and D-loop formation (Seitz and Kowalczykowski, 2006; Sigurdsson et al., 2002). Recruitment of RAD51, as well as replacement of RPA, is dependent on breast cancer type 2 susceptibility protein (BRCA2) (Holloman, 2011; Liu et al., 2010). After the D-loop formation, the damaged sequence is restored by the activity of various polymerases including polymerase β and translesion polymerases (Sebesta et al., 2013). Finally the resulting double-Holiday junction structure is resolved by the BLM-TOPOIII complex (Bussen et al., 2007) or the endonuclease GEN1 in concert with SLX1-SLX4 resolvases for crossover and non-crossover products (Fekairi et al., 2009; Rass et al., 2010). Alternatively, in some cases the D-loop can also be resolved by migration of the Holiday junction towards the 3' end that is promoted by BLM helicase and results in non-crossover repair product (Karow et al., 2000).

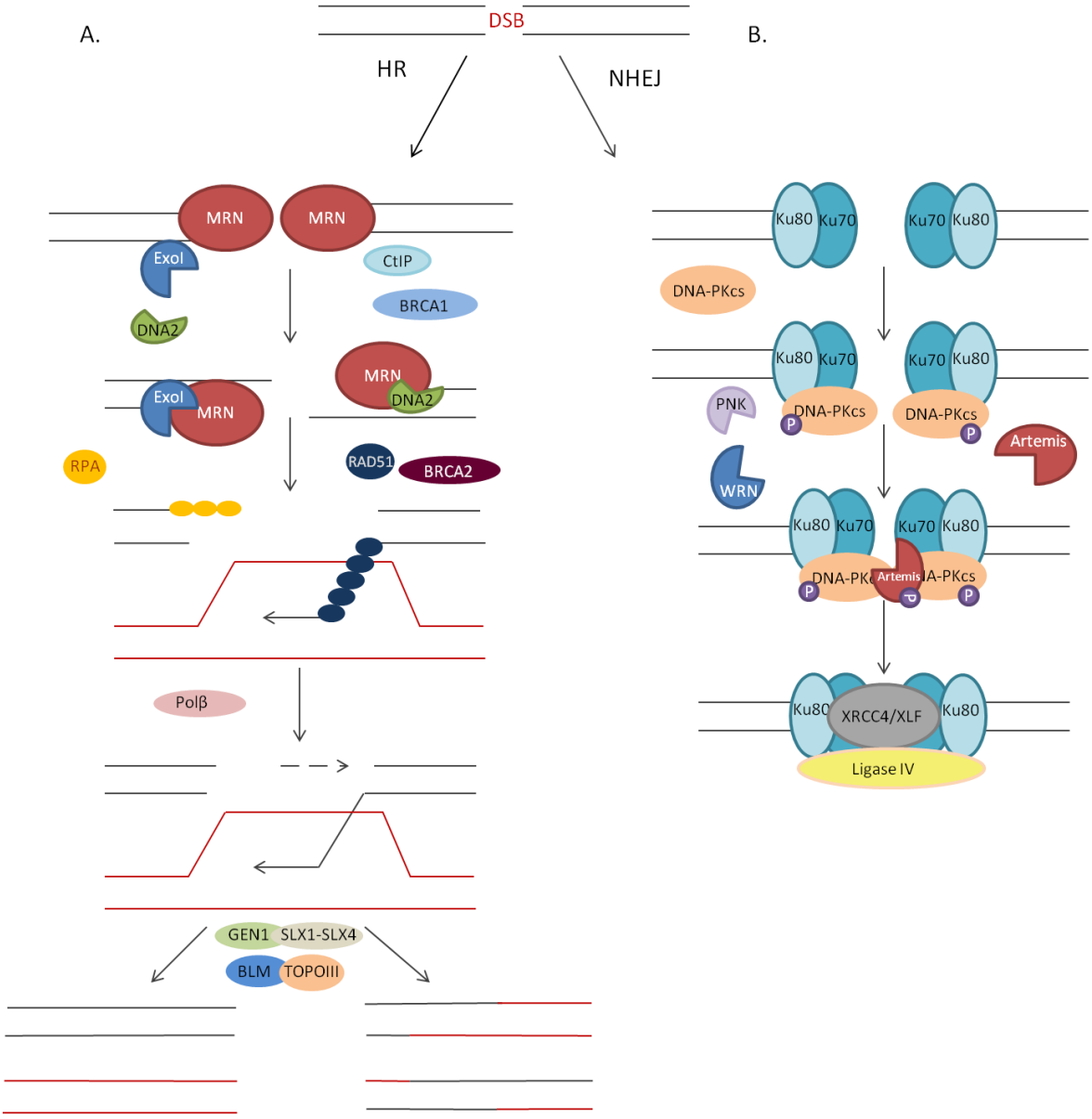

Figure 1.1. Schematic representation of major DNA DSB repair pathways. A. Homologous recombination (HR). DNA ends are recognized by the MRN complex following recruitment of CtIP, ExoI and DNA2 nucleases and 5'-3' end resection in. Next the single-stranded 3'-overhanging end is bound by RPA, following replacement with RAD51 which facilitate the strand exchange with an undamaged homologous template and then the damaged region can be restored. Finally, the resolution of the resulting structure occurs by resolvases such as GEN1/SLX1-SLX4 or BLM/TOPOIII to form crossover or non-crosover products. B. Non-homologous end joining (NHEJ). Ku70/80 heterodimer specifically binds to DNA ends and interacts with the DNA-PK catalytic subunit facilitating synapse of the ends. DNA-PK catalytic subunit recruits factors like PNK, Artemis or WRN which process DNA ends preparing ends for ligation. DNA Ligase IV, in complex with XRCC4 and XLF, rejoins the ends to complete the repair process.

The other major mechanism used to repair DSBs does not utilise any template for break restoration but instead directly religates the DNA ends and therefore is called non-homologous end joining (NHEJ). It is considered to be a more error-prone repair process as there is a possibility of deletion or mutation of parts of the damaged sequence during the end processing steps (Lieber, 2010). Similarly to HR, the initial part is the recognition of free DNA ends. In NHEJ the first factor performing rapid recognition and binding to the DSB is the Ku70/80 heterodimer (Fig. 1.1 B) (Mimori and Hardin, 1986; Walker et al., 2001). Ku70/80 not only protects DNA ends from processing by nucleases but also serves as a platform for recruitment of other NHEJ factors (Downs and Jackson, 2004). The first factor recruited to the break by Ku is protein kinase DNA-PKcs (Li and Comai, 2000; Spagnolo et al., 2006) whose activity results in recruitment of other factors such as Artemis, WRN, Aprataxin, Aprataxin-and-PKN-like factor (APLF) and polynucleotide kinase-phosphatase (PNK). All of the listed factors can perform end processing if the damaged DNA ends are not suitable for direct ligation, for example by lacking a 5'-hydroxyl, 3'-phosphate, attached adenylate groups or other modifications (Ahel et al., 2006; Jilani et al., 1999; Li et al., 2011; Neale et al., 2005; Perry et al., 2006; Povirk et al., 2007). End processing is then followed by filling of any gaps by polymerases μ and λ that are recruited to Ku via its phosphor-protein binding BRCT domains (Ma et al., 2004). Ligation of the final structure is performed by Ligase IV which is recruited to the break in a complex with XRCC4 and XLF that stabilise the location of the complex at the break via interaction with Ku and DNA and have also been shown to stimulate Ligase IV activity (Grawunder et al., 1998; Gu et al., 2007).

Interestingly, apart from canonical NHEJ cells utilise an alternative end ligation process independent of the presence of Ku and DNA-PKcs, alternative-NHEJ (alt-NHEJ) (Bennardo et al., 2008). This process is mainly occurring when canonical NHEJ is disabled

although some studies have shown the activity of this pathway in the presence of both NHEJ and HR (Bothmer et al., 2010; Coussens et al., 2013). In alt-NHEJ free DNA ends are not protected by Ku and therefore are available for the binding of other factors including Mre11 and CtIP that perform the initial end resection and generate short 3'-overhangs (Zhang and Jasin, 2011). This in turn leads to strand annealing in case of the existing microhomology between the strands or just subsequent end ligation by either the Ligase III/XRCC1 complex or Ligase I activity (Audebert et al., 2004; Paul et al., 2013). Alt-NHEJ is the most mutagenic among the major DSB repair pathways as genetic information is deleted during the end resection and subsequent annealing and unlike HR this cannot be restored by the use of an undamaged homologous template.

It is important to mention that DSB repair pathways both collaborate and compete with each other and repair pathway choice is tightly regulated in cells (Kass and Jasin, 2010). Primarily, regulation occurs with the particular cell cycle phase where HR is favoured in the S and G2 phases when sister chromatids are available in close proximity to serve as a template for accurate break restoration whereas NHEJ operates throughout the whole cell cycle (Rothkamm et al., 2003). This regulation is dependent on the action of cyclin-dependent kinases (CDK) that have been shown to promote end resection and favour HR via phosphorylation of CtIP and facilitating the formation of the CtIP-BRCA1 complex (Chen et al., 2008; Yun and Hiom, 2009). Recently, 53BP1 has also been proposed to be a point of regulation by competing with BRCA1 and inhibiting end resection performed by CtIP (Bunting et al., 2010; Escribano-Diaz et al., 2013). Generally, the crucial point of pathway choice is thought to be initial recognition of DNA ends by either Ku70/80 or MRN complexes leading to end protection versus resection respectively (Pierce et al., 2001; Shibata et al., 2014). Interestingly, the ADP-ribosyl transferase PARP1 has recently been proposed to compete for the initial binding of DNA ends with Ku and therefore serve

as another regulator of NHEJ activity ((Wang et al., 2006), further discussed in section 1.4).

1.2 Role of chromatin in DNA double-strand break repair

Alongside the DNA repair machinery, the chromatin environment surrounding the break plays an important role in both mechanism choice and efficiency of restoration of the break. Chromatin is a nucleoprotein complex where the fundamental unit, the nucleosome, consists of approximately 147bp of DNA wrapped around an octamer of core histones (Kornberg, 1977; Luger et al., 1997). The histone octamer is composed of two H3-H4 dimers surrounded by two H2A-H2B dimers (Campos and Reinberg, 2009). Additionally, linker histone H1 connects adjacent nucleosomes and promotes the formation of higher order chromatin structure (Happel and Doenecke, 2009). Apart from canonical histones, divergent histone variants are present in cells and differ from canonical histones in aminoacid composition, expression patterns and chromatin localization (Talbert and Henikoff, 2010). The structure of chromatin is highly regulated, involving histone post-translational modifications and activity of chromatin remodelling complexes (Campos and Reinberg, 2009; Clapier and Cairns, 2009). Euchromatin and heterochromatin represent two diverse states of chromatin compaction where the former represents relaxed regions associated with actively transcribed genes and histone acetylation and the latter is considered as a transcriptionally silent, highly compact form enriched in repetitive sequences and H3 K9 trimethylation (de Wit and van Steensel, 2009; Guenther et al., 2007; Peng and Karpen, 2008).

Initial studies hypothesised the active involvement of chromatin in the DNA damage response (DDR) as nucleosome rearrangements were observed after UV-induced DNA

damage as judged by the nuclease sensitivity of newly synthesised DNA (Smerdon and Lieberman, 1978). Nowadays, several features of chromatin have been proposed to facilitate DNA repair including involvement of histone variants, histone post-translational modifications, chromatin remodelling as well as general chromatin organisation.

1.2.1 DNA double-strand break repair in heterochromatin

DNA repair pathways are generally described in a context of euchromatin where the break is easily accessible for the repair machinery. However, general compaction of chromatin around the DNA break can also influence the repair process (Falk et al., 2008). DNA damage repair in heterochromatin has been demonstrated to have slower kinetics of break restoration than that of euchromatin as judged by one of the commonly used marks of DNA damage – serine139 phosphorylated H2AX (γ-H2AX) induction and decay (Cowell et al., 2007; Goodarzi et al., 2011). Furthermore, more recent studies have shown the reorganisation of chromatin structure in the event of a heterochromatic DNA break and the subsequent relocation of the break to a peripheral region of the heterochromatin (Chiolo et al., 2011). Thus, γ-H2AX has been detected early after the induction of the DSB located in the chromocenters and this then relocates to the periphery within 20 min (Jakob et al., 2011). In agreement with this, the recruitment of early sensors of DSB such as BRCA1, MDC1 and RPA is not delayed in the heterochromatic DSB whereas the recruitment of late factors such as RAD51 requires the relocation of the break to the less packed forms of chromatin (Chiolo et al., 2011; Jakob et al., 2011). Involvement of heterochromatin associated proteins as well as heterochromatic histone modifications in DNA damage response has also been revealed. Histone H3 on K9 trimethylation is a known mark enriched in heterochromatin (Barski et al., 2007). This modification is essential for binding of a key factor of heterochromatin maintenance – heterochromatin protein 1 (HP1) (Maison and Almouzni, 2004). The presence of mammalian HP1 variant HP1β on the chromatin has been shown to prevent phosphorylation of H2AX in response to DSBs

(Ayoub et al., 2008). Further studies have demonstrated that the release of HP1β from chromatin is regulated by its phosphorylation by casein kinase 2 and is also dependent on the phosphorylation of its counterpart KAP1 (Bolderson et al., 2012). Interestingly, KAP1 also contributes to DNA damage-induced heterochromatin relaxation via interaction with ataxia-telangiectasia mutated (ATM) kinase (White et al., 2012). Phosphorylation of KAP1 by ATM has been shown to facilitate the release of the nucleosome remodelling factor CHD3 from the damaged region promoting chromatin relaxation (Goodarzi et al., 2011). Additionally, desumoylation of KAP1 by SENP7 peptidase has been shown to further stimulate CHD3 release by preventing the interaction of the latter with sumoylated KAP1 (Garvin et al., 2013). Interestingly, release of HP1 from the H3 containing K9 trimethylation makes it accessible for other factors to bind this heterochromatin mark including the acetyltransferase Tip60 and this binding has been suggested to be critical for its activity and subsequent acetylation of histones promoting chromatin relaxation ((Murr et al., 2006; Sun et al., 2009) further discussed in section 1.2.2).

1.2.2 Role of histone variants and histone post-translational modifications in DNA damage repair

Histones comprise a core of the nucleosome particle and therefore have an important role to signal the break and recruit the repair machinery to the DNA lesions (Campos and Reinberg, 2009). As mentioned above, one of the most studied responses of chromatin to DNA damage is phosphorylation of histone H2A variant H2AX (Rogakou et al., 1998). H2AX is phosphorylated on serine-139 by members of the phosphatidylinositol kinase (PIK) family such as ATM and DNA-PKs in a matter of minutes following DNA DSB break induction (Friesner et al., 2005; Stiff et al., 2004). The phosphorylated form is known as γ-H2AX. γ-H2AX is then recognized by the mediator of DNA damage

checkpoint protein 1 (MDC1) which facilitates H2AX phosphorylation spreading up to 2Mbp on both sides of the damaged site and recruits other factors of the repair machinery such as the MRN complex, 53BP1 and BRCA1 (Jungmichel and Stucki, 2010; Lukas et al., 2004; Paull et al., 2000; Wang et al., 2002). Interestingly, MDC1 has also been shown to promote the formation of another histone post-translational modification around the break site, namely ubiquitylation (Bekker-Jensen and Mailand, 2011). The ubiquitin ligase RNF8 has been shown to be recruited to the phosphorylated form of MDC1 at the break via its FHA domain followed by subsequent recruitment of its counterpart RNF168 (Doil et al., 2009; Mailand et al., 2007). This in turn triggers K36-linked ubiquitylation of histone H2A and H2B and recruitment of repair factors such as BRCA1 and CtIP (Doil et al., 2009; Kolas et al., 2007; Wu et al., 2009). Furthermore, RNF186 dependent ubiquitylation of H2A serves as a marker of transcription silencing by contributing to the inhibition of RNA polymerase II elongation (Shanbhag et al., 2010). Thus, H2AX phosphorylation serves as a signal of DNA damage and promotes recruitment of DNA repair factors to the break as well as promoting transcription suppression to favour the repair process.

Another H2A variant has also been shown to have a distinct role in the DNA repair process. Studies in *Saccharomyces cerevisiae* have demonstrated recruitment of the H2A.Z variant to the site of double-strand breaks and deletion of the gene encoding H2A.Z led to DSB sensitivity and genetic instability (Morillo-Huesca et al., 2010; van Attikum et al., 2007). Recent studies in mammalian cells provide a mechanistic insight into the role of H2A.Z in DSB repair. Depletion of H2A.Z has been shown to decrease the level of RNF8 induced chromatin ubiquitylation and therefore reduced BRCA1 recruitment (Xu et al., 2012). Furthermore, the absence of H2A.Z has been shown to limit the binding of the Ku70/80 heterodimer to DNA ends and instead promote recruitment of RPA and therefore

favour DNA end resection by CtIP. Indeed, the activity of the chromatin remodelling factor INO80 and the histone chaperone ANP32E that are responsible for the H2A.Z/H2A exchange have recently been shown to promote the homologous recombination pathway and facilitate IR-induced RPA and RAD51 foci formation (Alatwi and Downs, 2015).

Alongside phosphorylation, histone acetylation plays an important role in DNA repair. Generally, acetylation is linked to the relaxed state of chromatin and is thought to promote DNA accessibility for the machinery responsible for both transcription and DNA repair by destabilising DNA-histone interactions (Campos and Reinberg, 2009; Simpson, 1978) and/or leading to the recruitment of specific factors. Several studies have demonstrated the critical role of H2AX, H3 and H4 acetylation in DNA double-strand break repair (Murr et al., 2006). Thus, the Tip60/TRRAP complex, in which Tip60 functions as an acetyltransferase, has been shown to be involved in the HR pathway (Courilleau et al., 2012; Murr et al., 2006). Either prevention of Tip60 acetyltransferase activity or deletion of the gene encoding the TRRAP subunit leads to the abolishment of DNA DSB-induced H4 and H2AX hyperacetylation and prevents the recruitment of 53BP1, BRCA1 and RAD51 to the break (Ikura et al., 2000; Murr et al., 2006). Moreover, another acetyltransferase complex, p300/CBP, has been shown to be critical for the DNA DSB damage response. CBP/p300-dependent H2AX K36 acetylation has been shown to be important for mammalian cell survival following exposure to IR (Vempati et al., 2010). Furthermore, acetylation of histones H3 at K18 and K56 as well as histone H4 at K5/K8/K12/K16 have been shown to be involved in both HR and NHEJ pathways in *Saccharomyces cerevisiae* (Ogiwara et al., 2011; Tamburini and Tyler, 2005). H3 K36 acetylation also increases in response to DNA DSB induction in mammalian cells in a p300 and CBP dependent manner (Vempati et al., 2010). Additionally, depletion of either p300 or CBP leads to a defect in recruitment of Ku70/80 to the break, indicating

involvement of these acetyltransferases in the NHEJ pathway (Ogiwara et al., 2011). It is important to mention that some studies have also demonstrated a decrease in H3 K56 acetylation upon DNA DSB induction performed by histone deacetylases HDAC1 and HDAC 2 and proposed this hypoacetylation to play a role in NHEJ repair, perhaps highlighting the importance of dynamic regulation of chromatin acetylation surrounding the break (Miller et al., 2010; Tjeertes et al., 2009). Another enzyme contributing to H4 acetylation is MOF (Sharma et al., 2010). MOF has been shown to be the major acetyltransferase responsible for DNA damage-induced H4 K16 acetylation and its loss results in global chromosome aberrations in conditional MOF-null mouse models, with the abolishment of recruitment of MDC1 and, as a consequence, 53BP1 and BRCA1 to IR-induced DNA damage (Li et al., 2010b). ATM-induced phosphorylation of DNA-PKcs has also been shown to be reduced in MOF-depleted cells suggesting a potential involvement of MOF dependent H4 K16 acetylation in the action of DNA-PK (Sharma et al., 2010).

A number of other histone post-translational modifications have also been shown to contribute to the DNA DSB response. For example, MMSET-mediated methylation of H4 at K20 has recently been shown to be increased at the DSB sites and yet again facilitate recruitment of 53BP1 to the break via its Tudor domain (Botuyan et al., 2006; Pei et al., 2011). Another methyltransferase responsible for H4K20 methylation, SET8, has also been shown to be recruited to laser-induced DNA damage sites and contribute to the 53BP1 accumulation, although its recruitment is dependent on PCNA (Oda et al., 2010). Additionally, histone ADP-ribosylation has been shown to be triggered upon DNA damage and its role in DNA double-strand break repair will be further discussed in section 1.4 (Burzio et al., 1979).

1.3 ADP-ribosylation

1.3.1 ADP-ribosylation in mammalian cells

ADP-ribosylation is a protein post-translational modification occurring in response to different types of genotoxic stress and involved in different cellular processes including the DNA damage response. ADP-ribosylation activity has been shown to be conserved in many organisms including species from all six major eukaryotic supergroups as well as in some representatives of bacteria and viruses (Mattiussi et al., 2007; Perina et al., 2014; Slade et al., 2011). Interestingly, ADP-ribosylation has not been reported in *Saccharomyces cerevisiae* and *Schizosaccharomyces pombe*, two of the most commonly used model organisms for DNA repair studies (Citarelli et al., 2010). Recently the importance of ADP-ribosylation has been further highlighted as its inhibition has been shown to lead to the synthetic lethality of cancer cells carrying BRCA1/2 mutations (Bryant et al., 2005; Farmer et al., 2005).

ADP-ribosylation occurs by the transfer of the ADP-ribosyl moiety from NAD^+ to the acceptor protein enzymatically by ADP-ribosyl transferases (ARTs) (Fig. 1.2). Currently, ADP-ribosylation has been reported to occur on the glutamate, aspartate, lysine, cysteine and arginine residues *in vitro* in mammalian cells as well as phosphoserine, asparagine and diphthamide in bacterial cells (Hassa et al., 2006; Vyas et al., 2014). Mono ADP-ribosylation (MAR) can occur when only one ADP-ribosyl unit is transferred to the acceptor site or poly-ADP-ribosylation when ADP-ribosyl units are attached to each other forming long poly-ADP-ribosyl (PAR) chains up to 200 units in length (Corda and Di Girolamo, 2002; D'Amours et al., 1999).

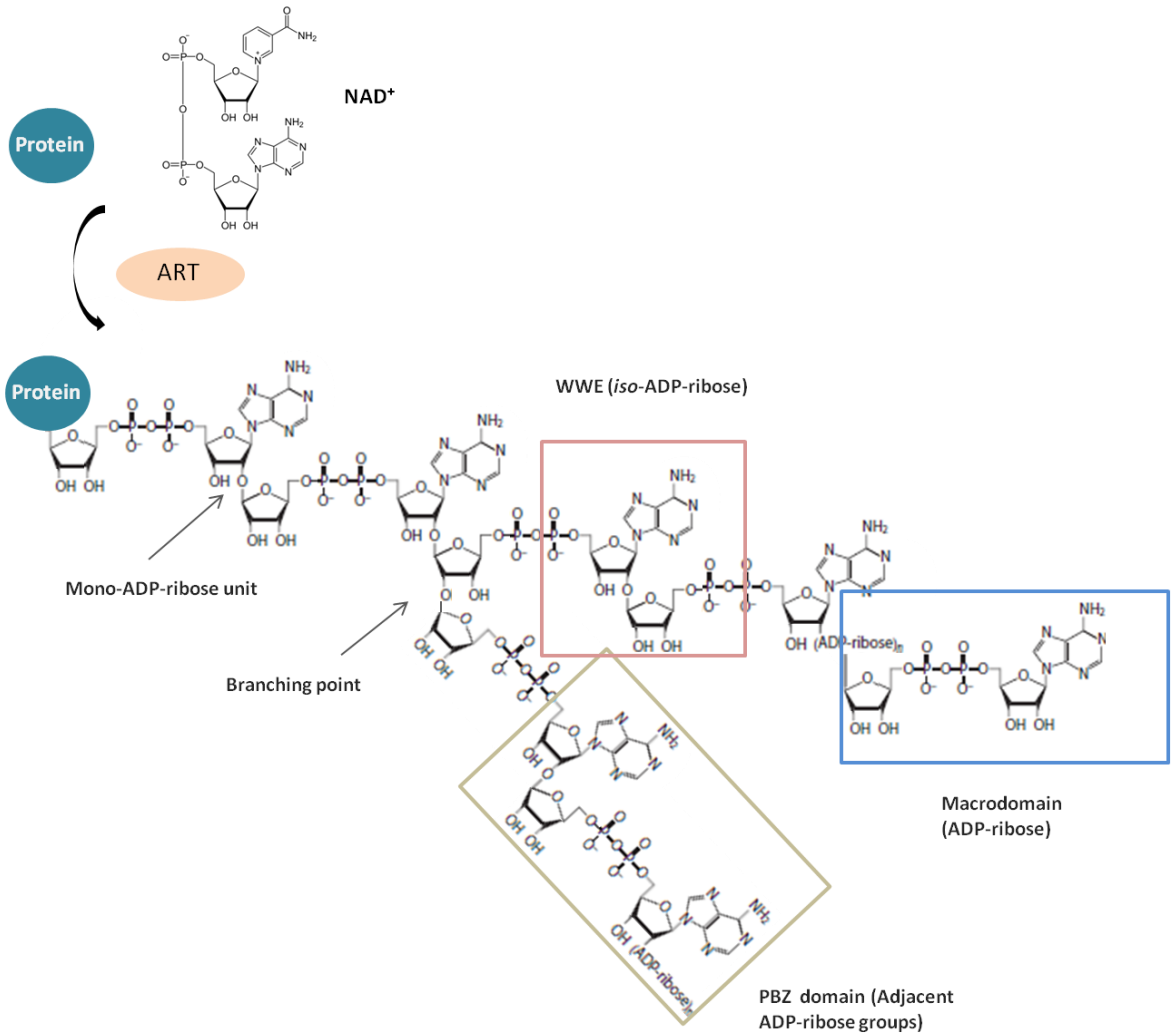

Figure 1.2 ADP-ribosylation reaction and the structure of the ADP-ribose polymer. ADP-ribosyl transferases catalyse transfer of the ADP-ribose moiety from NAD^+ to acceptor proteins forming either mono- or poly-(ADP-ribose) chains. Polymer branching point and structures recognised by specific ADP-ribose binding domains are indicated. Adapted from (Hottiger, 2015).

Historically, ADP-ribosylation was discovered by demonstrating the incorporation of radioactively-labeled NAD^+ into the nuclear fraction purified from rat liver cells (Nishizuka et al., 1967; Sugimura et al., 1967). The polymeric structure of the resulting nuclear product incorporating NAD^+ was identified (Sugimura et al., 1967). Soon the major nuclear enzyme that performs ADP-ribosylation in mammalian cells, PARP1, was purified and characterized (Kawaichi et al., 1981; Shimizu et al., 1967). Thus, the catalytic domain as well as a critical residue for catalyzing the formation of the poly-ADP-ribose chains, glutamate 988, was identified by crystal structure analysis and comparison with the previously known bacterial ADP-ribosyl toxins (Kim et al., 1997; Marsischky et al., 1995).

Furthermore, the branching structure of the ADP-ribosyl polymer was characterised suggesting a branching event to occur on average every 20-50 units and to represent around 2% of the total polymer (Keith et al., 1990; Miwa et al., 1979). The ADP-ribosylation has been shown to be increased by the presence of DNA breaks *in vitro* by stimulating PARP auto-modification activity by the presence of DNA breaks (Benjamin and Gill, 1980). Treating cells with DNA damaging agents has led to a dramatic increase in total ADP-ribosylation as judged by the incorporation of ^{14}C-labeled NAD^+ to the nucleus (Adamietz and Rudolph, 1984; Wielckens et al., 1982). Since the initial discovery of PARP1, many more enzymes catalysing protein post-translational ADP-ribosylation have been discovered comprising a family of ADP-ribosyl transferases (Hottiger et al., 2010).

1.3.2 ADP-ribosyl transferases

The most well-studied ART is PARP1 which has been proposed to perform up to 90% of the whole cellular ADP-ribosylation (Shieh et al., 1998). PARP1 contains six independently folded domains (Fig. 1.3) and the crystal structure of the separate domains bound to DNA is determined (Langelier et al., 2012). PARP1 has been shown to interact

both with native and damaged DNA via its N-terminal DNA binding domain containing two zinc finger domains (Eustermann et al., 2011; Langelier et al., 2011). A third zinc finger domain has also been discovered and is implicated in enzyme activation upon DNA binding (Langelier et al., 2008). The DNA binding domain is followed by the so-called auto-modification domain containing a BRCT domain responsible for protein-protein interactions and found in many DNA repair proteins (Bork et al., 1997). Most PARP1 *in vitro* auto-modification sites are found within this domain, however more recent studies suggest auto-modification can also occur outside of the BRCT domain (Altmeyer et al., 2009; Duriez et al., 1997; Vyas et al., 2014). The WGR domain contains conserved repeats of tryptophan, glycine and arginine. Its function is still unknown although it has been shown to be important for the ART enzymatic activity (Altmeyer et al., 2009).

Finally, at the C-terminus is located the catalytic domain (CAT). This domain is particularly important as it is required for both binding NAD^+ (donor site) and also for transferring the ADP-ribose units to the acceptor proteins (acceptor site) (Ruf et al., 1998; Ruf et al., 1996). The CAT domain includes an ART homology domain and a highly conserved NAD^+ binding pocket including a so-called ART signature HYE motif. This motif has been shown not only to be responsible for the coordination of the NAD^+ molecule at the binding pocket but also to be important for producing poly-ADP-ribosylation as the mutation of glutamate 988 from this motif led to the inability of PARP1 to catalyse the transfer of more than one ADP-ribosyl unit in auto-catalysis and reduced the overall PARP1 activity by more than 2000-fold (Marsischky et al., 1995; Otto et al., 2005).

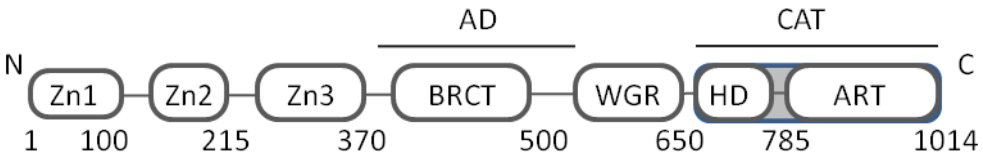

Figure 1.3 PARP1 domain organization. N- to C-terminus domain structure is shown. Auto-modification domain and ART catalytic domain are indicated. Adapted from (Langelier et al., 2012).

The catalytic domain is the most conserved domain among the known ARTs. Currently 22 human genes potentially encoding proteins containing a highly conserved ART domain have been identified and at least 17 ART-related enzymes have been characterized (Hottiger et al., 2010).

The most similar to PARP1 in domain composition and organisation are PARP2 and PARP3. Both PARP2 and 3 have the WGR, HD and ART domains including the fully conserved HYE motif (Karlberg et al., 2010; Lehtio et al., 2009; Otto et al., 2005). Like PARP1, both PARPs 2 and 3 are activated by the presence of DNA breaks *in vitro* (Ame et al., 1999; Langelier et al., 2014; Loseva et al., 2010). Interestingly, although PARP3 contains the conserved glutamate in the HYE motif, it can only catalyse either mono-ADP-ribosylation in autocatalysis or the formation of the short oligo-ADP-ribose chains on acceptor proteins (Loseva et al., 2010; Rulten et al., 2011). Three more ARTs containing fully conserved HYE motif are PARP4, 5a and 5b and these have been shown to perform poly-ADP-ribosylation (Kickhoefer et al., 1999; Smith et al., 1998).

The remaining 11 PARPs do not contain the full HYE motif in their catalytic domain and have the catalytic glutamate replaced with either isoleucine for PARP6-8 and PARP10-12, leucine for PARP14 and 15, and valine or tyrosine for PARP13 and 16 respectively (Aguiar et al., 2005; Kleine et al., 2008; Otto et al., 2005). Consistent with the lack of the catalytic glutamate most of the listed ARTs were shown to perform only mono-ADP-ribosylation in auto-catalysis (Vyas et al., 2014). It is important to mention that both PARP9 and PARP13 lack not only the glutamate but also the histidine in the NAD^+ binding motif and are therefore predicted not to have any ADP-ribosyl transferase activity and none has been detected *in vitro* assays with purified recombinant protein (Aguiar et al., 2005; Vyas et al., 2014).

Together with the differences in domain structure and biochemical characteristics, cellular distribution and functions of the known ARTs also differ. PARPs 1-3 are localised predominantly in the nucleus and were shown to play a role in DNA damage repair by recruiting factors of DNA repair machinery to the sites of single and/or double strand breaks (discussed further in chapter 1.4). Furthermore a role for the same ARTs in transcription and cell cycle regulation has been shown. PARP1 has been shown to interact with up to 90% of genes transcribed by Pol II and to recruit and promote the exchange of different transcription co-factors such as NF-kB, Elk1, Oct1, Sp1, NFAT (Kraus, 2008; Krishnakumar et al., 2008). Deletion of PARP2 leads to the change of expression of more than 600 genes (Szanto et al., 2012) and it have been proposed to regulate transcription of cell-cycle related genes through interaction with histone deacetylases and the methyltransferase G9a (Liang et al., 2013). PARP3 has been suggested to regulate transcription via association with the polycomb group protein complex (Rouleau et al., 2007). Additionally, PARP3 has been identified to play a role in the stabilization of the mitotic spindle by stimulating spindle components NuMA directly and via Tankyrase 1 (Boehler et al., 2011b).

Some ARTs have only been shown to have a more specific localisation and function. PARP4 has been mainly found as a part of a ribonucleoprotein complex and shown to have a major vault protein as its main substrate (Kickhoefer et al., 1999). Tankyrases PARP5a and 5b have been found to localise on telomeres and be involved in telomere length regulation (Cook et al., 2002; Smith et al., 1998). PARP7, 10, 12, 13 and 15 are mainly found in the cytoplasm and are involved in cytosolic mRNA processing (Ji and Tulin, 2013; Leung et al., 2012). Another role of the ARTs is regulation of inflammatory gene expression. For example, promotion of T helper cells 2 gene expression for PARP1 and

PARP14 and involvement in *S.aureus*-induced astrocyte activation for PARP1-3 (Cho et al., 2009; Riley et al., 2013; Rosado et al., 2013).

1.3.3 Removal of protein ADP-ribosylation

Like most protein post-translational modifications, ADP-ribosylation is reversible. Poly-ADP-ribosylation is known to be degraded rapidly in the cell in a matter of seconds whereas the removal of mono-ADP-ribosylation requires a minute timescale (Wielckens et al., 1982). The major enzyme responsible for PAR chain degradation is poly-ADP-ribose glycohydrolase (PARG). Using biochemical *in vitro* assays as well as crystal structure data analysis, this enzyme has been shown to have both endo- and exo-glycohydrolase activity, hydrolysing ribose-ribose bonds in the PAR polymer but not cleaving the final moiety from the protein (Lin et al., 1997; Slade et al., 2011; Ueda et al., 1972). The importance of PARG activity in cell survival has been demonstrated as disruption of gene encoding nuclear localised PARG led to increased sensitivity to cytotoxisity and early lethality of mouse embryos (Koh et al., 2004). Although PARG degrades the majority of PAR chains another enzyme hydrolysing ribose-ribose linkages, ADP-ribosyl hydrolase (ARH3), has been identified (Oka et al., 2006). Unlike PARG ARH3 is able to hydrolyse only the terminal ADP-ribose bond in the PAR chain and has much less activity compared to PARG (Mueller-Dieckmann et al., 2006; Slade et al., 2011).

However, both PARG and ARH3 hydrolyse only the PAR chains leaving the last ADP-ribosyl moiety on the acceptor protein. Recently a family of macrodomain containing proteins have been discovered to be enzymes able to fully remove mono-ADP-ribosylation (Jankevicius et al., 2013). The major representatives of the family are MacroD1, MacroD2 and TARG. Both MacroD1 and 2 have been shown to remove auto-mono-ADP-ribosylation of PARP10 and weakly modified PARP1 *in vitro* and the enzymatic activity of

MacroD2 has been shown to be functional as it reversed the inhibition of GSK3β kinase brought about by mono-ADP-ribosylation (Jankevicius et al., 2013; Rosenthal et al., 2013). It is important to mention that it is predicted from X-ray crystal structure and structure homology modelling analysis that MacroD1/2 are only able to remove ADP-ribosyl units attached to acidic residues. During the de-ADP-ribosylation the substrate is thought to be located within the active site of the MacroD1/2 together with a water molecule where it gets deprotonated and performs a nucleophilic attack on the carbonyl carbon of the acceptor acidic residue (Rosenthal et al., 2013). Indeed MacroD1 is unable to remove the ADP-ribosylation of actin performed by the bacterial arginine specific ADP-ribosyltransferase CTDa.

1.3.4 ADP-ribosylation signal recognition

ADP-ribosylation can play a role in cellular processes not only by directly altering the structure of modified acceptor proteins but also through reader proteins which bind noncovalently to the ADP-ribosylated target proteins. Currently such readers are divided into four major groups depending on the presence of different conserved domains sensing the ADP-ribosylation (see Fig. 1.2).

One of the first domains that was determined to interact with PAR chains is the PAR-binding motif (PBM) (Malanga et al., 1998). PBM contains repeats of primarily basic residues and has a defined sequence [HKR][X][X][AIQVY][KR][KR][AILV][FILPV] (Gagne et al., 2008; Pleschke et al., 2000). PBMs have been found in a large number of proteins including DNA damage signalling and repair proteins like XRCC1, DNA ligase III, DNA-PKs, Ku70/80, p53 and others (Gagne et al., 2008). Although there is not much structural data defining the interaction of PMBs with ADP-ribose units, they are thought to bind long and branched ADP-ribosyl polymers and be utilised in the recruitment of DNA

repair proteins to the damaged site (Fahrer et al., 2007; Gagne et al., 2008). Apart from a role in DNA damage repair, the PAR-binding motif present in apoptosis-inducing factor has been demonstrated to be critical for its role in PARP1-induced cell apoptosis (Wang et al., 2011).

Interestingly, one of the classes of ADP-ribosylation readers are macrodomain containing proteins (Karras et al., 2005). Together with the previously mentioned enzymatically active MacroD1/2 and TARG there are 11 genes encoding macrodomain-containing proteins identified in the human genome (Feijs et al., 2013). A macrodomain is a globular domain containing between 120 to 190 amino acids and, by contrast to other ADP-ribose recognition domains, it has been shown to recognise both mono-ADP-ribosylation and PAR chains, as well as their degradation products (Allen et al., 2003; Karras et al., 2005). Macrodomains were initially found in the macroH2A histone variant and recently also been shown to be present and have functional significance in a chromatin remodelling enzyme ALC1 and ADP-ribosyl transferases ADPRT8 and 9 (Forst et al., 2013; Gottschalk et al., 2009; Timinszky et al., 2009; Yan et al., 2013).

A third class of ADP-ribosyl recognising proteins have a conserved WWE domain. This domain is named after highly conserved tryptophan and glutamate residues and has been shown to have PAR and more precisely *iso*-ADP-ribose binding activity (Aravind, 2001; Wang et al., 2012). Like the macrodomain, the WWE domain has been identified to be present in ADPRT8, and 11-14 ARTs suggesting a role in their ADP-ribosylation activity (He et al., 2012). Interestingly, the WWE domain has also been identified in E3 ubiquitin ligases like RNF146, potentially linking ubiquitylation and ADP-ribosylation processes in cells (Kang et al., 2011). Indeed, RNF146 has been shown to interact with ADP-

ribosylated axin via its WWE domain and promote its degradation by ubiquitylation (Zhang et al., 2011).

The final class is the PAR-binding Zinc-finger (PBZ) domain that recently been shown to bind poly-ADP-ribose chains (Ahel et al., 2008). The specificity to PAR versus MAR is defined by the simultaneous recognition of the ribose of one moiety and the pyrophosphate of the adjacent ADP-ribosyl unit (Li et al., 2010a; Oberoi et al., 2010). Currently only three proteins bearing PBZ domain have been identified in human cells and are the check-point protein CHFR, and two DNA repair proteins DCLRE1a and APLF (Ahel et al., 2008; Rulten et al., 2008). The functional role of the latter will be further discussed in the section 1.4.1.

Recent studies suggest Forkhead-associated (FHA), BRCA1 C-terminal (BRCT) and oligonucleotide/oligosaccharide binding fold (OB-fold) domains also have PAR binding activity (Li et al., 2013; Zhang et al., 2014). The OB-fold motif has long been known to recognise DNA and RNA structures but the OB-fold domain of human ssDNA-binding protein 1 has recently been shown to recognise iso-ADP-ribose and be responsible for its recruitment to DNA breaks (Flynn and Zou, 2010; Zhang et al., 2014). Both FHA and BRCT domains are known to be phosphoprotein-binding motifs and also recognise phospho-groups within the ADP-ribose unit for latter and iso-ADP-ribose for former (Mahajan et al., 2008; Manke et al., 2003). A lot of DNA repair proteins have been shown to carry these domains and the functional significance of some of these will be also discussed further in the next section.

1.4 ADP-ribosylation in DNA damage response and repair

One of the major roles of cellular ADP-ribosylation is its involvement in DNA damage response (DDR). The level of ADP-ribosylation has been shown to increase rapidly up to 500-fold in response to different types of genotoxic stresses consuming the majority of cellular NAD^+ (Wielckens et al., 1983; Wielckens et al., 1982). Out of all known mammalian ARTs only three have been reported to play a role in DDR – PARP1, PARP2 and PARP3. Indeed, PARP1 null mice have been shown to have increased sensitivity to DNA damaging agents such as gamma-irradiation leading to mutation accumulation and genomic instability in fibroblasts derived from these *parp1-/-* mice (Phulwani and Kielian, 2008; Trucco et al., 1998). Similarly, *parp2-/-* mice show increased sensitivity to DNA damage and cells derived from these animals show a delay in the repair of DNA breaks caused by the alkylating agents (Boehler et al., 2011a). By contrast, *parp3-/-* mice do not show sensitivity to γ-irradiation but depletion of PARP3 in mammalian cells sensitises cells to DNA DSB inducing agents (Beck et al., 2014; Boehler et al., 2011b; Rulten et al., 2011).

One of the mechanisms for ADP-ribosylation involvement in the DDR is through DNA damage-induced chromatin remodelling. Firstly, all DDR ARTs have been reported to have core histones as well as linker histone H1 as ADP-ribosylation substrates both *in vitro* and in cells (Burzio et al., 1979; Huletsky et al., 1985). Having two negatively charged phosphate groups in each ADP-ribosyl unit, PAR polymers greatly increase the negative charge of the acceptor protein and potentially destabilise protein-DNA or protein-protein interactions. Indeed, ADP-ribosylation of histone H1 and core histones leads to chromatin structure relaxation when studied on reconstituted polynucleosomes and has been shown to directly destabilise histone-DNA interactions judged by increased accessibility of nucleosomal DNA to nucleases (Hough and Smulson, 1984; Niedergang et al., 1985).

Secondly, auto ADP-ribosylation of ARTs themselves as well as other proteins on the DNA damage site promotes recruitment and activation of chromatin remodelling factors. For example, an SHF2 family ATPase ALC1 has been shown to be activated following ADP-ribosylation of nucleosomes by PARP1 *in vitro* and to be rapidly recruited to the chromatin by its macrodomain in PAR-dependent manner in cells (Ahel et al., 2009; Gottschalk et al., 2012). Recruitment of chromatin remodelling complexes ISWI and NuRD to the DNA damage sites also depends on the activity of PARP1 (Chou et al., 2010; Smeenk et al., 2013). Depletion of PARP1 in U2OS cells leads to the reduced recruitment of ISWI core component SMARCA5 to laser-induced DNA damage sites and PAR chains are required for its full accumulation at the damaged sites (Smeenk et al., 2013). Similarly, CHD4, a component of NuRD complex, has been shown to be recruited to the laser-induced damaged DNA in a PARP1 dependent manner, potentially through its PBZ domain and subsequently facilitate loading of other components of the complex (Chou et al., 2010; O'Shaughnessy and Hendrich, 2013). Interestingly, recruitment of the NuRD deacetylase complex may lead to the formation of repressive chromatin whereas ISWI components promote chromatin relaxation suggesting a regulatory role of ADP-ribosylation-induced chromatin remodelling (Chou et al., 2010).

1.4.1 ADP-ribosylation in DNA single- and double-strand break repair

The most defined function of ARTs in the DDR is participation in DNA single-strand break repair. Single-strand breaks (SSBs) occur in cells on a daily basis due to both endogenous and exogenous reasons and get repaired rapidly by well established pathways, generally involving break recognition, DNA end processing, gap filling and ligation to repair the break (Caldecott, 2014). ADP-ribosylation has been demonstrated to participate at all of these steps. Firstly, both PARP1 and PARP2 have been shown to be recruited to and get activated by the DNA SSBs both *in vitro* and *in vivo* and serve as initial signal for

accumulation of other factors on the break (Ame et al., 1999; Okano et al., 2003; Schreiber et al., 2002). Thus, XRCC1, one of the first factors that recognises SSBs and recruits other members of the repair machinery to the break, has been shown to have affinity for PAR chains *in vitro* and *in vivo* through its BRCT domain (Breslin et al., 2015; Li et al., 2013). XRCC1 has also been shown to be recruited to sites of oxidative DNA damage shortly after induction of poly-ADP-ribose chain synthesis and its recruitment is dependent on the presence of PARP1 and XRCC1 BRCT domain (Breslin et al., 2015; Schreiber et al., 2002). Next, aprataxin and aprataxin-and-PNK-like factor (APLF) have been reported to be recruited to SSBs in a PAR- dependent manner via FHA and PBZ domains respectively (Li et al., 2010a; Li et al., 2013). The former is responsible for the release of the adenylate groups from the 5'-ends of the break and the latter participates in DNA end resection (Ahel et al., 2006; Li et al., 2011). Finally, Polynucleotide kinase 3'-phosphatase (PNKP), an enzyme performing both phosphorylation of 5'- hydroxyl and hydrolysis of 3'-phosphate groups for subsequent ligation, also interacts with PAR polymers through its FHA domain (Jilani et al., 1999; Li et al., 2013).

Apart from facilitating single-strand break repair other studies suggest ADP-ribosylation has an important role in DNA double-strand break repair pathways. Similarly to DNA SSB repair, the function of PARP1 in the repair of double-strand breaks is defined the most. Firstly, PARP1 both interacts with and gets activated by different DNA DSB *in vitro* and also gets recruited to the DNA double-strand break sites *in vivo* in a matter of seconds (Ali et al., 2012; Haince et al., 2008; Kun et al., 2002; Tartier et al., 2003). Then its activity on DNA DSBs promotes recruitment of other factors of the DNA repair machinery including members of both major DSB repair pathways. Indeed, two key factors of the MRN complex initiating DNA repair via homologous recombination pathway,Mre11 and NBS1, have been reported to have a PAR-binding motif and an FHA domain respectively and

have been shown to interact with PAR chains *in vitro* (Haince et al., 2008; Li et al., 2013). Furthermore, study of the kinetics of Mre11 and NSB1 recruitment to laser-induced DNA damage *in vivo* have demonstrated the requirement of the presence and activity of PARP1 on the break for the subsequent rapid accumulation of these factors (Haince et al., 2008). Another HR complex recruited to the DSBs in a PAR-dependent manner is the BARD1/BRCA heterodimer. BARD1 has been shown to interact with PAR chains through its BRCT domain and this domain has been shown to be critical for the BARD1/BRCA recruitment to the DSB during early DNA damage response *in vivo* (Li et al., 2013; Li and Yu, 2013). Interestingly, both PARP1 and PARP2 have been reported to be required for DSB repair by HR following stalled replication forks (Bryant et al., 2009; Ying et al., 2012). Depletion of either PARP1 or PARP2 has been shown to sensitise cells to hydroxyurea treatment and excess of thymidine and both PARPs have been demonstrated to be required for efficient RAD51 foci formation and subsequent break resolution by HR.

However, apart from facilitating repair of DSB by homologous recombination PARP1 has been suggested to participate in the NHEJ pathway too, although its role is controversial. PARP1 has been shown to interact with DNA-PK *in vitro* and the kinase activity of the latter has been shown to be dependent on ADP-ribosylation (Ruscetti et al., 1998). The formation of a PARP1 – DNA-PK complex *in vivo* has also been reported (Gagne et al., 2008; Spagnolo et al., 2012). However, the formation of such complex has not been shown to be critical for the DNA-PK activity *in vivo* yet, although several reports suggest that PARP1 and DNA-PK could co-operate by having similar functions in NHEJ DSB repair in cells as shown by the lack of additional sensitivity to IR in *dna-pk-/-* null mice after PARP inhibition and vice versa (Rybanska et al., 2013; Veuger et al., 2003). Another example of PARP1 – DNA-PK co-operation is their function in V(D)J recombination where the repair step occurs via NHEJ pathway (Morrison et al., 1997). PARP1 has been

shown to decrease mutation rate during V(D)J recombination of *dna-pk-/-* T cells. However, there is also evidence that, instead of facilitating the canonical NHEJ pathway, PARP1 promotes repair by the more mutagenic alt-NHEJ. Several studies have shown that PARP1 competes with the initial factor of c-NHEJ Ku70/80 for binding to the free DNA ends on the break (Hochegger et al., 2006; Paddock et al., 2011). As discussed previously, PARP1 also facilitates rapid recruitment of Mre11 endonuclease favouring end processing versus Ku70/80 binding and therefore preventing the fast recruitment of other c-NHEJ factors (Haince et al., 2008). Indeed, cells deficient in Ku80 have been shown to have significantly increased sensitivity to ionizing radiation after depletion of PARP1 further confirming its role in alt-NHEJ (Wang et al., 2006).

Interestingly, recent studies suggest PARP3 to have a defined role in DSB repair be NHEJ. Like PARP1, PARP3 has been shown to be activated by DNA DSB *in vitro* and to be recruited to DSB sites *in vivo* (Boehler et al., 2011b; Loseva et al., 2010; Rulten et al., 2011). Recently, PARP3 have been reported to ADP-ribosylate and interact with Ku80 and promote the recruitment of Ku70/80 to the laser-induced DNA breaks (Beck et al., 2014) Furthermore, depletion of PARP3 leads to the increased level of DNA damage-induced Mre11 phosphorylation as well as an increase in the general level of end-resection, suggesting PARP3 participates in repair pathway choice by favouring Ku70/80 directed canonical NHEJ, as opposed to PARP1 (Beck et al., 2014). Additionally, PARP3 has been shown to facilitate c-NHEJ by interaction with APFL (Rulten et al., 2011). As mentioned before, APLF has a PBZ domain which is responsible for its interaction with PAR *in vitro* and has been shown to be recruited to DNA damage sites *in vivo* (Li et al., 2010a; Rulten et al., 2008). Recently initial recruitment of APLF to DSBs has been reported to be dependent on the activity of PARP3 (Rulten et al., 2011). This in turn led to the subsequent

acceleration of recruitment of XRCC4/Ligase IV and promoted accurate ligation of the ends.

Thus, current findings suggest PARP1 and PARP2 to participate in the repair of single-strand DNA breaks and mainly play a role in the homologous recombination DSB repair pathway with PARP1 also playing a role in promoting alternative NHEJ whereas PARP3 is mainly involved in facilitating canonical NHEJ. However the precise role and molecular mechanisms of the function of ARTs in DSB repair still remains to be determined.

1.5 Dictyostelium discoideum as a model organism

1.5.1 Chromatin organization in *Dictyostelium*

Lower eukaryotes are widely used as model organisms for studying a variety of processes including the DNA damage response, transcription control, cell cycle regulation and many others (Mathiasen and Lisby, 2014; Nichols et al., 2015; Tissenbaum, 2015). Use of the social amoeba *Dictyostelium discoideum* in such studies has grown rapidly during the last decade as its full genome sequence, completed in 2005, revealed the presence of around 12,250 genes encoding proteins including many homologues of mammalian factors suggesting the potential of using *Dictyostelium* as a genetically tractable model (Eichinger et al., 2005).

Dictyostelium is a haploid organism containing a genome of 34Mb located on six chromosomes (Stevense et al., 2011). Similarly to higher eukaryotes *Dictyostelium* chromatin contains relaxed gene enriched regions as well as more compact clusters rich in *Dictyostelium* intermediate repeat sequences (DIRS) that thought to include centromeric regions. Indeed, DIRS have been shown to associate with centromeric histone CenH3, and

be enriched in the heterochromatin mark H3K9 methylation (Dubin et al., 2010), ref). Additionally, functional orthologues of the HP1 protein have been found in *Dictyostelium* and have also been shown to localise at the telomeric reagions (Kaller et al., 2006).

Orthologues of all four core histones and the linker histone H1 have been shown to be present in *Dictyostelium*. Histone H1 is encoded by a single gene and is expressed in cells as shown by mass spectrometry analysis of acid extracts of nuclear fractions (Hauser et al., 1995; Stevense et al., 2011). Histone H2A has been shown to have two major variants: H2AX and H2A.Z, where H2AX represents the majority of expressed H2A proteins ((Stevense et al., 2011), dictyexpress). Importantly, phosphorylation of H2AX on C-terminally located serine S150 have been shown to be present in *Dictyostelium in vivo* in response to DNA DSBs demonstrating the conservation of this DNA damage signalling modification (Hudson et al., 2005; Stevense et al., 2011). Histone H2B is encoded by three different genes representing three potential variants (Eichinger et al., 2005). However, the major expressed H2B variant is H2Bv3 whereas the other two variants represent a hybrid of an *h2b* domain linked with other domain sequences and are not expressed in cells as judged by mRNA levels (dictyexpress). With use of mass spectrometry post-translational methylation and acetylation of lysines have been identified on histone H2Bv3 although their functional significance has not been revealed yet (Stevense et al., 2011). The most rich in variants is histone H3. It is encoded by five different genes proposed to represent five variants: H3a, H3b, H3c, H3v1 and 2. Expression of H3a and b variants has been shown by mass spectrometry although H3c and H3v2 have not been detected (Stevense et al., 2011). H3v1 has recently been shown to be an ortholog of centromeric histone CenH3 (Dubin et al., 2010). Interestingly, critical post-translational modifications involved in transcription have been identified on *Dictyostelium* H3 (Stevense et al., 2011). Thus, trimethylation of H3K4 and H3K79 dimethylation, marks of actively transcribed

chromatin, have been shown to be performed by Set1 and Dot1 methyltransferases respectively and their activity has been demonstrated to be important for cell differentiation and development (Chubb et al., 2006; Muller-Taubenberger et al., 2011). Additionally, acetylation of H3 K9, 14, 18, 23 and 27 have also been demonstrated by mass spectrometry (Stevense et al., 2011). Finally, *Dictyostelium* histone H4 is encoded by two genes responsible for the expression of identical proteins (dictybase). Lysine acetylation has also been demonstrated to be present on H4 including of lysine K17 which could potentially have similar functions to mammalian H4K16 acetylation (Stevense et al., 2011). It is important to mention that all core histones and histone variants are encoded by a single copy gene as opposed to arrays of genes encoding mammalian histone variants enabling genetic manipulations in *Dictyostelium* and facilitating its employment as a model organism to study chromatin dynamics (dictybase).

1.5.2 DNA double-strand break repair in *Dictyostelium*

Alongside conservation of chromatin components, core factors of both DNA double-strand break repair pathways are also conserved in *Dictyostelium* (Table 1). Vegetative *Dictyostelium* cells have been shown to be predominantly in the G2 phase with a short S phase interval and therefore perform DNA repair predominantly through HR pathway whereas germinating spores are more dependent on the NHEJ (Muramoto and Chubb, 2008), (Hudson et al., 2005), . This observation is supported by the requirement of HR factors for survival of vegetative cells as deletions of RAD51 and other core components result in cells lethality (Hudson et al., 2005; Zhang et al., 2009). Interestingly, disruption of the gene encoding the Exo1 nuclease doesn't lead to cell lethality but does sensitise cells to the DNA DSB-inducing agent bleomycin (Hsu et al., 2011). This is consistent with HR being the major DSB repair pathway in growing cells but perhaps suggests, as in other cells, the involvement of at least one other nuclease in the end resection process (Raynard

et al., 2008). However, such sensitivity of *Dictyostelium* to the disruption of HR components makes it difficult to use this organism for further investigation of HR mechanisms alone.

Homo sapiens	***S. cerevisiae***	***D. discoideum***
Ku70	Hdf1	DDB0232001
Ku80	Hdf2	DDB0232002
DNA-PKcs	-	DDB0229336
XRCC4	Lif1	DDB0204503
DNA ligase IV	Dnl4	DDB0184548
Artemis	-	DDB0169391
Rad50	Rad50	DDB0184568
Mre11	Mre11	DDB0191996
NBS1	Xbs1	-
Polβ	Pol4	DDB0232376
PARP1-3	-	DDB0214818, DDB0185172

Table 1. Conservation of key DNA double-strand break repair factors in *Dictyostelium*. Adapted from (Hsu et al., 2006).

By contrast, the NHEJ pathway has been studied in *Dictyostelium*. Interestingly, together with key NHEJ components such as Ku70/80, XRCC4 and Ligase IV, two of the initial NHEJ components DNA-PKcs and an ortholog of Artemis, Dclre1, that were previously thought to be present only in vertebrate organisms have been identified in *Dictyostelium* (Table 1), (Block and Lees-Miller, 2005; Hsu et al., 2011; Hudson et al., 2005; Muramoto and Chubb, 2008). In agreement with the operation of NHEJ in hatching spores, the Ku70/80 heterodimer has been shown to be critical for the survival of germinating spores but not vegetative cells after exposure to bleomycin (Hudson et al., 2005). DNA-PKcs has also been shown to be required for bleomycin sensitivity of germinating spores and, similarly to mammalian cells, DNA-PKcs is responsible for DNA DSB-induced H2AX phosphorylation in germinating spores (Hudson et al., 2005). However, more recent studies showed the functionality of NHEJ in vegetative cells too. Restriction enzyme plasmid integration of non-genomic sequences into the *Dictyostelium* genome in vegetative cells is dependent on the presence of DNA-PKcs and Ku80 and therefore performed by NHEJ (Hsu et al., 2011). Furthermore, disruption of the *dclre1* gene led to the slower kinetics of DSB repair in vegetative cells after exposure to bleomycin as judged by γ-H2AX decay.

The observation that the abolishment of the latter factor leads to a delay in the break repair suggests that NHEJ is normally involved in the response of vegetative cells to DNA damage. However the lack of sensitivity to DSBs following disruption of key NHEJ factors suggests that, in the absence of NHEJ, the breaks can be repaired by other pathways. These observations propose *Dictyostelium* can serve as a model not only for DNA repair pathway mechanisms but also for DNA DSB repair pathway choice. Indeed, the observed delayed DSB repair phenotype of *dclre1-null* cells can be rescued by simultaneous disruption of *ku80* proposing that, similarly to mammalian cells, *Dictyostelium* Ku70/80 plays a role in the choice DSB repair pathway (Hsu et al., 2011; Pierce et al., 2001).

Recently, the regulation of Ku retention on chromatin has been proposed to be dependent on ADP-ribosylation, revealing another level of DSB repair regulation in *Dictyostelium* (Galande and Kohwi-Shigematsu, 1999; Paddock et al., 2011).

1.5.3 ADP-ribosylation in *Dictyostelium*

By contrast to yeast, ADP-ribosylation is conserved in *Dictyostelium* (Rajawat et al., 2007; Rickwood and Osman, 1979). A protein containing ADP-ribosyltransferase activity was identified, purified and characterized more than 20 years ago (Auer et al., 1995; Kofler et al., 1993). It was shown to be activated and perform auto-poly-ADP-ribosylation in the presence of damaged DNA *in vitro* and further increase enzyme activity by the addition of histone H1 to the reaction mixture (Auer et al., 1995). More recently with the sequencing of the whole genome, 15 genes encoding putative ART catalytic domains have been identified (Citarelli et al., 2010; Otto et al., 2005; Pears et al., 2012). Out of these four, namely Adptr1a, Adprt1b, Adprt2 and Adprt4 possess a strong similarity in the domain structure and organisation to the mammalian ARTs involved in DNA repair (Otto et al., 2005; Pears et al., 2012). Furthermore, homologues of ADP-ribosyl degradation enzymes PARG and MacroD1/2 have also been identified in *Dictyostelium* (Perina et al., 2014).

The role of some of these ARTs in DNA damage repair has been demonstrated. Firstly, protein poly-ADP-ribosylation has been shown to occur in *Dictyostelium* in response to oxidative stress, DNA single- and double-strand break inducing agents (Couto et al., 2011; Rajawat et al., 2007). Further, Adprt1b and Adprt2 have been demonstrated to be required for cell resistance to DNA single-strand break inducing agents methyl methanesulfonate (MMS) and H_2O_2 as their disruption increased cell sensitivity to the indicated agents (Couto et al., 2011). This is reminiscent of the requirement for PARP1 and PARP2 for resistance to SSB in mammalian cells (Le Page et al., 2003; Menissier de Murcia et al., 2003; Schreiber et al., 2002). However, loss of Adprt1a has no effect on survival to MMS

(Couto et al., 2011). Interestingly, cells lacking Adprt2 still show DNA damage-induced ADP-ribosylation after exposure to the DSB inducing agent phleomycin similar to parental Ax2 cells, suggesting Adprt2 plays a role predominantly in SSB repair. However, *adprt2*$^{-}$ and to a greater extend *adprt1a*$^{-}$ strains have decreased level of the ADP-ribosylation foci formation in response to phleomycin treatment indicating their involvement in DSB repair mechanisms (Couto et al., 2011). Indeed, involvement of Adprt1a in NHEJ pathway have been suggested to occur via retention of Ku70/80 to the DSB as either deletion of *adprt1a* or deletion of the PAR-binding zinc finger (PBZ) domain of Ku70 resulted in reduced enrichment of Ku80 to chromatin following phleomycin induced DNA damage and reduced levels of NHEJ judged by efficiency of REMI (Couto et al., 2011). Furthermore, Adprt1a has been shown to contribute to the DNA damage signalling following MMS treatment in the absence of Adprt2 suggesting an overlap in functions of these two ARTs (Couto et al., 2013). Altogether, these findings suggest that, similarly to mammals, ADP-ribosylation have an active role of in DNA damage repair in *Dictyostelium* although more detailed investigation of the mechanism of its action is required.

1.6 Aims

Histone variants and histone post-translational modifications have been studied extensively and shown to have an important role in regulating cellular processes including the DNA damage response. Whilst there is much known about the involvement of core histones in the DNA repair process, the role of particular histone variants (apart from H2AX) remains unclear. One of the histone H3 variants H3.3 has been recently shown to be selectively recruited to sites of UV damage in mammals suggesting a potentially distinct role in DNA damage repair (Adam et al., 2013). This question will be addressed in this work with the use of *Dictyostelium* strains lacking two out of the three histone H3 variants – H3b and H3c (H3b/c$^{-/-}$) by testing:

- Resistance of H3b/c$^{-/-}$ cells to DSBs induced by chemical agent phleomycin.
- The ability of H3b/c$^{-/-}$ cells to signal and repair DSBs caused by phleomycin.
- Dynamics of histone H3 variant association with the site of double-strand break by developing an assay to introduce a site-specific break into the *Dictyostelium* genome.

Various histone post-translational modifications are known to participate in the DNA damage response by facilitating recruitment of factors of the DNA repair machinery as well as damage-induced remodelling of chromatin. All four mammalian core histones have been found to be ADP-ribosylated in response to DNA damage both *in vitro* and *in vivo*, however the functional significance of such modification is still unknown. In this work the ADP-ribosylation status of *Dictyostelium* core histones and any function in DNA DSB repair will be investigated. The ability of Adprt1a, the major ART involved in DNA DSB repair, to ADP-ribosylate core histones will be addressed by:

- Biochemical characterisation of the Adprt1a auto-modification activity *in vitro*.
- ADP-ribosylation *in vitro* of recombinant *Dictyostelium* core histones H2AX, H2B, H3a, H3b and H4 by Adprt1a.
- Mapping modification sites of the discovered histone(s) by deletion and point mutation analysis.
- Investigating *in vivo* the validity of the histone modification site(s) mapped *in vitro* by determining the ADP-ribosylation status of epitope-tagged histone(s) lacking the ADP-ribosylation acceptor sites.

If verified, these strains would facilitate investigation of the significance of the histone ADP-ribosylation in DNA repair process.

2 Materials and Methods

2.1 Materials

All solutions were prepared using distilled water and sterilized either by autoclaving for 15 min at 125^0C or filtration through 0.2µm filter (Nalgene).

2.1.1 Solutions and media

SM agar

1% bactopeptone

56mM glucose

0.1% yeast extract

16mM KH_2PO_4

5.5mM K_2HPO_4

4mM $MgSO_4$

1.7% agar

Autoclaved

HL5

53mM maltose

1.4% bactopeptone

0.7% yeast extract

4mM Na_2HPO_4

3.5mM KH_2PO_4

340µM dihydrostreptomycin sulphate

74µM vitamin B12

82µM biotin

532μM riboflavin

Adjusted to pH6.5

Autoclaved

KK2

19mM KH_2PO_4

3.6mM K_2HPO_4

Autoclaved

LB agar

1% bactotryptone

0.5% yeast extract

85mM NaCl

1.5% agar

Autoclaved

LB broth

1% bactotryptone

0.5% yeast extract

85mM NaCl

Autoclaved

2xSDS gel loading buffer

50mM Tris pH6.8

4% SDS

20% glycerol

0.2% bromophenol blue

100mM dithiothreitol

SDS-PAGE Running buffer

25mM Tris

250mM Glycine

Adjusted to pH8.3

0.1% SDS

SDS-PAGE Transfer buffer

50mM Tris

500mM Glycine

Adjusted to pH8.3

0.1% SDS

20% methanol

Towbin buffer

25mM Tris

192mM Glycine

Adjusted to pH8.3

20% methanol

Phosphate-Buffered Saline (PBS)

137mM NaCl

2.7mM KCl

10mM Na_2HPO_4

1.8mM KH_2PO_4

Adjusted to pH7.4

Autoclaved

Tris-Buffered Saline (TBS)

2.48mM Tris

250mM Glycine

Adjusted to pH8.3

Autoclaved

Chemiluminescent detection reagent (ECL)

Solution 1:

10mM Tris pH8.5

0.386mM P-coumaric acid

2.5mM luminal

Solution 2:

10mM Tris pH8.5

0.19% H_2O_2

2.2 Methods

2.2.1 *Dictyostelium* cell culture and assays

2.2.1.1 General cell culture

Dictyostelium discoideum cells were grown on SM agar plates in association with *Klebsiella aerogenes* or axenically in HL5 media (Ashworth and Quance, 1972) containing

0.25 mg/ml streptomycin in shaking suspension at 220rpm or on Petri dishes at 22^0C. Ax2 strain (from Jonathan Chubb) was used as a wild-type and parental cell line. *H3b/c*$^{-/-}$ strain was generated in the lab previously by Dr. D-W. Hsu (Hsu et al., 2012).

2.2.1.2 Electroporation

Dictyostelium cells were harvested during exponential growth ($2x10^6$ – $6x10^6$ cells/ml), washed three times with the ice-cold electroporation buffer (20mM HEPES, 50mM KCl, 10mM NaCl, 1mM $MgSO_4.7H_2O$, 5mM $NaHCO_3$, 1mM $NaH_2PO_4.2H_2O$, pH=7.0) and resuspended in the same buffer at a density of $5x10^6$ cells/ml. 7μg of the required DNA construct was added to the cells in a chilled 1-mm gap electroporation cuvette (BioRad). Cells with constructs were then incubated on ice for 5 min followed by direct exposure to two consecutive pulses of 0.65 kV with a capacitance of 25 μF with 5 second recovery between pulses. Cells were left on ice for 5 min and then plated onto a 9cm dish containing 10ml of HL5 media. 10μg/ml Blasticidin was added the next day to select for transformants. Cells were selected for 7-10 days at 22°C and then harvested for further experiments.

2.2.1.3 Generation of gene disruption strains

Dictyostelium cells were electroporated with the disruption construct as described above and were resuspended in 50ml of HL5. Cell suspensionss were then plated onto the 96-well plates either undiluted or at a 1:10, 1:100 and 1:1000 dilutions. 10μg/ml Blasticidin was added the next day to each well. Cells were left for 14-18 days until the colonies start to appear. Blasticidin resistant colonies were then confirmed by colony PCR as described in 2.2.2.2 and successful clones were expanded for further confirmation.

2.2.2 Molecular biology and *in vitro* assays

2.2.2.1 DNA manipulations and PCR

Plasmid DNA was purified from *E.coli* using NucleoSpin Plasmid mini- or midi-purification kit (MN) by following the manufacturer's protocol.

PCR was performed using Taq DNA Polymerase mix (PCRBio) or Hi-Fi Polymerase mix (PCRBio) by following the manufacturer's protocols. Primer sets were ordered from Sigma Aldrich. Primer sequences are listed in Appendix.

Plasmid DNA ligation was performed using T4 DNA ligase (NEB) using the manufacturer's protocol. Ligation of PCR products to pJET vector were performed using CloneJET PCR cloning kit (Thermo Scientific).

Sequences of the PCR and ligation products were confirmed using the sequencing service from SourceBioscience.

Genomic DNA was purified from *Dictyostelium* cells using Wizard genomic DNA purification kit (Promega) by harvesting $5x10^6$ cells and then following the manufacturer's protocol.

2.2.2.2 Colony DNA PCR

Blasticidin resistant *Dictyostelium* colonies were lysed by resuspension in lysis buffer (50mM KCl, 10mM TRIS pH8.3, 2.5mM $MgCl_2$, 0.45% NP40 and 0.45% Tween 20) containing Proteinase K (0.8µg/µl) followed by its inactivation at 95^0C for 2 min and BSR cassette integration was investigated by PCR using either gene or BSR-cassette primers (Appendix 1).

2.2.2.3 Western Blot analysis

Unless otherwise specified western blot analysis were performed by separating samples boiled in SDS loading buffer by SDS-PAGE (8, 12 or 18%) using standard procedures followed by transferring to PVDF membrane for 4h or overnight. The membrane was then soaked in methanol, air dried for 20 min and blocked with 5% milk for 30min. After blocking, the membrane was subjected to the indicated primary antibody diluted in 5% milk (Table 2) for 1 hour followed by 3 washes with TBST buffer. The same procedure was performed subsequently for the secondary antibody incubation. The presence of the secondary antibody was detected by incubating membrane with ECL solution followed by exposure to the X-ray film (GE Healthcare).

Primary antibody	Manufacturer	Concentration
α-Flag-M2 (mouse, monoclonal)	Sigma	1:1000
α -penta-His (mouse, monoclonal)	Qiagen	1:2000
α -HA (rabbit, polyclonal)	Invitrogen	1:4000
α –Myc (mouse, monoclonal)	Santa Cruz	1:2000
α -Actin (goat, polyclonal)	Santa Cruz	1:1000
α-Gamma-H2AX(rabbit, polyclonal)	Abcam	1:2000
α -H2B (sheep, serum)	Generated in the lab (unpublished)	1:1000
α -H3(goat, polyclonal)	Abcam	1:2000
α -Ku80 (goat, serum)	Generated in the lab (Couto et al., 2011)	1:1000
α -PAR (rabbit, polyclonal)	Trevigen	1:500
anti-pan-ADP-ribose binding reagent (rabbit)	Millipore	1:1000
anti-poly-ADP-ribose binding reagent (rabbit)	Millipore	1:1000

Table 2. Antibody and dilutions used for the Western blot analysis.

2.2.2.4 Membrane stripping for Western blot

For reprobing the PVDF membrane with a second antibody, membrane were stripped by incubating with the 100mM β-mercaptoethanol, 2% SDS and 62.5 mM Tris-HCl pH6.7 at 50^0C for 30 min followed by two 10min washes with 1xPBST buffer. Membranes were then incubated with appropriate blocking solution before reprobing.

2.2.2.5 His-tagged protein purification

His-tagged Histone proteins were expressed by transforming the expression construct to *E.coli* M15 strain and inducing the expression in appropriate amount of culture with 0.1mM IPTG for 4h at 22^0C. Cells were then harvested by centrifugation at 5000rpm for 30 min and resuspended in ice-cold column buffer (50mM Tris-HCl pH8, 150mM NaCl, 10% glycerol, 30mM Imidazole) complemented with protease inhibitor cocktail tablet (Roche) and 1mM PMSF (Sigma). Cell lysis was performed by sample sonication on ice with 20% amplitude four times for 30sec with 2 min breaks. Soluble proteins were then collected by centrifugation of lysates at 15000rpm for 30min and collecting the supernatant. The latter was filtered through a 0.45µm pre-filter (Millipore) and loaded onto a column containing prewashed Ni-NTA beads (Qiagen). Beads were then washed three times with 10x bed volume column buffer containing 30mM, 50mM and 100mM Imidazole (Sigma) respectively. Proteins of interest were eluted using column buffer substituted with 200mM Imidazole, then dialyzed against storage buffer (50mM Tris-HCl pH8, 10% glycerol), snap frozen in liquid nitrogen and stored at -80^0C.

His-tagged Adprt1a and Adprt1a^{H789AY823A} were purified in a similar way but following lysis using Bugbuster (Merck) instead of the sonication step to avoid the activation of the enzyme by sheared DNA during the purification process. IMAC buffer (50mM HEPES

pH=8, 500mM NaCl, 10% glycerol, 1mM DTT, 1mM Imidazole) was used instead of the column buffer.

2.2.2.6 ADP-ribosylation and de-ADP-ribosylation assays

100ng of recombinant His-tagged Adprt1a was mixed with 75μM NAD^+, 25μM Biotinylated NAD^+ (Trevigen) in 50mM Tris-HCl pH8 and 2mM $MgCl_2$ either with or without 100μg/ml of sheared salmon sperm DNA (Sigma). 100ng of recombinant His-tagged *Dictyostelium* histone were added where indicated. Reaction mixtures were incubated at room temperature for 30min. The reaction was stopped by adding 2xSDS loading buffer and boiling for 5 min. Samples were then analysed by Western blot. For ADP-ribosylation signal detection PVDF membrane with proteins was soaked in methanol and air-dried for 20 min. After blocking with 1% BSA for 2h membrane was incubated with HRP-conjugated Streptavidin (Sigma) diluted to 1:5000 with PBST. The membrane was then washed six times with PBST and subjected to ECL for the signal detection.

Where indicated, 100nM ^{32}P-labeled NAD^+ was used instead of Biotinylated NAD^+. In this case, the ADP-ribosylation status of proteins was assessed by separating samples by SDS-PAGE, vacuum-drying the latter at 80^0C for 1h and exposing to the X-ray film overnight.

For de-ADP-ribosylation assays, ADP-ribosylation reactions using Biotinylated NAD^+ were terminated by adding 10mM 3-aminobenzamide. Then 3μl of 2.4μM MacroD1 protein (kindly provided by Prof. Keith Caldecott, Sussex) or 9nM PARG enzyme (Trevigen) were added to the reaction either undiluted or diluted 1:5 and 1:10. Mixtures were incubated at 37^0C for 30min and the de-ADP-ribosylation reaction was stopped by adding 2xSDS loading buffer and boiling for 5 min. ADP-ribosylation status was then assessed by Western blot as described above.

2.2.3 Phenotypic assays

2.2.3.1 Chromatin Enrichment

Dictyostelium cells were harvested at the exponentially growing stage and resuspended at a density of $1x10^7$ cells/ml in HL5. Phleomycin was added to cells at a dose of 300 μg/ml and incubated for 1h on a rotating wheel at room temperature. Cells then were washed 3 times with KK2 buffer and resuspended in Extraction buffer (50mM HEPES pH7.5, 150mM NaCl, 1mM EDTA, 200 μM DEA, protease inhibitor cocktail 2,3 Roche) containing 0.1% Triton-X100 at a density of $5x10^7$ cells/ml. Cells were incubated at 4^0C for 15 min followed by centrifugation at 14,000g for 3 min. The resulting pellet was resuspended in Extraction buffer and the extraction procedure was then repeated one more time. The resulting pellet was resuspended in extraction buffer containing 200 μg/ml RNAse A and was then incubated on a rotation wheel for 30 min at room temperature followed by collection of the chromatin pellet by centrifugation at 14,000g for 3 min. The resulting chromatin pellet was resuspended in 2xSDS-loading buffer and boiled for 5 min.

2.2.3.2 Immunoprecipitation from chromatin

Chromatin pellets were obtained as described in section 2.2.3.1 and resuspended in 2xSDS buffer (100mM Tris-HCl pH6.8, 4% SDS) and boiled for 10 min. After 10 times dilution of the resulting mixtures with IP buffer (50mM Tris pH8, 200mM NaCl, 1mM EDTA, 1mM DTT, 10% glycerol, 1% Triton X-100, phosphatase inhibitor cocktail 2 and 3 (Roche), 200 μM DEA, 500 μM benzamide, protease inhibitor cocktail tablet (Roche). Anti-Flag M2 affinity beads (Sigma) were added and the solution was incubated on a rotating wheel for 1h at 4^0C. Beads were then collected by centrifugation at 1000rpm for 2 min and washed three times with IP buffer. Washed beads were resuspended in 2xSDS

loading buffer, boiled for 10 min and centrifuged at 1000rpm for 2 min. The resulting supernatant was loaded onto an SDS-Polyacrylamide gel for subsequent analysis. (Couto et al., 2011).

2.2.3.3 Acid extraction to enrich for histones

$2x10^8$ exponentially growing *Dictyostelium* cells were harvested and washed with ice cold KK2 buffer. Cells then were resuspended in lysis buffer (50mM Tris-HCl pH8, 10mM NaCl, 3mM $MgCl_2$, 3mM $CaCl_2$, 0.5M D-Sorbitol, 0,6% Triton-X, 10mM Sodium butyrate, Phosphatase inhibitor cocktail 2,3 Roche, 200 μM DEA, protease inhibitor cocktail tablet) at a density of $2x10^8$ cells/ml and incubated on rotating wheel at 4^0C for 10 min. The nuclear pellet was collected by spinning down lysates at 5,000 rpm for 5 min. The pellet was then resuspended in lysis buffer containing 4M Urea and 10 μg/ml β-mercaptoethanol and incubated on a rotation wheel for 10 min at 4^0C followed by 5 min centrifugation at 5,000 rpm. The resulting nuclear pellet was resuspended in 0.4M HCl and incubated for 1h at 4^0C. The extracts were centrifuged at 13,000 rpm for 15 min and the resulting supernatant enriched in histones was transferred to a fresh tube. Acetone was added and the mixtures were left at -20^0C overnight. Histones were then pelleted by centrifuging at 13,000 rpm for 15 min at 4^0C. The pellet was washed twice with ice cold acetone followed by air drying. Resulting pellets, enriched in histones, were then resuspended in 8M Urea with 10 μg/ml β-mercaptoethanol and were used for subsequent experiments. (Hudson et al., 2005).

2.2.3.4 Histone immunoprecipitation

Acid extracts from cells expressing 3xFlag-tagged histones were dialyzed with 20mM Tris-HCl pH8 for 2h and then diluted 10 times with IP buffer (50mM Tris pH8, 200mM

NaCl, 1mM EDTA, 1mM DTT, 10% glycerol, 1% triton X-100, phosphatase inhibitor cocktail 2,3 (Roche), 200 μM DEA, 500 μM benzamide, protease inhibitor cocktail tablet (Roche). Anti-Flag M2 affinity beads (Sigma) were added and the mixture was incubated on a rotating wheel for 1h at 4^0C. Subsequent procedures were carried out as described in 2.2.3.3.

2.2.3.5 REMI (Restriction Enzyme Mediated Integration)

Exponentially growing *Dictyostelium* cells were prepared for transformation as described in 2.2.1.3 and electroporated with BSR cassette with or without BamHI and were then transferred to 96-well plates containing 10ml of HL5. The BSR cassette was prepared by restriction digest of the pLPBLP plasmid using BamHI restriction endonuclease. Blasticidin at 10μg/ml was added to plates on the next day. Blasticidin resistant colonies were counted after 10 days and REMI efficiency was addressed by the number of colonies from cells electroporated with BamHI relative to no enzyme sample. (Hsu et al., 2011).

Alternatively the BSR cassette was excised from the pLPBLB-2n plasmid using NotI restriction endonuclease cleavage and electroporated into Ax2 cells with or without 75U of NotI. 50ml aliquots of undiluted or 10 and 100 times diluted samples were prepared and plated into 96-well plates with 100μl sample per well. 10μg/ml Blasticidin was added to all wells on the next day. After 2 weeks Blasticidin resistant colonies were counted.

2.2.3.6 Analysis of γ-H2AX by Immunofluorescence

Exponentially growing *Dictyostelium* cells were harvested and resuspended at a density of $1x10^6$ cells/ml in HL5 media. Phleomycin was added at concentration of 250μg/ml and

samples were left in shaking suspension at 100 rpm at 22°C for 1 hour. Cells were then washed three times with HL5 and resuspended at a density of $1x10^6$ cells/ml in HL5 with shaking (100 rpm at 22°C). $1x10^6$ cells were removed at the time points indicated and left to adhere to polylysine-coated cover slips for 10 minutes prior to incubation in pre-extraction buffer (10 mM PIPES pH 6.8, 300 mM sucrose, 3 mM $MgCl_2$, 20 mM NaCl, 0.5% Triton X-100) for 5 minutes. Cells were washed in Tris-buffered saline (TBS) and fixed for 5 minutes in 70% ethanol. After removal of ethanol, cover slips were washed once in ice-cold methanol, twice in TBS and blocked with 10% swine serum in TBS for 1 hour. Samples were subsequently incubated for 1 hour with anti-γ-H2AX (Abcam) diluted to 1:1000 in blocking solution and washed three times with TBS before incubation for 1 hour with anti-rabbit labeled with TRITC (DAKO) diluted at 1:4000 in blocking solution. Cover slips were washed three times with TBS and mounted using Vectorshield containing DAPI (Vector Labs). Immunofluorescence was detected using an Axioscope 2 fluorescent microscope equipped with Axiovision imaging software (Zeiss). At least 200 cells were counted for each point.

2.2.3.7 Sensitivity to DSB assays

Dictyostelium cells were harvested at an exponentially growing stage and resuspended at a density of $1x10^6$ cells/ml in HL5 media. Phleomycin was added to cells at the indicated concentrations in shaking suspension at 100 rpm at 22°C for one hour. To assess survival rates cells were diluted in KK2 to a density of $1x10^4$ cells/ml. Replicates of 250 cells were plated on 15 cm SM agar plates in association with *Klebsiella aerogenes*. Survival was assessed by counting the number of colonies 3, 4 and 5 days after plating.

3 Role of histone H3 variants in DNA damage response in *Dictyostelium*

3.1 Introduction

Chromatin plays an important role in the DNA damage response by remodeling its structure around the damaged region (Chubb and Rea, 2010; House et al., 2014). However, investigation of the role of particular histone variants (other than H2AX) remains challenging. Mammalian cells contain three main histone H3 variants each encoded by arrays of genes which hinders performing genetic manipulation to investigate their role. It is generally thought that H3.3 is enriched at active genes and contains higher levels of modifications associated with active genes such as H3K4me3 and H3 acetylation whereas H3.1/3.2 are enriched in non-active regions of the genome and in modifications associated with gene silencing such as H3K9me2 (Hake et al., 2006; McKittrick et al., 2004). Histone H3.3, for example, has been found to incorporate into the promoter regions of actively transcribed genes and also at so-called nucleosome-free regions together with H2A.Z (Jin et al., 2009). However, H3.3 is also enriched in telomeres and some heterochromatic regions (Szenker et al., 2011). Recently histone H3.3 has been reported to be recruited to sites of UV damage suggesting a potential role in the DNA damage response (Adam et al., 2013).

Lower organisms contain either several H3 variants, like *Drosophila* or *Caenorhabditis elegans*, and also have several copies of each gene (Ahmad and Henikoff, 2002; Ooi et al., 2006), or contain only one histone H3, like *Saccharomyces cerevisiae* and *S. pombe* (Dion et al., 2007). *Dictyostelium*, however, like mammals contains genes encoding three H3 variants but each is encoded by a single gene. It has been shown that the gene encoding H3c gives rise to only a very low level of mRNA compared to H3a and H3b as determined

by RNA seq analysis (dictybase) and mass spectrometry of histones is consistent with this variant being expressed at very low levels in growing cells (Hsu et al., 2012; Stevense et al., 2011). Expression of the H3b variant protein has been shown to be 32% of that of H3a (Hsu et al., 2012). All *Dictyostelium* histone H3 variant are resemble histone H3.3 class protein. Histone H3a variant differs from H3b only with presence of three additional amino acids at the N-terminal tail (Hsu et al., 2012). Post-translational modifications of histone H3 associated with transcription or chromatin architecture are also conserved in *Dictyostelium* together with enzymes responsible for the modifications, though often in lower numbers than in mammals, again facilitating genetic manipulation (Stevense et al., 2011). Cells containing disruption of the genes encoding two of H3 variants H3b and H3c and also H3b/c double-disruptants are available (Hsu et al., 2012). This offers a unique opportunity to investigate the role of histone H3b and c variants in DNA DSB break repair.

3.2 Results

3.2.1 *H3b/c*$^{-/-}$ strains are not sensitive to DNA double-strand breaks

In order to investigate the importance of histone H3b and c variants in DSB repair during vegetative cell growth of *Dictyostelium* first the sensitivity of cells disrupted in the *H3b* and *c* genes (*H3b/c*$^{-/-}$ cells) to DNA DSB induction was tested. This sensitivity assay has been used previously to investigate the sensitivity of *Dictyostelium* strains lacking DNA repair proteins such as *exo1, ku80, dnapkcs* or *dclre1* to DSB (Hsu et al., 2011; Hudson et al., 2005). Thus, *H3b/c*$^{-/-}$ cells were treated with the DNA DSB inducing agent phleomycin for 1 hour before diluting and plating on lawns of *K. aerogenes* and the number of surviving cells assessed 3-4 days after treatment. Surprisingly, the *H3b/c*$^{-/-}$ cells showed no additional sensitivity to phleomycin in comparison to the parental Ax2 cell line but if anything had a higher level of survival (Fig. 3.1). This indicates higher resistance of

Dictyostelium cells lacking H3b and c variants to DSBs and can serve as a marker that DNA repair is altered in these cells.

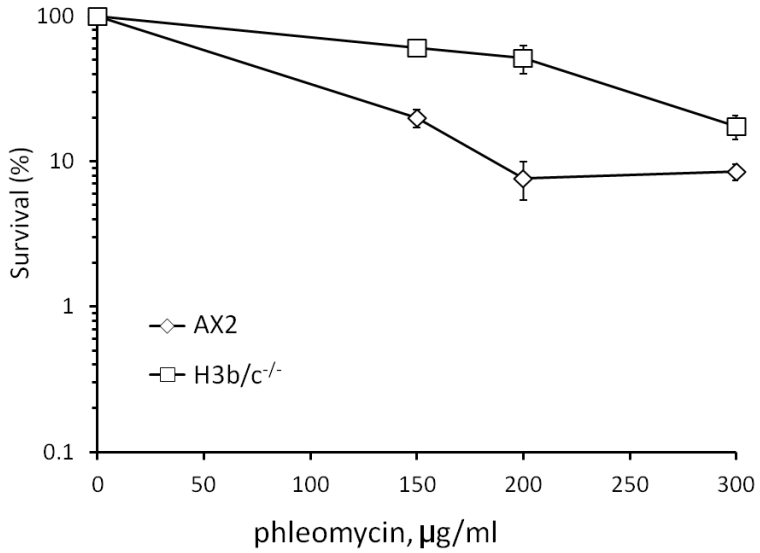

Figure 3.1. Sensitivity of *H3b/c*$^{-/-}$ cells to DSBs. Cells were treated with the indicated concentrations of phleomycin for 1 hour. Cells were diluted and 250 cells were plated on agar plates in association with *Klebsiella* and cell survival assessed by counting the number of colonies apparent after 3-4 days. The percentage of surviving cells relative to untreated is shown. Error bars represent three independent experiments.

3.2.2 *H3b/c*$^{-/-}$ cells are normal in γ-H2AX signalling and decay

Loss of a number of known DNA repair proteins, such as Ku70, Ku80, DNA-PKcs does not lead to overt sensitivity to DNA DSB in growing *Dictyostelium* cells (Hudson et al., 2005). Some strains however show differences in their rate of repair, such as *dclre1*$^{-}$ cells (Hsu et al., 2011). The ability of *H3b/c*$^{-/-}$ cells to signal DNA DSB was assessed. Histone H2AX is phosphorylated on Ser139 to form γ-H2AX in response to DNA damage and in particular DNA DSBs (Rogakou et al., 1998). Therefore the level of γ-H2AX can be used as a marker of the level of DSBs present and the ability of cells to signal DNA damage. Thus, the kinetics of γ-H2AX appearance and disappearance in *H3b/c*$^{-/-}$ cells were monitored following induction of DSBs with phleomycin. In order to investigate the accumulation of breaks, cells were treated with phleomycin and γ-H2AX levels determined at several times up to 2 hours by Western blot using an antibody specific for this modification. For all time points *H3b/c*$^{-/-}$ cells show similar levels of γ-H2AX as are seen in parental Ax2 cells (Fig. 3.2 A). This indicates no significant role for histone H3b and c variants in accumulation of γ-H2AX in response to phleomycin in *Dictyostelium* cells. Therefore phosphorylation of H2AX is not dependent on the presence of H3b or H3c.

Although *H3b/c*$^{-/-}$ cells show normal accumulation of γ-H2AX, they could be defective in recovery after DSB induction. To investigate this *H3b/c*$^{-/-}$ and parental Ax2 cells were treated with phleomycin for 1h and, following removal of the damaging agent, γ-H2AX nuclear foci were observed using immunofluorescence. Phleomycin treatment caused γ-H2AX foci induction in more than 90% of cells in both strains. This was accompanied by a gradual decrease in the number of positive cells after several hours of recovery (Fig. 3.2 B). However, both initial and prolonged rates of γ-H2AX decay were comparable in both cell types suggesting that general DSB repair rates are similar and that cells lacking histone H3b and c variants are normal in or timely repair of double-strand breaks.

A.

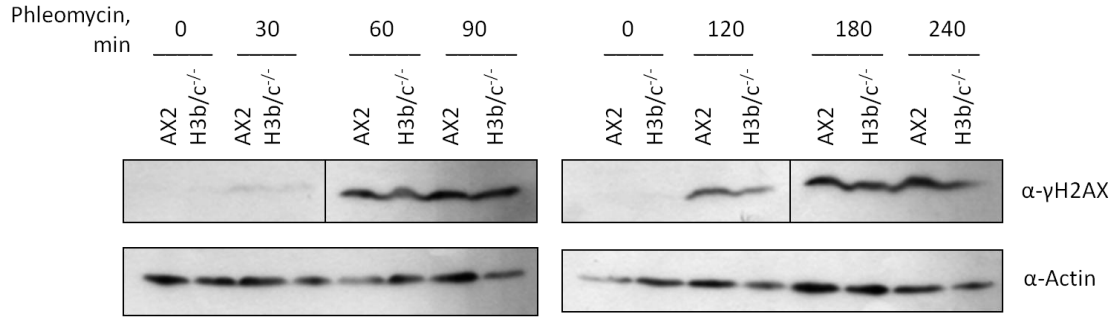

B.

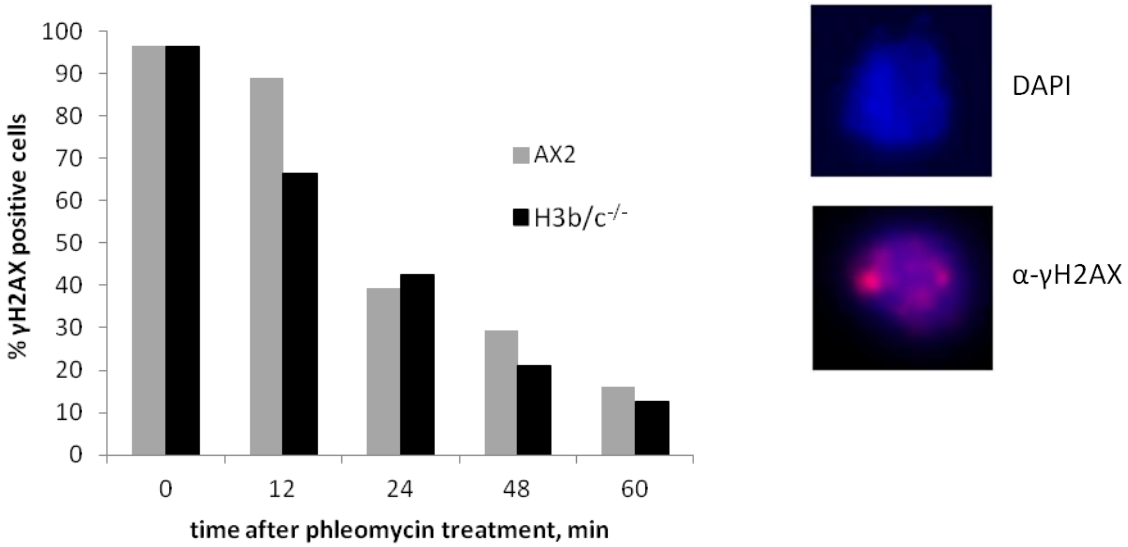

Figure 3.2. γ-H2AX signalling and decay in response to DSB in *H3b/c*$^{-/-}$ cells. A. γ-H2AX induction following phleomycin treatment. Cells were treated with 200μg/ml phleomycin for the time indicated and then whole cell lysates resolved by SDS PAGE and analysed by Western blot using an antibody specific for γ-H2AX. Actin was used to control for loading of the samples. B. Recovery of γ-H2AX after phleomycin treatment. Cells were treated with 100μg/ml phleomycin for 1h, washed and the levels of γ-H2AX were determined after the indicated time intervals by immunofluorescence using an antibody specific for γ-H2AX and DAPI to stain DNA to mark the location of nuclei. At least 200 cells were analysed at each time point. One experiment representative of at least three is shown. Typical images of cells scored as positive (upper) and negative (lower) for γ-H2AX staining are shown.

3.2.3 H3 b and c variants are not essential for NHEJ

The general DNA DSB repair rate is not reduced in *H3b/c*$^{-/-}$ cells as judged by γ-H2AX induction and decay following DNA damage. However, *H3b/c*$^{-/-}$ cells show a higher resistance to DSBs than their parental strain. Higher resistance of cells to DSB has been observed previously for vegetative *Dictyostelium* cells lacking one of the ADP-ribose polymerases, Adprt1a (Anne-Marie Couto, personal communication). Although DNA repair in these cells has not been assessed by γ-H2AX, it was shown that *adprt1a*$^{-}$ cells are deficient in NHEJ but upregulated for HR (Couto et al., 2011). This makes it possible to speculate that cells lacking H3b and c variants could similarly be deficient in the NHEJ pathway. To test this, the ability of *H3b/c*$^{-/-}$ cells to perform NHEJ was assessed using restriction enzyme mediated plasmid integration (REMI). The principle of the REMI assay is that an antibiotic resistance cassette is cut out of a plasmid using a restriction endonuclease and then electroporated into *Dictyostelium* in the presence or absence of the same endonuclease, or one which can generate compatible ends. The enzyme cuts genomic DNA, generating sites of integration for the cassette and this integration is dependent on NHEJ in *Dictyostelium* (Hsu et al., 2011). Finally cells are selected by resistance to the antibiotic and the proportion of resistant cells electroporated with enzyme to those without enzyme indicates the rate of NHEJ (Hsu et al., 2011; Kuspa and Loomis, 1992). The level of NHEJ in *H3b/c*$^{-/-}$ cells was similar to the parental AX2 strain suggesting that overall DSB repair by NHEJ was not impaired (Fig. 3.3). Thus, H3 b and H3c variants are not essential for general DNA repair by NHEJ in *Dictyostelium*.

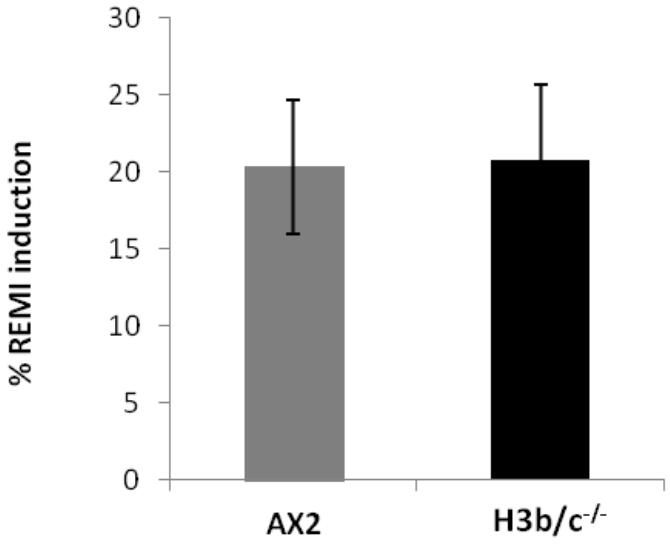

Figure 3.3. NHEJ in *H3b/c*$^{-/-}$ cells. Exponentially growing AX2 or *H3b/c*$^{-/-}$ cells were electroporated with the BSR cassette excised from pLPBLP using BamHI restriction endonuclease either with or without the same enzyme. Cells were then plated into 96-well plates, followed by the addition of blasticidin on the next day and colony number was assessed 10 days after. REMI induction was calculated for each strain as fold induction in the number of blasticidin-resistant colonies achieved by addition of BamHI. Error bars represent three independent experiments.

3.2.4 Assay development to interrogate DNA repair on site-specific breaks

In the experiments described above, the general level of overall DNA repair and NHEJ efficiency were shown not to be impaired in *H3b/c*$^{-/-}$ cells using phleomycin for DSB introduction. Although this method allows the introduction of multiple breaks in a dose-dependent manner, it has limitations as the introduced breaks are located at multiple random sites in the genome that only allows investigation of the overall repair rate and such treatments could also alter other cell processes which could influence the repair process. By contrast, a site-specific break allows observation of the whole repair process at one or several defined places in the genome and also facilitates analysis of chromatin dynamics surrounding the break using chromatin immunoprecipitation (ChIP). Thus, in order to investigate the efficiency of the repair at the particular DSB and the dynamics of H3 variants present at the break the development of an assay to introduce a site-specific break into the genome of *Dictyostelium* is required.

Site-specific break introduction has been widely used previously in mammalian and yeast systems (Hicks et al., 2011; Rouet et al., 1994). The most common method is to induce expression recombinant I-SceI meganuclease to cut an existing or artificially introduced recognition site(s) in the genome, often in connection to a GFP reporter which can be used to measure the efficiency of HR- and NHEJ-dependent repair of the break (Kriegs et al., 2010; Rieckmann et al., 2013). *Dictyostelium* doesn't contain an I-SceI recognition site in its genome, so another rare-cutting endonuclease, NotI, was chosen. NotI has only three recognition sites in the genome located on chromosome 3 within DDB_G0282409 gene coding sequence and chromosome 6 within DDB_G0291974 and DDB_G0292728 genes (dictyBase). Unfortunately, the sequence surrounding the NotI site located within the latter

gene is very AT rich making it extremely difficult to design specific PCR primers flanking the site (dictybase). The following analysis includes only the remaining two of the three sites.

Rather than using the common technique of driving expression of the nuclease by an inducible promoter, the possibility of break detection following electroporation of the enzyme was tested. As Not1 introduces only a maximum of 3 DSBs into the genome, in an initial attempt to optimize break detection the frequently cutting restriction enzyme DpnII was used. DpnII was electroporated into Ax2 cells and γ-H2AX levels were analysed by western blot. The initial γ-H2AX signal was relatively high in the cells electroporated in the presence or absence of enzyme and presumably represents damage caused by the electroporation procedure itself (Fig. 3.4 A). Nevertheless, the signal from cells electroporated with enzyme is still slightly higher than those without enzyme. Furthermore, after 8 hours cells electroporated in the absence of restriction enzyme have reduced levels of γ-H2AX whereas cells electroporated with DpnII have a higher signal which remains for at least 24 hours. This data suggests that the endonuclease continues to create DSBs for up to 24 hours post electroporation, which are due to be repaired, or initially generates a large number of breaks and the repair process takes 24 hours or more.

Next the ability of NotI to similarly induce DSBs and their repair was addressed. NotI, is C5-methylation sensitive and *Dictyostelium* DNA contains a low level of methylation (Katoh et al., 2006) so first the ability of Not1 to cut *Dictyostelium* genomic DNA *in vitro* was confirmed (data not shown). Then the possibility of the break detection by observing γ-H2AX levels following NotI electroporation was checked (Fig. 3.4 B). Although the initial level of γ-H2AX was increased similarly to DpnII experiment, the signal after 8h was compatibly low in both NotI and mock treated cells reaching a minimum at 24h.

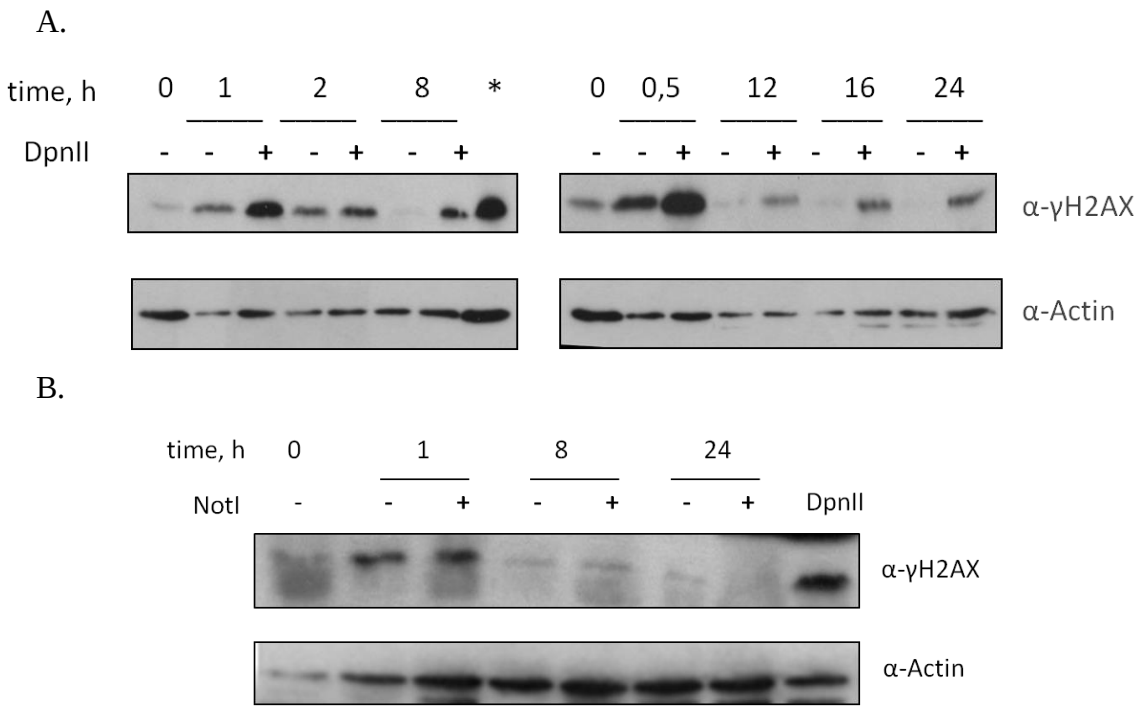

Figure 3.4. γ-H2AX levels following restriction endonuclease electroporation. A. Cells were electroporated in the presence (+) or absence (-) of 50 units of DpnII. Whole cell lysates were made after indicated time points for Western blot analysis using antisera specific for γ-H2AX. Actin was used as control for loading of samples. * represents a positive control from Ax2 cells treated with phleomycin for 1h. B. Cells were electroporated in the presence (+) or absence (-) of 75 units of NotI. Whole cell lysates were made after indicated time points for Western blot analysis using antisera specific for γ-H2AX. Actin was used as control for loading of samples. Cell lysates from cells 8 hours following electroporation with DpnII were used as a positive control.

This could suggest that either this method is not sensitive enough for detection of NotI introduced breaks as there are only 3 potential DSB sites, that DSBs introduced by NotI are repaired more efficiently than those introduced by DpnII or that NotI is not active in the cell and doesn't introduce breaks at all. In order to test the former two, a REMI assay was utilized to try and detect both the introduction of the break and its repair by NHEJ. To perform REMI of plasmid at NotI sites, the pLPBLP-2n plasmid was constructed in which a second NotI site was introduced. A second NotI site was introduced at the 5'end of the BSR cassette in addition to the existing site at 3'end by inserting a double-stranded oligonucleotide into a HindIII recognition site (Fig. 3.5 A). pLPBLP was linearised using HindIII and then a 14-bp oligonucleotide containing NotI site and compatable HindIII ends (see Appendix) was hybridized and ligated to the plasmid. Positive clones were confirmed by digestion analysis and sequencing (Fig. 3.5 B). The cassette was then cut out with Not1 and electroporated into *Dictyostelium* in presence or absence of NotI. No consistent increase in numbers of colonies was apparent in cells electroporated in the presence of restriction enzyme in comparison to the absence of enzyme (data not shown). A probable explanation for this is the low number of acceptor sites for the cassette in the genome. However, a lack of increase in number of colonies doesn't exclude the possibility of the integration at a Not1 site which may occur at low efficiency.

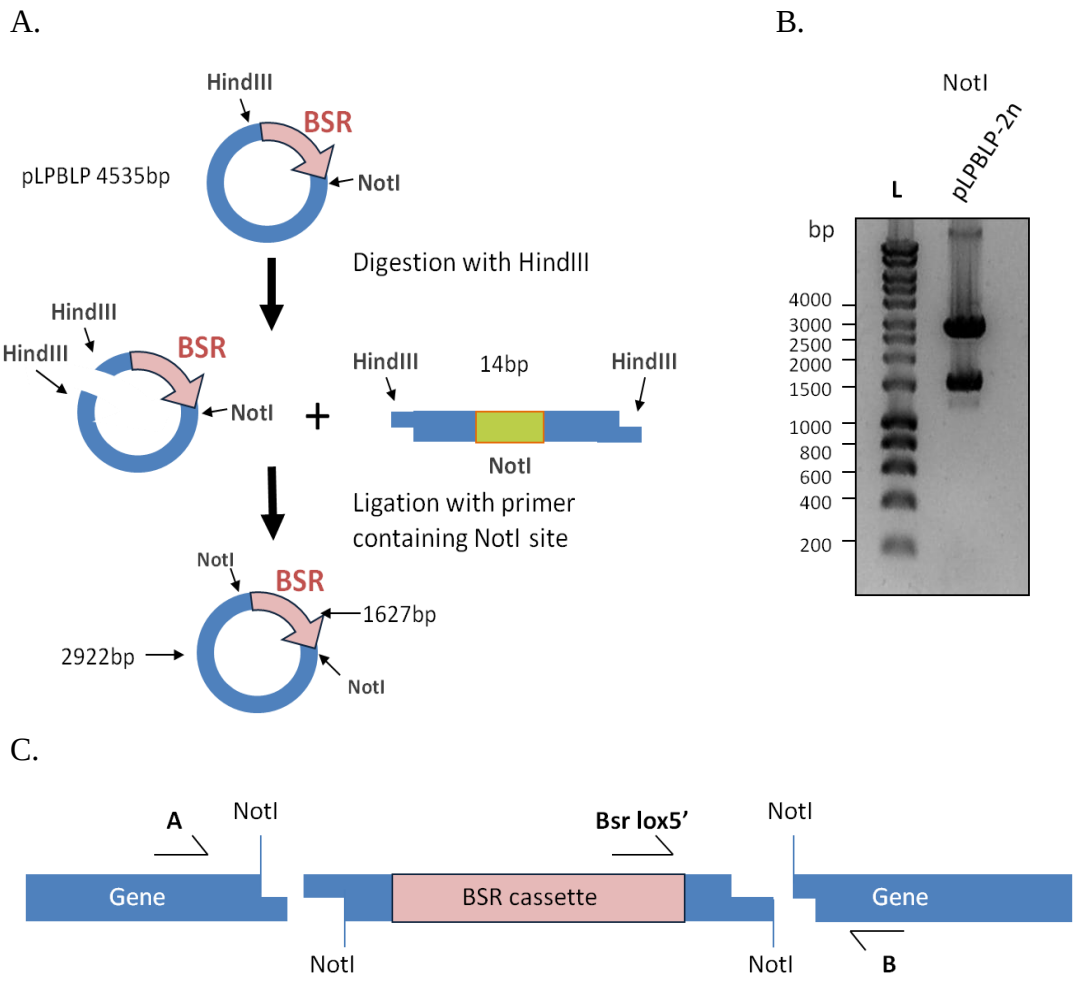

Figure 3.5. A. Schematic representation of the pLPBLP-2n plasmid construction. pLPBLP was linearised with HindIII and a double-stranded oligonucleotide (ARNot1) containing a Not1 recognition site and ends compatible with HindIII was then ligated into the vector. B. The resulting pLPBLP-2n plasmid was digested with NotI for 1h and fragments were resolved on a 1% agarose gel. Expected fragment sizes are 2922bp and 1627bp. C. Schematic representation of the resulting cassette integration and the primers used for the PCR screening. In brief, genomic DNA was isolated from the individual or pooled colonies resistant to blasticidin after electroporation with BSR cassette obtained from NotI digested pLPBLP-2n along with NotI. PCR was performed using all combinations of gene A and B primers and a primer located at the 5' end of the BSR cassette.

To assess if low efficiency cassette integration into Not1 sites is detectable, genomic DNA was extracted from blasticidin resistant colonies and analyzed by PCR using primers flanking the two analyzable Not1 sites and primers located inside the BSR cassette. PCR analysis of more than 300 individual colonies as well as screening of pools of colonies from a number of separate electroporations was performed but integration of the cassette wasn't detected (Fig. 3.5 C and data not shown). In order to increase the sensitivity of the screen and eliminate the intact genomic DNA without the integration event from the analysis in the pools of clones, the assay was modified by cutting out the BSR cassette from pLPBPL-2n vector using BstZI endonuclease that creates ends compatable with NotI but does not regenerate its recognition site in case of the integration event. This makes it possible to cut genomic DNA purified from the blasticidin resistant colonies with NotI prior to PCR analysis and eliminate the uninterrupted NotI recognition sites from the screen. However, the integration of the BSR cassette was not detected even in the pre-digested samples suggesting that the integration event is very rare and could not be detectable or just doesn't occur in cells at all (data not shown).

Another high throughput approach to detect the integration event is to use a phenotypic assay. *Dictyostelium* has an unusual life cycle being a unicellular organism during the vegetative stage and aggregating in the absence of food to form a multicellular organism that goes on to generate a fruiting body (Strmecki et al., 2005). One of the genes containing a NotI recognition site encodes a Dock-family protein DocA. The interruption of this gene leads to the developmental arrest of *Dictyostelium* cells at the mound stage preventing formation of fruiting bodies (Santorelli et al., 2008). This fact was used to perform a phenotypic assay to try and detect the integration of the BSR cassette at this site in Ax2 cells. 89 blasticidin resistant single colonies were analyzed. All cells were normal

in their development and formed fruiting bodies (data not shown). Although this analysis could only detect insertion at one of the NotI sites, it further suggests the inability to detect the integration event and that NotI site-specific break introduction assay is not a common event following electroporation of Not1 in *Dictyostelium*.

Therefore, another approach needs to be developed in order to monitor repair at a site-specific DSB in the genome. Given the evidence presented here that H3b and c variants are not required for overall DNA DSB repair and NHEJ in particular, it was decided not to continue with this line of research.

3.3 Discussion

Histone variants such as H2AX and H2A.Z have been shown to have defined roles in the DNA damage response and repair by signalling damage, facilitating chromatin flexibility and recruitment of DNA repair factors (Redon et al., 2002). At the outset of this project there was no information on any role for histone H3 variants in DNA double-strand break repair. However it was known that in mammalian cells the H3.3 variant is enriched in actively transcribed regions and differences in repair between euchromatin and heterochromatin have been reported (Ahmad and Henikoff, 2002; Goodarzi et al., 2010). Cells lacking two out of three H3 variants were demonstrated to have no sensitivity to DSBs compared to wild-type cells. A similar effect has previously been described for *Dictyostelium* strains lacking DNA repair factors such as DNA-PKcs, Ku80, and Dclre1 (Hsu et al., 2011; Hudson et al., 2005). In the case of *ku80* disruption such lack of sensitivity has been explained by elevated HR in the vegetative cells as an alternative repair pathway when NHEJ is prevented. However, *dclre1*$^{-}$ strains do not show increased HR levels although NHEJ is still defective. Consistent with impaired NHEJ, *dclre1*$^{-}$ cells

show delay in recovery from DSB induction both by resumption of cell growth and γ-H2AX decay after treatment with DSB inducing agent bleomycin (Hsu et al., 2011). Here *H3b/c*$^{-/-}$ cells were shown to be normal in DNA damage signaling and repair by monitoring γ-H2AX signal induction and decay following exposure to phleomycin. The growth rate of *H3b/c*$^{-/-}$ cells after transient exposure to phleomycin was also not impaired (data not shown) supporting the lack of a DSB repair deficiency. Indeed, non-homologous end joining was not impaired as was shown by REMI assay. Altogether these findings indicate that NHEJ is not altered in cells lacking H3b and c variants and no DNA repair defect was detected with methods used.

Interestingly, one year after the completion of this part of the project a role of the histone H3.3 variant in DNA repair was reported. Chicken DT40 cells lacking both isoforms of the H3.3 variant have been shown to be hypersensitive to UV light and exhibit a delay in maintaining replication fork progression on damaged DNA after UV irradiation (Frey et al., 2014). Furthermore, *h3.3* null cells have sensitivity to the DNA cross-linking agent cisplatin and the alkylating agent MMS although neither of these agents have any effect on the progression of the replication fork in these cells. This data suggests that the histone H3.3 variant has a role in maintenance of replication fork progression at sites of UV damage and is also somehow involved in the DNA interstrand cross-link and single-strand break repair pathways. Importantly, the *h3.3* null cells did not show any sensitivity to ionizing radiation consistent with the H3.3 variant not having a major role in DNA DSB repair.

In contrast to replication-dependent H3.1 and H3.2 variants, H3.3 is known to be expressed throughout the whole cycle independently of transcription and has recently been shown not to be essential for cell survival. In our lab it was only possible to disrupt the *h3b* and *h3c*

genes in *Dictyostelium*, whereas deletion of *h3a* has not been successful (Dr. D-W Hsu personal communication). This could suggest that H3a could have a closer resemblance in function with replication dependent H3 variants whereas H3b may be more equivalent to H3.3. Further supporting this H3K9ac, one of the markers of euchromatin, is preferentially detected in H3b but not in H3a similarly to H3.3 and H3.1 respectively (Hake et al., 2006; Hsu et al., 2012) Altogether, these observations suggest that it would be worth investigating whether, similarly to histone H3.3, *Dictyostelium* histone variant H3b has a role in DNA single-strand break and cross-link repair rather that in double-strand break repair pathways. This would require performing sensitivity assays of *H3b/c*$^{-/-}$ cells to chemical agents inducing different types of DNA strand damage.

An attempt to develop a system for site-specific break introduction into *Dictyostelium* genomic DNA was made. NotI endonuclease was chosen for the enzymatic DNA break as it only has three recognition sites within the *Dictyostelium* genome. Transfection of NotI into cells via electroporation was chosen rather than expression of recombinant enzyme from an extrachromosomal vector under an inducible promoter. This was done primarily because of the lack of *Dictyostelium* vectors where the promoter is not "leaking" and the enzyme is not expressed at all without induction. However, it was impossible to detect either a break or a repair event via NHEJ at NotI recognition sites after NotI electroporation. This could indicate either the inability of NotI to introduce a break into the genomic DNA *in vivo* despite of its ability to cut isolated genomic DNA *in vitro*, or the fact that the efficiency of NotI cutting is low in the cell and the introduced breaks are repaired with high efficiency so that they cannot be detected with available techniques. Such repair might predominantly occur by HR as introduction of BSR cassette with NotI compatible ends via NHEJ could not be detected either, but introduction of the cassette at the break site is presumably a low efficiency event and NHEJ is presumably more likely to

occur without insertion. In both cases the method used in this work is not applicable for monitoring chromatin dynamics at the break and specifically H3b turnover. Thus, development of another approach to introduce a site-specific break is required. This could be done by either testing available vectors for internal conditional expression of NotI and break detection using γ-H2AX signaling or preferentially by introducing an artificial recognition site of one of the endonucleases used in mammalian cells assays like I-SceI. In the latter case, the artificial sequence introduction could be performed by replacing a known sequence by homologous recombination similarly to gene disruption and could be carried out both within a gene and within non-coding sequences to allow comparison of repair in different chromatin environments (Hsu et al., 2011). For example, Sfo1 was successfully expressed in *Dictyostelium* using a tetracycline-regulated expression system to access the function of the mitochondrial genes (Chida et al., 2008). The fluorescent protein reporter system could also be used to give the possibility of detection of the repair event by either NHEJ or HR pathways (Kriegs et al., 2010; Rieckmann et al., 2013).

4 Characterization of the auto-modification activity of *Dictyostelium* ADP-ribosyl transferase Adprt1a *in vitro*

4.1 Introduction

Protein ADP-ribosylation serves as one of the early responses to DNA damage in living cells (Haince et al., 2008). It was confirmed that ADP-ribosylation plays an important role in DNA single- and double-strand break repair by mediating recruitment of key players of repair pathways e.g. XRCCI for SSB, Mre11 and NBS1 for DSB (Breslin et al., 2015; Haince et al., 2008). It has also been shown that ADP-ribosylation plays a role in DNA damage associated chromatin reorganization by recruiting chromatin remodelling proteins such as ALC1 ATFase, CHD4 and the macro-domain-containing histone variant MacroH2A.1.1 to DNA damage sites (Chou et al., 2010; Gottschalk et al., 2009; Timinszky et al., 2009). Furthermore, core histones have been shown to be targets of ADP-ribosylation in response to DNA damage (Poirier et al., 1985). However, the exact sites and functional significance of core histone ADP-ribosylation still remains unclear. In this study I am aiming to address these issues by using *Dictyostelium discoideum* as a model organism.

ADP-ribosylation is conserved in different organisms from mammals to lower eukaryotes and bacterial species (Perina et al., 2014). *Dictyostelium* contains 15 genes with putative ART catalytic domains (Pears et al., 2012). Among them, 4 ARTs are predicted to have similar domain organization and contain similar catalytic motifs to mammalian PARPs involved in the DNA damage response. One of these ARTs, Adprt1a, has recently been shown to be involved in DNA double-strand break signalling and repair (Couto et al., 2011). ADP-ribosylation observed in *Dictyostelium* vegetative cells after DSB induction was compromised in strains deficient in Adprt1a. Also, DNA double-strand break repair

pathway choice has been shown to be altered in the absence of Adprt1a as repair by NHEJ is decreased drastically in *adprt1a*$^{-}$ strains whereas HR by contrast is elevated, indicating involvement of this ART in DSB repair pathway choice in *Dictyostelium* (Couto et al., 2011). Collectively, these observations suggest Adprt1a to be a functional orthologue of mammalian DSB repair ARTs and therefore to potentially play a role in the DNA damage response by damage-induced histone modification. In order to investigate this, first functional characterization of Adprt1a is required. Mammalian ARTs implicated in the DNA damage response PARP1, PARP2 and PARP3 have been shown to be catalytically activated and auto-modified in the presence of DNA breaks *in vitro* (Altmeyer et al., 2009; Ame et al., 1999; Rulten et al., 2011). Furthermore, PARP1 and PARP2 have been shown to catalyse the formation of poly-ADP-ribosyl chains as shown by gel mobility of the ADP-ribosyl polymers removed from the auto-modified PARP1 and PARP2 by phosphodiesterase, whereas PARP3 performs predominantly mono-ADP-ribosylation (Ame et al., 1999; Loseva et al., 2010; Marsischky et al., 1995). Auto-modification sites on glutamates, aspartates and lysines have also been mapped for these ARTs by performing both *in vitro* point mutation analysis and mass-spectrometry of *in vitro* auto-modified enzymes (Altmeyer et al., 2009; Chapman et al., 2013; Haenni et al., 2008; Vyas et al., 2014). In this chapter I aim to investigate *in vitro* characteristics of the recombinant Adprt1a.

4.2 Results

4.2.1 Purification of recombinant Adprt1a

In order to characterize the enzymatic activity of Adprt1a, a version of Adprt1a tagged with 6xHistidines at the N-terminus (6xHis-Adprt1a) was expressed in *E.coli* and affinity purified using the His tag. The pQE30 vector containing 6xHis-Adprt1a was made by Dr. D-W Hsu (unpublished, Fig. 4.1 A). Previously it has been shown that mammalian ARTs are activated *in vitro* by the presence of damaged DNA (Altmeyer et al., 2009; Ame et al., 1999; Rulten et al., 2011). The standard method of protein purification using sonication for cell lysis is not suitable for investigating the DNA-dependence of ARTs as the enzyme can be pre-activated by sheared DNA (K Caldecott, personal communication). To avoid this, Bugbuster reagent was chosen for cell lysis and the affinity column purification of 6xHis-Adprt1a was performed using a protocol optimized by Dr. D-W. Hsu as described in Methods. A typical purification is shown in Figure 4.1 B.

A.

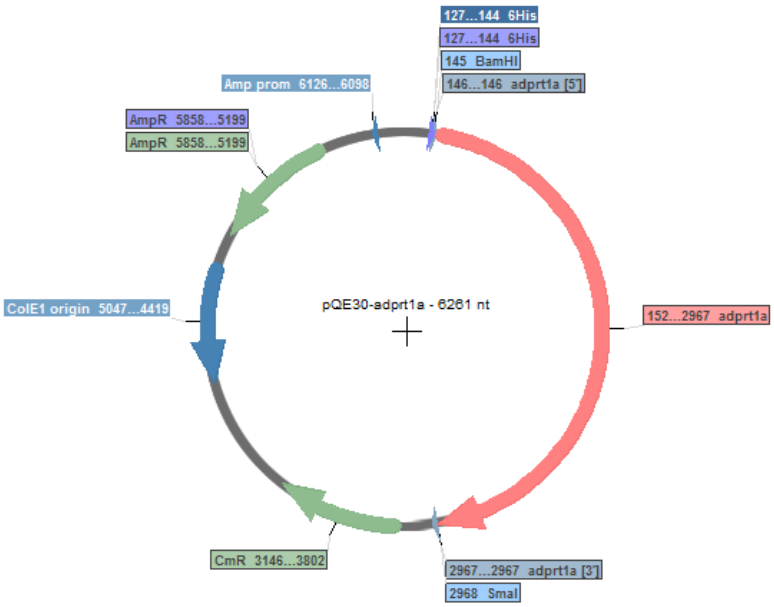

B.

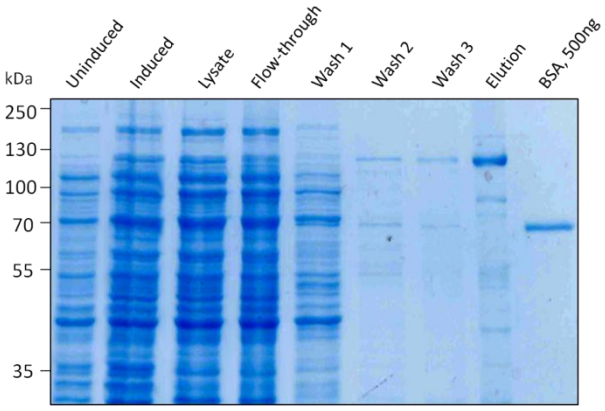

Figure 4.1. Recombinant 6xHis-Adprt1a. A. pQE30-Adprt1a vector used for the Adprt1a affinity purification. The Adprt1a coding sequence was PCRed from *Dictyostelium* cDNA and inserted into pQE30 vector using BamHI and SmaI restriction endonucleases. B. 6xHis-Adprt1a affinity purification. *E.coli* M15 cells were transfected with pQE30-Adprt1a vector, expression induced with 0.1mM IPTG for 4 hours and affinity column purification was performed as described in Methods using Ni-NTA beads (Qiagen) and eluting the 6xHis-Adprt1a with 200mM imidazole. A representative 12% polyacrylamide gel of the purification process, stained with Coomassie blue, is shown. The predicted molecular weight of Adprt1a is 107 kDa

4.2.2 Adprt1a auto-ADP-ribosylation: DNA DSB dependency

Mammalian ARTs have been shown to perform auto-ADP-ribosylation in the presence of different types of DNA breaks contained in sheared DNA (Loseva et al., 2010). In order to address if Adprt1a could also be auto-modified in the presence of sheared DNA recombinant 6xHis-Adprt1a was incubated with ^{32}P-labelled NAD^+ in the presence or absence of sheared salmon sperm DNA. Then the auto-ADP-ribosylation status of Adprt1a was addressed by resolving the reaction by SDS-PAGE followed by autoradiography (Fig. 4.2 A). Incorporation of radioactivity at the desired molecular weight consistent with automodification is dependent on NAD^+ and increased in the presence of sheared DNA suggesting the stimulation of Adprt1a auto-ADP-ribosylation in the presence of sheared DNA. In order to further confirm the finding, another method of signal detection was used. 6xHis-Adprt1a was incubated with NAD^+ spiked with 25% Biotin-conjugated NAD^+ and the Adprt1a auto-modification signal was detected by Western blot using Streptavidin conjugated to horseradish peroxidase (Strep-HRP) (Fig. 4.2 B). Similarly to the previous data Adprt1a was auto-modified only in the presence of sheared DNA indicating stimulation of its enzymatic activity. The kinetics of ADP-ribosylation was addressed by incubating 6xHis-Adprt1a with ^{32}P-labelled NAD^+ either in the absence or presence of sheared DNA and the reaction was stopped at the indicated times (Fig. 4.2 C). The auto-modification signal is detectable immediately after the addition of sheared DNA (0 time point) and is saturated after approximately 15 minutes incubation. The intensity of the modification signal remains unchanged for longer incubation times.

Sheared DNA used in the assay was produced by sonication of salmon sperm DNA and therefore contains all types of DNA breaks including single- and double-strand breaks. Since the aim of this work is to address the role of Adprt1a ADP-ribosylation activity in double-strand break repair, investigation of Adprt1a enzymatic activation by DNA double-

strand breaks is necessary. For this, pUC19 plasmid DNA was used in the ADP-ribosylation assay either uncut or cut with restriction endonuclease DpnI to generate 15 double-strand breaks. As described above, Adprt1a was incubated either with or without different DNA preparations in the presence of ^{32}P-labelled NAD^+ and the auto-ADP-ribosylation status of Adprt1a was addressed by autoradiography (Fig. 4.2 D). As before strong activation of Adprt1a auto-catalysis occurs in the presence of sheared DNA containing a mixture of damage (lane 2). Interestingly, uncut pUC19 induced some level of Adprt1a auto-modification, although to a much lower extent. This could be due to the presence of small number of nicks in the purified plasmid DNA. However, the presence of DNA double-strand breaks triggers Adprt1a activation above the level of uncut plasmid, consistent with double strand breaks activating Adprt1a auto-modification (line 4). These findings indicate that Adprt1a gets activated and auto-modified in the presence of DNA double-strand breaks *in vitro* consistent with its previously demonstrated role in the DNA double-strand break response in living cells (Couto et al., 2011).

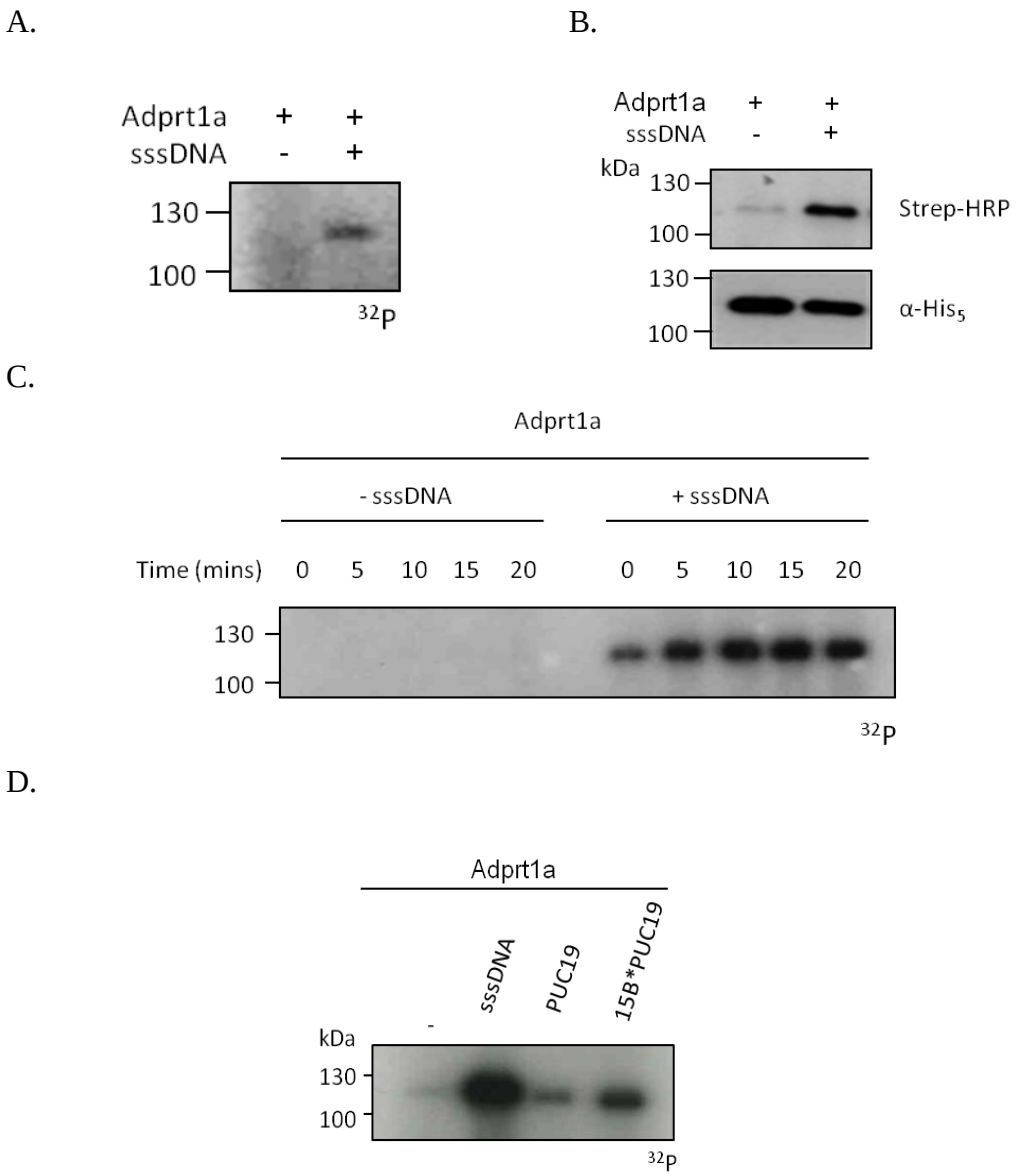

Figure 4.2. Characterisation of Adprt1a activity. A,B. 6xHis-Adprt1a was incubated for 30 min with ^{32}P-labelled NAD$^+$ or Biotin-NAD$^+$ either in the presence or absence of sheared salmon sperm DNA as described in Methods. Samples were then resolved by 8% SDS-PAGE and the ADP-ribosylation signal was detected A. using autoradiography for 12h, B. by Western blot using Strep-HRP. Reprobing with anti-His antibody confirmed equal loading. C. 6xHis-Adprt1a was incubated with ^{32}P-labelled NAD$^+$ either in the presence or absence of sheared salmon sperm DNA and the reaction was stopped after the indicated time by boiling samples in SDS loading buffer. D. 6xHis-Adprt1a was incubated for 30 min with ^{32}P-labelled NAD$^+$ in the presence of 0.1μg of either salmon sperm sheared DNA, pUC19 plasmid DNA, or pUC19 plasmid DNA cut with DpnI for 1h. For C and D samples were resolved by 8% and the ADP-ribosylation signal was detected using autoradiography.

4.2.3 Purification and characterization of catalytically inactive Adprt1a^{H789AY823A}

Having shown that Adprt1a gets activated and auto-modified in the presence of DNA breaks, the question of whether the observed modification was dependent on the catalytic activity of the enzyme itself was addressed. ARTs found in different organisms contain highly conserved "PARP signature" motifs including a catalytic domain HYE motif. This motif serves as a catalytic core located within six anti-parallel β-sheets forming an NAD^+ binding pocket (Ruf et al., 1998). Sequence alignment of *Dictyostelium* ARTs with the catalytic domains of the three major mammalian ARTs involved in the DNA repair process, PARP1, PARP2 and PARP3, reveals conservation of this HYE motif in Adprt1a (Fig. 4.3 A). In order to check whether the HYE motif could be functional in binding NAD^+, the 3D structure of the Adprt1a catalytic domain was modelled by performing sequence homology modelling using the crystal structure of the PARP3 catalytic domain (PDB 3fhb 1.A) as a template. Alignment of the resulting structure with the structure of PARP3 catalytic domain revealed strong superimposition of the HYE motifs of the two proteins, as well as the general location of the surrounding β-sheet structures, further suggesting the Adprt1a HYE motif to be functional in interactions with NAD^+ co-factor (Fig. 4.3 B).

To address whether the HYE motif is essential for the Adprt1a catalytic activity two out of these three residues, Histidine (H^{789}) and Tyrosine (Y^{823}), were mutated to Alanine (Adprt1a^{H789AY823A}) (Dr. D-W. Hsu, unpublished) and I expressed and purified 6xHis-tagged recombinant Adprt1a^{H789AY823A} from *E.coli*. An ADP-ribosylation assay was then performed with wild-type Adprt1a and Adprt1a^{H789AY823A} in the presence or absence of sheared DNA using either ^{32}P-labelled NAD^+ or Biotin-NAD^+ as a substrate (Fig. 4.3 C, D). An auto-ADP-ribosylation signal is apparent only in the presence of both wild-type

Adprt1a and sheared DNA (lane 2) but not in the presence of catalytically inactive version (lane 4). This finding suggests that the auto-modification is due to the catalytic activity of Adprt1a and that HYE motif is essential for the Adprt1a auto-catalysis *in vitro*.

A.

```
tr|Q54XI2|Q54XI2_DICDI      RTN-ICVQDILSLERENESERFTPWAKDKNRLLLWHGSRLTNFVSIVSQGLRIAPPSAPK
sp|Q9Y6F1|PARP3_HUMAN       RCP--TLQHIWKVNQEGEEDRFQAHSKLGNRKLLWHGTNMAVVAAILTSGLRIMPH----
sp|P09874|PARP1_HUMAN       NAYDLEVIDIFKIEREGECQRYKPFKQLHNRRLLWHGSRTTNFAGILSQGLRIAPPEAPV
sp|Q9UGN5|PARP2_HUMAN       SDYTMTLLDLFEVEKDGEKEAFR--EDLHNRMLLWHGSRMSNWVGILSHGLRIAPPEAPI
                                  :  : .::.:.* : :    .  ** *****:. :  ..*:: **** *

tr|Q54XI2|Q54XI2_DICDI      TGYRFGKGIYFADCISKSFSYCFTSS--DCPTALMLLCEVSLGDMNELKHDTYMEE-APH
sp|Q9Y6F1|PARP3_HUMAN       SGGRVGKGIYFASENSKSAGYVIGMKCGAHHVGYMFLGEVALGREHHINTDNPSLKSPPP
sp|P09874|PARP1_HUMAN       TGYMFGKGIYFADMVSKSANYCHTSQ--GDPIGLILLGEVALGNMYELKHASHISK-LPK
sp|Q9UGN5|PARP2_HUMAN       TGYMFGKGIYFADMSSKSANYCFASR--LKNTGLLLLSEVALGQCNELLEANPKAEGLLQ
                            :*  .*******.  *** .*           . ::* **:**    :   .   :

tr|Q54XI2|Q54XI2_DICDI      PFHSTKALGMAAPHKDGNHPLS-DSDGLVVPLGKISKTGL----STSCTHNEFIVYKIEQ
sp|Q9Y6F1|PARP3_HUMAN       GFDSVIARGHTEP--DPTQDTELELDGQQVVVPQGQPVPCPEFSSSTFSQSEYLIYQESQ
sp|P09874|PARP1_HUMAN       GKHSVKGLGKTTP--DPSANIS--LDGVDVPLGTGISSGV---NDTSLLYNEYIVYDIAQ
sp|Q9UGN5|PARP2_HUMAN       GKHSTKGLGKMAP--SSAHFVT--LNGSTVPLGPASDTGILNPDGYTLNYNEYIVYNPNQ
                               *. . *   *  .         :*  * :           . :   .*:::*.  *
```

B.

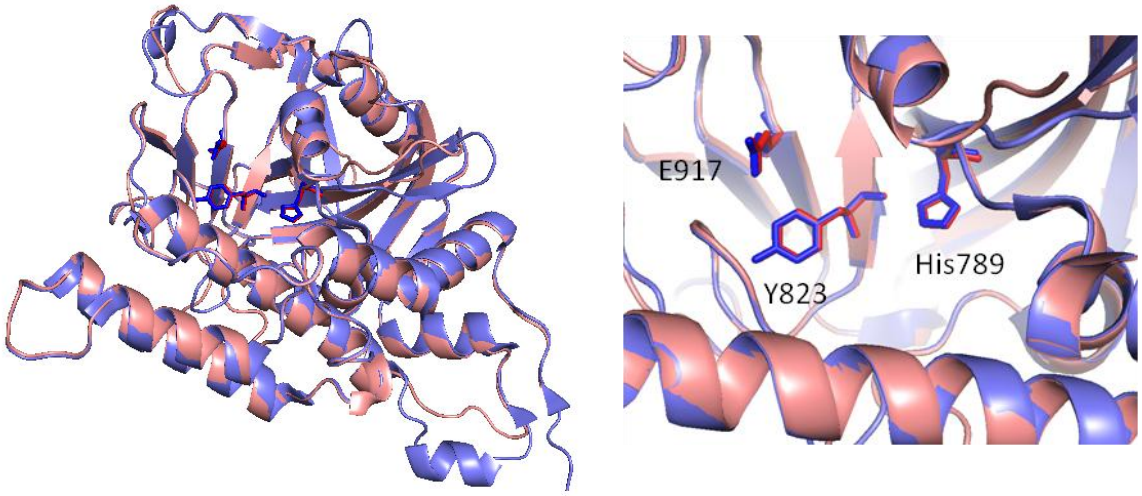

C.

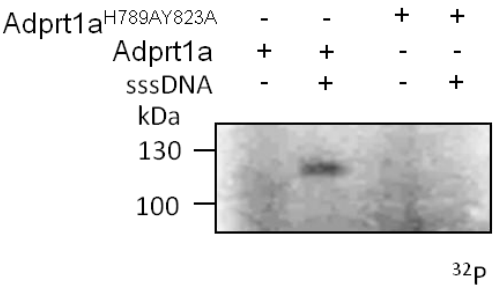

D.

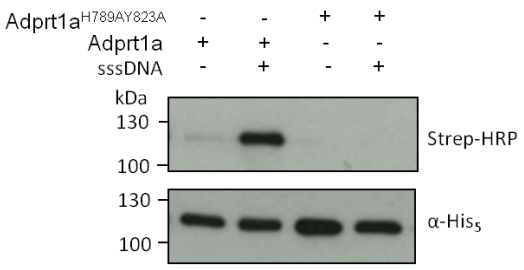

Figure 4.3. Adprt1a NAD^+ binding pocket characterisation. A. Protein sequence alignment of Adprt1a (Q54XI2) with human PARP1 (P09874), PARP2 (Q9UGN5) and PARP3 (Q9Y6F1). Protein sequences were obtained from UniProt, alignment was performed using MUSCLE online service. Conserved HYE motif residues are highlighted. B. Alignment of the PARP3 catalytic domain crystal structure (3fhb 1.A) with Adprt1a structure obtained by sequence homology modelling against 3fhb 1.A. Adprt1a structure is coloured in coral and PARP3 in blue (left). Superimposition of the HYE motif residues is shown (right). PARP3 residues are shown in blue, Adprt1a in red. Residue numbers of Adprt1a HYE motif are indicated. Sequence homology modelling was performed using online SWISS-MODEL service. Structure alignment was performed using PyMOL. C, D. 6xHis-Adprt1a and 6xHis- $Adprt1a^{H789AY823A}$ were incubated for 30 min with ^{32}P-labelled NAD^+ or Biotin-NAD^+ respectively either in the presence or absence of sheared salmon sperm DNA as described in Methods. Samples were then resolved by 8% SDS-PAGE and the ADP-ribosylation signal was detected C. using autoradiography after 12h of incubation with film, D. by Western blot using Strep-HRP. The blot was stripped and reprobed using anti-His tag antisera to confirm equal loading.

4.2.4 Adprt1a auto-modification can be removed by MacroD1 but not PARG

ADP-ribosyl transferases form a large family of enzymes that can be divided in two classes by the ability to catalyze either mono- or poly-ADP-ribosylation. The removal of the poly- and mono- ADP-ribosyl chains is catalysed by different enzymes. The major enzyme responsible for the degradation of poly-ADP-ribosyl chains is poly-ADP-ribosyl-glycohydrolase, PARG. PARG contains a macrodomain responsible for the hydrolysis of the ribose-ribose bonds in the PAR-polymers and effective degradation of PAR-chains (Slade et al., 2011). However, PARG hydrolysis affects only inner polymer bonds leaving the terminal mono-ADP-ribosyl moiety on the acceptor protein. By contrast, macrodomain family proteins MacroD1 and MacroD2 have the ability to hydrolyse the ester bond between the ADP-ribosyl moiety and a glutamate residue and therefore the capability to reverse mono-ADP-ribosylation occurring on acidic residues (Rosenthal et al., 2013).

To address whether Adprt1a acts as a mono- or poly-ADP-ribosyl transferase a de-ADP-ribosylation assay was designed. Adprt1a was auto-modified as described in 4.2.2 using Biotin-labelled NAD^+ as a cofactor. Then ADP-ribosylated Adprt1a was incubated with either MacroD1 or PARG and the ADP-ribosylation status of Adprt1a observed by Western Blot analysis (Fig. 4.4). The intensity of the ADP-ribosylation signal doesn't change in the presence of PARG suggesting its inability to reverse the auto-modification. By contrast, PARG shows efficient removal of signal from auto-modified mammalian PARP1, known to form poly-ADP-ribosyl chains *in vitro* (Fig. 4.4 right). However, increasing concentrations of MacroD1 facilitate the removal of Adprt1a ADP-ribosylation as the auto-modification signal decreases (Fig. 4.4 left). Taken together, these observations suggest that the auto-modification of Adprt1a is mono-ADP-ribosylation and Adprt1a acts as mono-ADP-ribosyl transferase in autocatalysis *in vitro*. Additionally, MacroD1/2 have

been shown to reverse mono-ADP-ribosylation occurring on acidic residues but not lysines (Rosenthal et al., 2013) suggesting that Adprt1a auto-modification occurs predominantly on acidic residues.

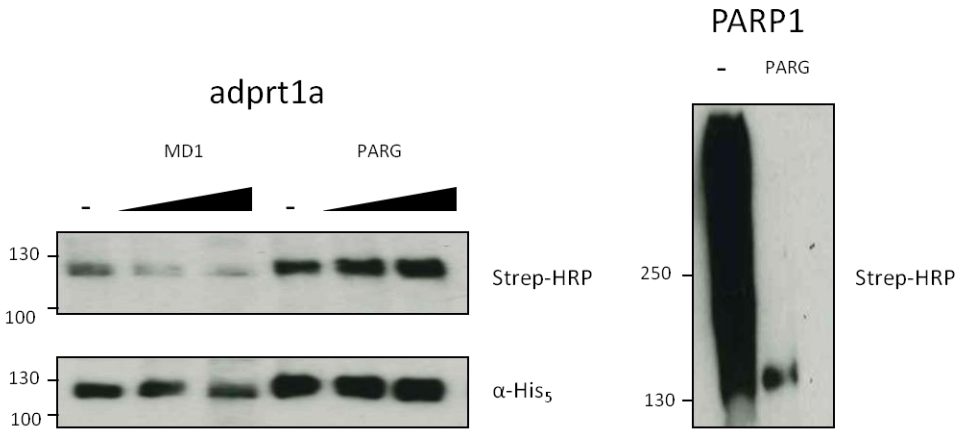

Figure 4.4. Adprt1a is a mono-ADP-ribosyl transferase *in vitro* autocatalysis. 6xHis-Adprt1a and PARP1 (Trevigen) were incubated for 30 min with Biotin-NAD^+ in the presence of sheared salmon sperm DNA as described in Methods. The reaction was then stopped by addition 10mM 3-aminobenzamide to inhibit further ART activity and auto-modified enzymes incubated with either MacroD1 or PARG for 30 min. Samples were then resolved by 8% SDS-PAGE and the ADP-ribosylation signal was detected by Western blot using Strep-HRP. The blot was stripped and reprobed with anti-His tag antibody.

4.3 Discussion

Mammalian ARTs known to be involved in DNA damage repair can be activated by damaged DNA *in vitro* (Altmeyer et al., 2009; Ame et al., 1999; Rulten et al., 2011). In order to investigate whether the *Dictyostelium* ART Adprt1a has similar enzymatic activity we designed an *in vitro* ADP-ribosylation assay where either unlabelled, Biotin-labelled or ^{32}P-labelled NAD^+ was used as a substrate for recombinant 6xHis-Adprt1a auto-modification. The ability of the Adprt1a to perform auto-modification was identified and the increase of this activity in the presence of sheared salmon sperm DNA was shown. The auto-ADP-ribosylation of Adprt1a also was stimulated by the presence of DNA double-strand breaks suggesting its potential activation by DNA double-strand breaks in living cells. It was also shown that Adprt1a auto-modification was dependent on its catalytic activity as it required the presence of an intact HYE catalytic motif responsible for NAD^+ binding in PARP1. These findings are consistent with the *in vitro* activity characteristics that have been identified for the mammalian ARTs involved in the DNA break repair. Thus, both PARP1 and PARP2 have been shown to be activated by the presence of DNase I-damaged DNA (Ame et al., 1999) as well as in the presence of the double-strand break mimicking DNA in the form of an annealed double-stranded oligomer (Altmeyer et al., 2009). PARP3 auto-ADP-ribosylation has also been shown to be stimulated by sheared salmon sperm DNA, double-stranded oligonucleotide as well as restriction enzyme digested pEGFP-C2 plasmid DNA (Rulten et al., 2011).

Further characterisation of Adprt1a *in vitro* enzymatic properties was performed by showing that it acts as a mono-ADP-ribosyl transferase in auto-catalysis. This observation is particularly interesting as PARP1 as well as PARP2 were shown to be poly-ADP-ribosyl transferases (Vyas et al., 2014). However, both of these enzymes were found to first

catalyse mono-ADP-ribosylation or form short oligo-ADP-ribosyl-chains when incubated with a low concentration of the NAD^+ or by decreasing the incubation time to 10sec (Haenni et al., 2008; Kleine et al., 2008). In the assays presented in this chapter both the concentration of NAD^+ and the auto-modification reaction time were used in saturating conditions suggesting that Adprt1a was fully active and still performed mono-ADP-ribosylation. The only ART involved in DNA repair that has been shown to catalyse predominantly mono-ADP-ribosylation *in vitro* is PARP3 (Loseva et al., 2010; Rulten et al., 2011). Auto-ADP-ribosylation of PARP3 generates a single distinct band when analysed by Western blot while PARP1 auto-modification gives a large, diffuse signal. Furthermore, ADP-ribosyl moieties cleaved from auto-modified PARP3 resolved as a single band on a sequencing gel whereas PARP1 again showed a ladder of different length PAR chains (Loseva et al., 2010). PARP3 auto-modification has also been shown to be reversed by MacroD1 *in vitro* when treatment with PARG didn't change the PARP3 ADP-ribosylation signal, further confirming it to be a mono-ADP-ribosyl transferase in auto modification *in vitro* (Vyas et al., 2014).

Interestingly, PARP3, like Adprt1a, contains the complete HYE motif, proposed to be a marker of poly-ADP-ribosyl transferases. Recently several more ARTs have been shown to catalyse mono-ADP-ribosylation; however most of them have only HY residues conserved in the catalytic domain while the glutamate is replaced by leucine, isoleucine, valine or tyrosine(Hottiger et al., 2010). In this chapter the conservation of full HYE motif in Adprt1a was shown by sequence alignment and its potential functionality was confirmed by performing sequence homology modelling with the PARP3 catalytic domain crystal structure. It is important to mention that two more mammalian ARTs, PARP4 and PARP10, have similar conservation of the HYE motif and recombinant proteins were shown to perform mono- or short oligo-ADP-ribosylation *in vitro* but their role in DNA

repair, or activation by DNA breaks, have not been reported (Kickhoefer et al., 1999; Kleine et al., 2008).

Taken together, these observations highlight similarities between Adprt1a and mammalian PARP3 in *in vitro* activity. However, in order to address the functional significance of Adprt1a enzymatic activity *in vivo* further characterisation is required. Thus, during this work, glutamates E11 and E399 as well as aspartate D16 have been identified as Adprt1a auto-modification sites using mass-spectrometry analysis (in collaboration with Prof. Caldecott, Essex). This observation is consistent with the ability of MacroD1 to remove the majority of the Adprt1a auto-modification since it can only catalyse the hydrolysis of ADP-ribose attached to acidic residues (Rosenthal et al., 2013). Next the authenticity of these sites found *in vitro* is required by deletion analysis and, if proven, the functional significance of Adptr1a auto-modification could be investigated by mutation of these residues in the endogenous gene by gene replacement technology followed by analysis of the DNA repair phenotype. Alternatively, not only Adprt1a auto-modification functionality but substrates of Adprt1a activity at DNA breaks can be identified. To address this, the ability of Adprt1a to modify core *Dictyostelium* histones will next be addressed.

5 Histone H2B ADP-ribosylation by Adprt1a *in vitro*

5.1 Introduction

Protein ADP-ribosylation has been shown to be involved in the variety of different cell processes including the DNA damage response (Bai, 2015). Apart from modifying and recruiting factors of the DNA repair machinery, ADP-ribosylation has also been shown to facilitate repair processes by remodelling chromatin structure and interacting with chromatin associated proteins (Ahel et al., 2009; Chou et al., 2010). Several factors have been suggested to be targets of ADP-ribosylation in response to DNA damage including histones. Initially, mammalian linker histone H1 and core histones (H2A, H2B, H3 and H4) were shown long ago to be acceptors of ADP-ribosylation *in vitro* by incubating nucleosomal histones purified from rat liver nuclei with ^{32}P-labelled or ^{14}C-labelled NAD^+ and detecting the radioactive signal following fractionation of samples for each histone (Burzio et al., 1979; Giri et al., 1978; Ogata et al., 1980a; Wong et al., 1977). Histones H1 and H2B were suggested to be modified the most among core histones *in vitro* (Burzio et al., 1979; Huletsky et al., 1985; Wong et al., 1977). Further studies showed the potential ADP-ribosylation of histones upon induced DNA damage *in vivo*. Mono- and poly-ADP-ribosylated protein conjugates purified from hepatoma AH 7974 cells that have been treated with dimethyl sulphate revealed proteins with the same molecular weight as core histones with potential H2B histone being modified to the greatest extent (Adamietz and Rudolph, 1984). Next, immunoblotting has been used to show that all core histones, but not H1, were present in the fraction of ADP-ribosylated proteins purified by affinity chromatography on ADP-ribosyl specific phenylboronate columns from human keratinocytes (HaCaT cells) after DNA damage induction by alkylating agents (Krupitza and Cerutti, 1989). Later, histones H1 and H2B were also proposed to be ADP-ribosylated *in vitro* in the context of native chromatin (Huletsky et al., 1989).

Several attempts have been made to identify the sites of mammalian histone ADP-ribosylation. Thus, histone H2B has been shown to be ADP-ribosylated on glutamate E2 *in vitro* by incubating chromatin fractions purified from rat liver with ^{14}C-labelled NAD^+ followed by preferential extraction of H2B, its digestion by trypsin and detection of radioactive peptides (Ogata et al., 1980a). Similarly histone H1 has been shown to be modified on E2, E14 at the N-terminus and C-terminal K213 residues (Ogata et al., 1980b). Later arginine 34 was also proposed to be an acceptor site of ADP-ribosylation of calf thymus histone H1 by purified ADP-ribosyl transferase (Ushiroyama et al., 1985). More recently, with the appearance of new techniques such as mass-spectrometry, more *in vitro* histone ADP-ribosylation sites have been reported (Zee and Garcia, 2010). All four core recombinant mammalian histones have been shown to be ADP-ribosylated by PARP1 on their amino-terminal tails and specific modification sites were identified by modifying synthetic peptides of full length or truncated histone terminal tails and subsequent analysis by electron transfer dissociation mass-spectrometry (Messner et al., 2010). By contrast to previous reports, histones were found to be ADP-ribosylated on lysines: K13 of H2A, K30 of H2B, K27 and K37 of H3 and K16 of H4.

However, no evidence confirming previously discovered potential glutamate or arginine ADP-ribosylation sites or their presence on full length recombinant histones or nucleosomal histones *in vivo* have been found yet. Thus, new models for identification of both *in vitro* and *in vivo* histone ADP-ribosylation and mapping modification sites are required. *Dictyostelium* is a good model for investigating core histone ADP-ribosylation as it contains orthologues of all mammalian core histones each encoded by single copy gene which makes it possible to perform genetic manipulations on endogenous genes (Stevense et al., 2011). *Dictyostelium*, unlike *S. cerevisiae*, also performs DNA damage-

induced nuclear protein ADP-ribosylation (Couto et al., 2011). In this chapter the ability of *Dictyostelium* ADP-ribosyl transferase Adprt1a to modify core histones *in vitro* will be investigated.

5.2 Results

5.2.1 Dictyostelium core histones are substrates of Adprt1a *in vitro*

5.2.1.1 Dictyostelium core histone purification

In order to investigate whether *Dictyostelium* histones are targets of ADP-ribosylation by Adprt1a recombinant histones were purified. The most abundantly expressed histones of each type were chosen for the initial verification. pQE30-vectors driving expression of N terminally 6xHis-tagged histones H2AX, H2Bv3 (H2B), H3a, H3b and H4, were provided by Dr. H-Y. Wang. Initial affinity purification of His tagged histones using the manufacturer's protocol proved to be inefficient. To improve this, the purification protocol was optimized by testing different conditions for protein induction. *E.coli* M15 cells were transformed with pQE30-Histone vectors and expression was induced using 0.1mM IPTG at 37^0C or 22^0C for 4h or overnight or 1mM IPTG at 16^0C overnight. A representative gel showing induction of 6xHis-H2B is shown (Fig. 5.1 A). The strongest expression was observed following 4 hours induction at 37^0C although induction for 4 hours at 22^0C was also effective. Increasing the induction time to 16 hours didn't result in more protein production so the first two conditions were chosen for further optimization. The next step was to check if the chosen induction conditions produced soluble target protein. For this, induced M15 cells were lysed using sonication and the soluble fraction was collected following centrifugation. Although the initial induction of expression was higher at 37^0C in comparison to 22^0C the amount of soluble protein was lower, so 22^0C was chosen for further purification (data not shown). Furthermore, the purity and efficiency of

recombinant histones purification was improved by increasing the concentration of imidazole in the initial lysis buffer from 10 to 30mM and replacing incubation of cell lysate with Ni-NTA agarose beads with a column. Representative purification gels using initial and optimised purification methods are shown for histone H2B (Fig. 5.1 B, C). The optimised protocol was used subsequently for purification of all *Dictyostelium* core histones (Fig. 5.1 D).

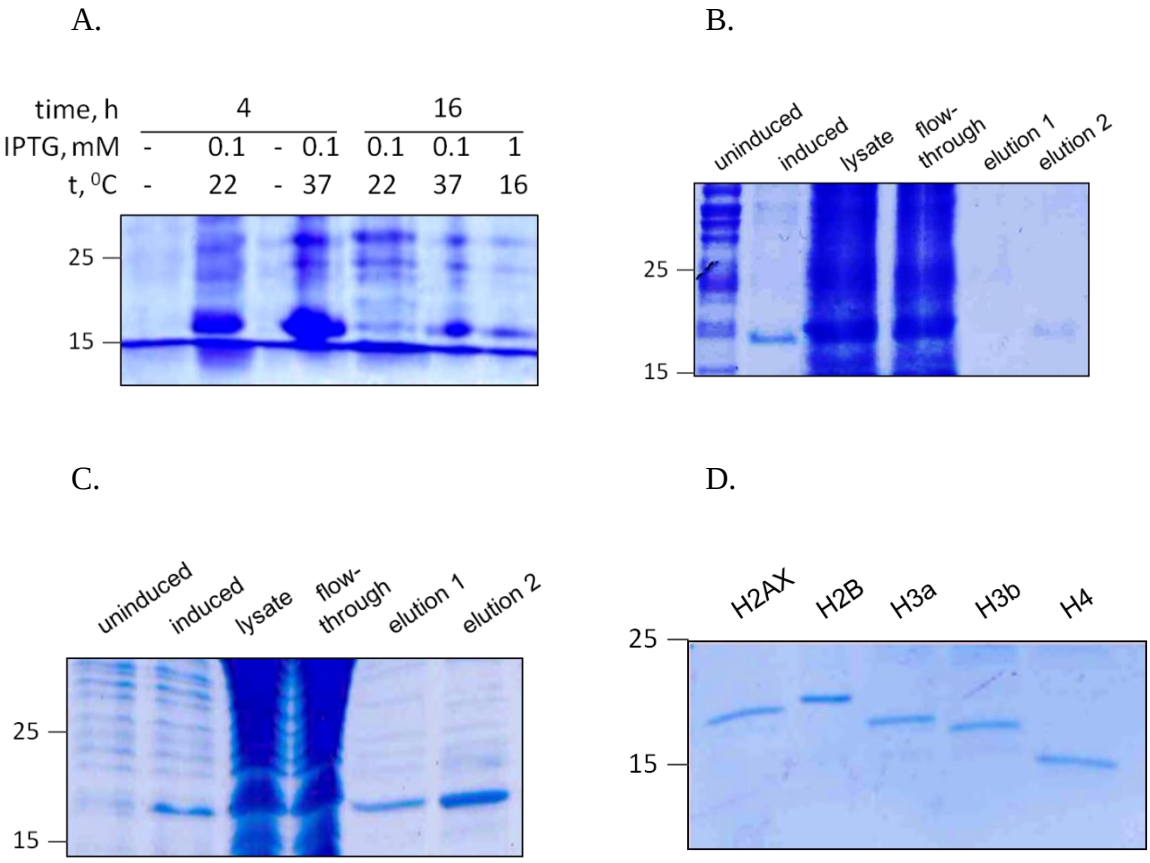

Figure 5.1. Optimisation of *Dictyostelium* recombinant core histone purification. A. E.coli M15 cells transfected with pQE30-H2B vector were incubated with the indicated concentrations of IPTG and incubation of the cell culture in the shaking incubator overnight at indicated temperatures. B,C. *E.coli* M15 cells were transfected with pQE30-H2B vector and protein expression induction has been performed at $22C^0$ for 4h. Cells were lysed using B. lysis buffer containing 10mM imidazole and lysates incubated with Ni^+-agarose beads on a rotation wheel, or C. lysis buffer containing 30mM imidazole and proteins purified using the column method. A representative gel of the purification process is shown. D.E. *E.coli* M15 cells were transfected with pQE30-Histone vectors and optimised affinity column purification was performed as described in Methods. In all cases proteins were resolved by 15% SDS-PAGE and visualized by staining with Coomassie blue.

5.2.2 ADP-ribosylation of core recombinant histones by Adprt1a *in vitro*

To determine if histones are substrates of ADP-ribosylation in *Dictyostelium* an ADP-ribosylation assay was performed with equal amounts of recombinant Adprt1a and core histones using biotinylated-NAD^+ and modified protein detected using Western blot analysis with Strep-HRP (Fig. 5.2 A). Among the core histones tested, histone H2B was modified the most efficiently *in vitro*. Among other core histones H3B and H4 also gave rise to an ADP-ribosylation signal although to a much lesser extent than H2B. Unfortunately, there was a background band in most of the samples appearing at approximately 17kDa. This band presumably corresponds to a contaminating protein coming through the affinity purification, as it reacts with Streptavidin-HRP reagent in all experiments containing recombinant 6xHis-tagged histones and/or 6xHis-Adprt1a, although in variable amounts. In order to avoid the appearance of this band, this experiment was repeated using ^{32}P-NAD^+ as a substrate (Fig. 5.2 B). Unfortunately, the general background signal was much higher in the area in which the histone proteins run (15-25kDa). The non-specific band of around 17kDa also appeared in this experiment too confirming that it is not an artefact of using the Biotin-labelled NAD^+ detection method. However, it is clear that H2B is still ADP-ribosylated, consistent with the Streptavidin-HRP experiment. Interestingly, by contrast to the previous experiment, histone H2AX, but not other histones, was also ADP-ribosylated suggesting it could also be the target of ADP-ribosylation by Adprt1a. Additionally, in both assays there was a strong ADP-ribosylation signal appearing at above 25kDa which presumably represents an N-terminal Adprt1a degradation product as it also reacts with α-His_5 antibody (Fig. 5.2 B and data not shown). However, since only H2B was ADP-ribosylated most robustly in both assays this histone was chosen for further analysis. Given the presence of high background noise in the

radiolabelling assay it was decided to perform further experiments using Biotinylated NAD^+ and Streptavidin-HRP for ADP-ribosylation signal detection.

A.

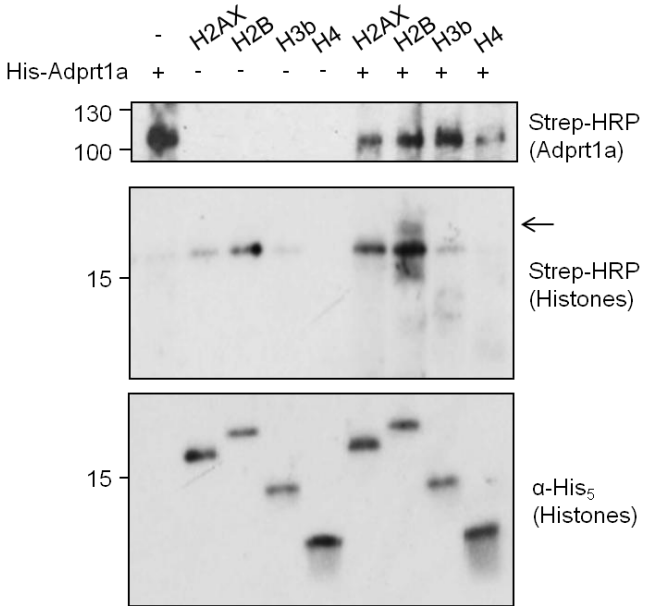

B.

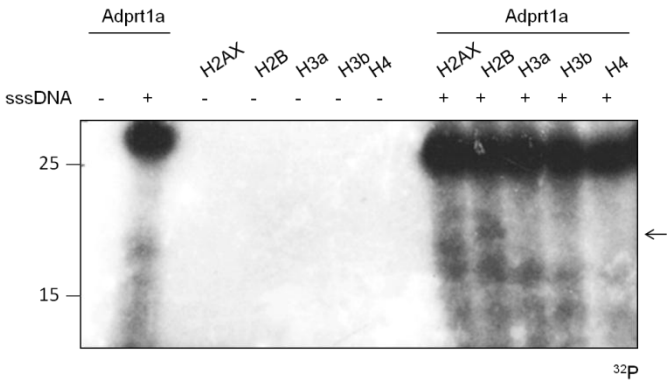

Figure 5.2. ADP-ribosylation of *Dictyostelium* core recombinant histone *in vitro* by Adprt1a. A. Recombinant 6xHis-tagged core histones (100ng) were incubated for 30 min either with or without 6xHis-Adprt1a (100ng) in the presence of salmon sperm sheared DNA and Biotin-NAD^+. Samples were then resolved by 18% SDS-PAGE and the ADP-ribosylation visualised by Western blot using Streptavidin-HRP. H2B modification is indicated with arrow. A representative of at least three experiments is shown. B. Recombinant 6xHis-tagged core histones (100ng) were incubated for 30 min either with or without 6xHis-Adprt1a (100ng) in the presence or absence of sheared salmon sperm DNA (sssDNA) and ^{32}P-labelled NAD^+. Samples were then resolved by 18% SDS-PAGE gel and the ADP-ribosylation signal was visualised by autoradiography. H2B modification is indicated with arrow.

In order to confirm that the observed H2B modification was dependent on DNA and Adprt1a, purified 6xHis-tagged H2B was incubated with or without 6xHis-Adprt1a in the presence or absence of sheared DNA. The ADP-ribosylation signal of H2B was detectable only in the presence of Adprt1a and sheared DNA (Fig. 5.3 A). The modification was also shown to be dependent on the catalytic activity of 6xHis-Adprt1a as it was not seen in the presence of the catalytically inactive mutant form Adprt1a^{H789AY823A} (Fig. 5.3 B).

Adprt1a acts as mono-ADP-ribosyl transferase in autocatalysis (see chapter 4.2.4). In order to determine if recombinant H2B was also modified by addition of a single ADP-ribose moiety, attempts were made to remove the modification from H2B using MacroD1 or PARG, but without success (data not shown). Reagents became available that are designed to either recognise only PARylated proteins (anti-poly-ADP-ribose binding reagent) or both poly- and mono-modifications (anti-pan-ADP-ribose binding reagent). In order to verify the specificity of these reagents, they were tested on auto-modified human PARP1, which is known to be auto-poly-ADP-ribosylated, and Adprt1a, which is mono-ADP-ribosylated (Chapter 4 Figure 4.4). Auto-modification of human PARP1, which is known to be auto-poly-ADP-ribosylated, was readily detected by both reagents (Fig. 5.3 C). Importantly, the Adprt1a auto-modification, as well as modification of the 25kDa Adprt1a degradation product, was only detectable with the anti-pan but not anti-poly-ADP-ribosyl binding reagent. This is consistent with the removal of the modification by MacroD1 and verifies the specificity of the reagents. Recombinant histone H2B was ADP-ribosylated by Adprt1a in the presence or absence of unmodified NAD^+ and then the ADP-ribosylation signal of H2B was detected using either reagent (Fig. 5.3 C). Modification of H2B was only detected by the anti-pan-ADP-ribosyl binding reagent, consistent with the notion that

histone H2B is mono-ADP-ribosylated by Adprt1a *in vitro*. Additionally, ADP-ribosylation signal of the Adprt1a and its degradation product but not H2B ADP-ribosylation was weakly detectable using a polyclonal α-PAR antibody raised against the poly-ADP-ribose polymer consistent with the H2B modification to be predominantly mono-ADP-ribosylation (Fig. 5.3 D).

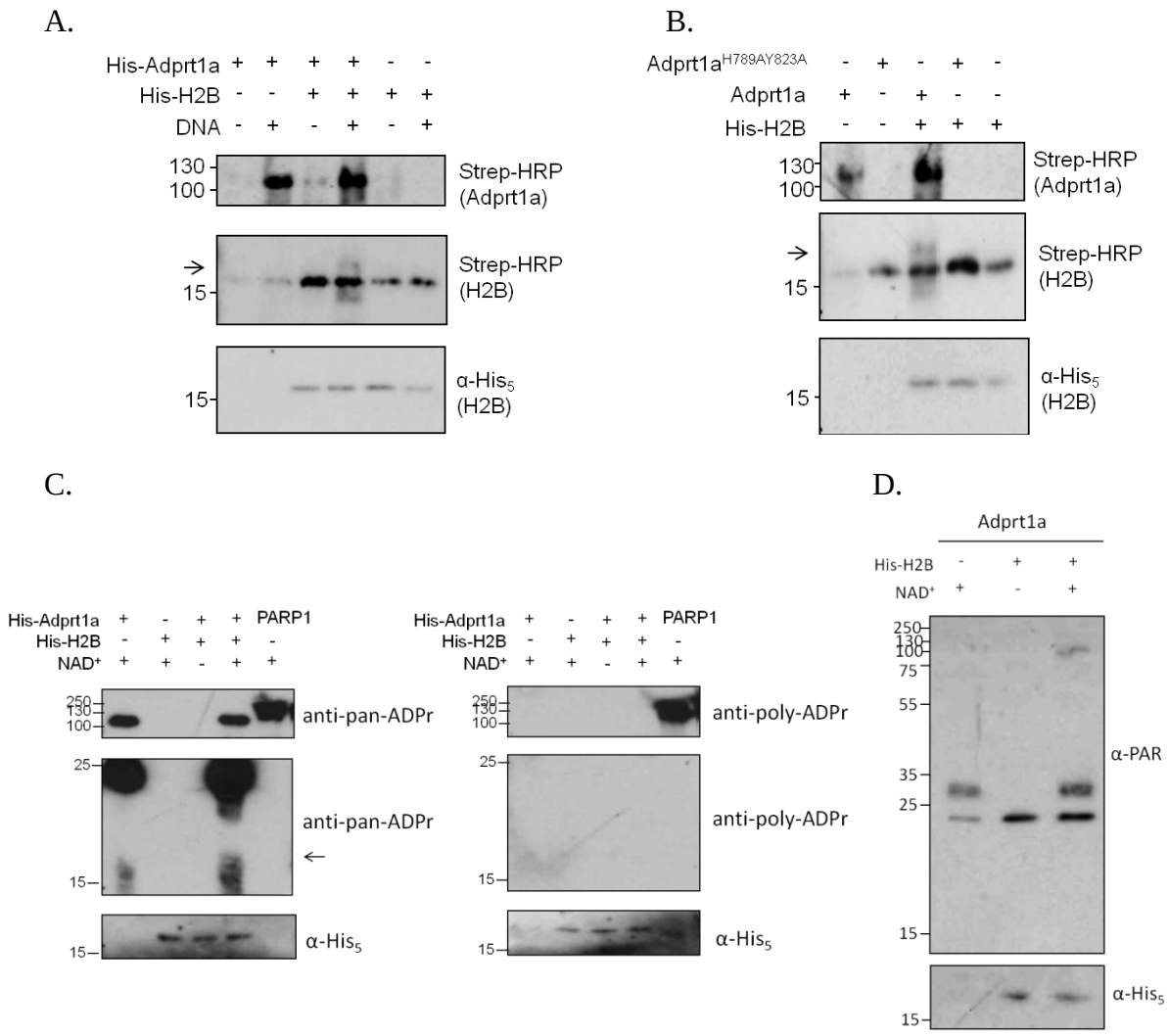

Figure 5.3. Characterisation of *Dictyostelium* histone H2B *in vitro* ADP-ribosylation by Adprt1a. A. Recombinant 6xHis-H2B (100ng) was incubated for 30 min either with or without 6xHis-Adprt1a (100ng) and salmon sperm sheared DNA in the presence of Biotin-NAD^+. Samples were then resolved by 18% SDS-PAGE and the ADP-ribosylation signal was visualised by Western blot using Streptavidin-HRP. H2B modification is indicated with arrow. A representative of at least three experiments is shown. B. Recombinant 6xHis-H2B was incubated for 30 min either with or without 6xHis-Adprt1a (100ng) and the catalytically inactive mutant 6xHis-Adprt1a^{H789AY823A} (100ng) in the presence of Biotin-NAD^+. Samples were then resolved by 18% SDS-PAGE and the ADP-ribosylation signal was visualised by Western blot using Streptavidin-HRP. H2B modification is indicated with arrow. A representative of at least three experiments is shown. C. Recombinant 6xHis-H2B was incubated for 30 min either with or without 6xHis-Adprt1a and unlabelled NAD^+. Samples were then resolved by 18% SDS-PAGE and the ADP-ribosylation signal was visualised by Western blot using either anti-pan (left panel) or anti-poly-ADP-ribose binding reagent (right panel). PARP1 was incubated for 30 min with unlabelled NAD^+ and the ADP-ribosylation signal was detected as described above. H2B modification is indicated with arrow. D. Recombinant 6xHis-H2B was incubated for 30 min either with or without unlabelled NAD^+. Samples were then resolved by 18% SDS-PAGE and the ADP-ribosylation signal was visualised by Western blot using polyclonal α-PAR antibody.

5.2.3 Histone H2B is ADP-ribosylated *in vitro* by Adprt1a predominantly in the first 25 amino acids

Among the most abundantly expressed *Dictyostelium* core histones, histone H2B is the major acceptor of ADP-ribosylation by Adprt1a *in vitro*. According to the literature, the majority of mammalian H2B post-translational modifications, including *in vitro* ADP-ribosylation, are found on the N-terminal tail (Messner et al., 2010; Ogata et al., 1980a), which in *Dictyostelium* is 50 amino acids. In order to determine if ADP-ribosylation of *Dictyostelium* H2B also occurs in this region a vector to drive the expression of a truncated version of H2B lacking the first 25 amino acids, approximately half of the N-terminal tail, was created. For this, the H2B coding sequence lacking the first 25 amino acids, was amplified by PCR from the initial pQE30-H2B vector using primers containing BamHI and XmaI restriction endonuclease sites on 5'- and 3'- sides respectively (Fig. 5.4 A, B). The PCR product was then ligated into the intermediate pJET2.1 vector and PCR fidelity was confirmed by sequencing. The BamHI and XmaI sites were then used to insert the fragment into the pQE30 vector to create a construct to drive expression of a 6xHis-tagged Δ25 H2B protein. Correct insertion was determined by digestion with EcoRV restriction endonuclease as there is one recognition site for this enzyme in the H2B sequence but not in pQE30 vector (Fig. 5.4 A, C). The 6xHis-tagged Δ25H2B recombinant protein was then expressed and purified using affinity chromatography as previously described (section 5.2.1) (Fig. 5.4 D).

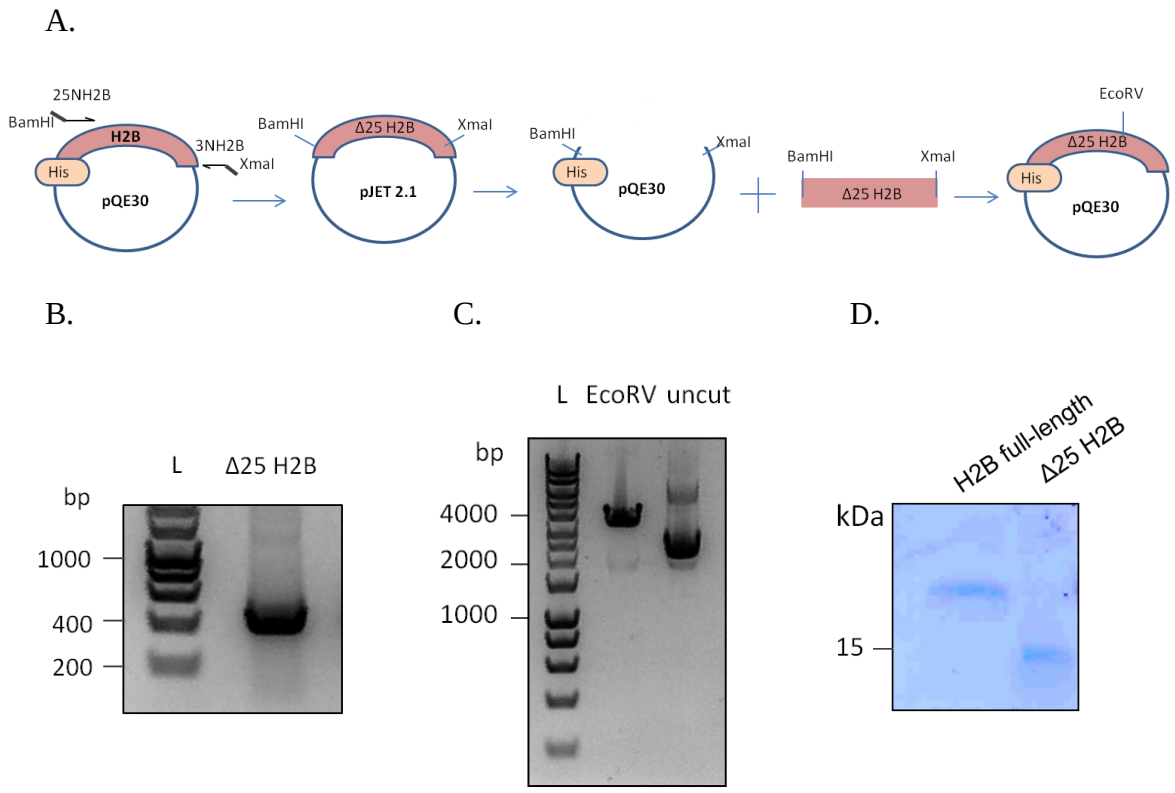

Figure 5.4. Generation of recombinant 6xHis-Δ25H2B . A. A schematic representation of the generation of 6xHis-Δ25H2B expression vector. The *h2b* coding sequence lacking the first 25 amino acids was amplified by PCR from genomic DNA using primer N25H2B and 3NH2B containing BamHI and XbaI restriction endonuclease sites respectively. The fragment was then ligated into pJET2.1 followed by sequence verification. The fragment was excised using BamHI and XbaI restriction endonucleases and ligated into the pQE30 vector pre-digested with the same enzymes. The final construct was confirmed by EcoRV digestion analysis. B. PCR fragment of the *h2b* coding sequence lacking the first 25 amino acids was resolved on a 1% agarose gel and visualised following staining with ethidium bromide. The product size (411bp) was confirmed by comparison with molecular weight markers (L). C. The final pQE30- Δ25H2B vector was digested with EcoRV endonuclease. Digested and undigested samples were resolved on a 1% agarose gel. The expected band size is 3851bp. D. *E.coli* M15 cells were transfected with pQE30-H2B or pQE30- Δ25H2B vectors and affinity column purification was performed as described in Methods. 6xHis-tagged proteins were resolved by 15% SDS-PAGE and visualized following staining with Coomassie blue.

The ability of Adprt1a to ADP-ribosylate the 6xHis-Δ25H2B protein in comparison to full-length H2B was determined (Fig. 5.5 A). Interestingly, the modification of 6xHis-Δ25H2B was decreased dramatically compared to the full-length protein. Quantification shows that 6xHis-Δ25H2B was ADP-ribosylated to less than 60% of the level of the full-length histone (Fig. 5.5 B). This suggests that a major site of histone H2B ADP-ribosylation *in vitro* occurs in the first 25 amino acids of the N-terminal tail, or is dependent on the presence of this stretch of amino acids.

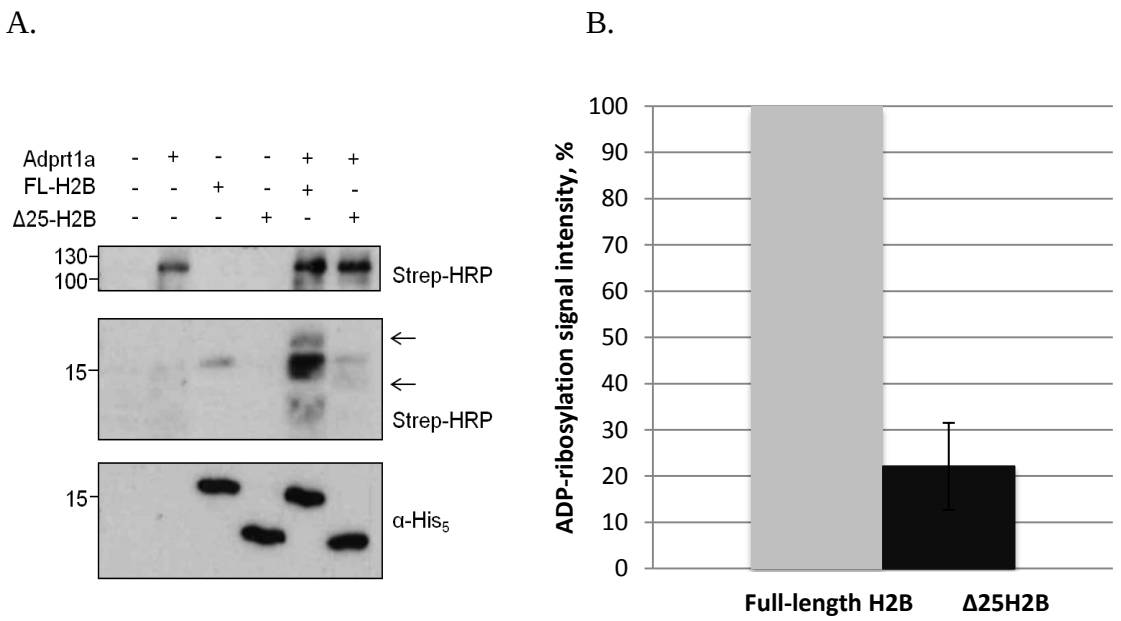

Figure 5.5. ADP-ribosylation of recombinant 6xHis-Δ25H2B protein by Adprt1a *in vitro*. A. Recombinant 6xHis-H2B (100ng) or 6xHis-Δ25H2B (100ng) were incubated for 30 mins either with or without 6xHis-Adprt1a (100ng) in the presence of Biotin-NAD^+. Samples were then resolved by 18% SDS-PAGE and the ADP-ribosylation signal was visualised by Western blot using Streptavidin-HRP. A representative of at least three experiments is shown. H2B and Δ25H2B modifications are indicated with arrows. B. Quantification of the ADP-ribosylation signal for 6xHis H2B and 6xHis-Δ25H2B. ADP-ribosylation carried out as in A was quantified by comparison of relative signal intensities using ImageJ. Signal reduction relative to full-length H2B is shown. Error bars represent three independent experiments.

5.2.4 Histone H2B is ADP-ribosylated by Adprt1a on glutamate 18 *in vitro*

It was shown previously that mammalian histones can be ADP-ribosylated on glutamic and aspartic acid residues *in vitro* (Ogata et al., 1980a; Ushiroyama et al., 1985). Recently it has been shown that mammalian core histones including histone H2B can also be PARylated on lysines by PARP1 *in vitro* (Messner et al., 2010). *Dictyostelium* histone H2B therefore contains 7 potential sites for ADP-ribosylation within the first 25 N-terminal amino acids: two glutamic acids (E18 and E19) and five lysines (K4, 7, 8, 11 and 20) (Fig. 5.6 A). In chapter 4 the ability of macro domain containing protein MacroD1 to remove the auto-modification of *Dictyostelium* Adprt1a was shown. MacroD1 and MacroD2 can only remove ADP-ribosylation occurring on glutamic and aspartic acid residues of acceptor protein but not lysines (Rosenthal et al., 2013). Consistent with this, mass-spectrometry data of Adprt1a *in vitro* auto-modification showed E11 and D16 to be acceptor sites for ADP-ribosylation, suggesting Adpr1a catalyses ADP-ribosylation of acidic residues. Therefore I hypothesized that in the first 25 amino acid residues of histone H2B the only two acidic residues, E18 and E19, would be the most probable potential acceptors of ADP-ribosylation by Adprt1a *in vitro*.

In test this hypothesis, recombinant H2B proteins containing point mutations were made. Glutamic acids E18, E19 or both E18 and 19 were mutated to alanine by site directed mutagenesis of the coding sequence of the pQE30-H2B vector using the QuikChange PCR mutagenesis system. Alterations and the integrity of the rest of the coding sequence were confirmed by sequencing across the coding region and then this region re-cloned into fresh pQE30 vector using BamHI and SalI sites to avoid potential mistakes introduced into the vector backbone (Fig. 5.6 B). Final positive clones were confirmed by digestion and sequencing (Fig. 5.6 C). 6xHis-tagged recombinant $H2B^{E18A}$, $H2B^{E19A}$ and $H2B^{E18AE19A}$

proteins were then expressed and purified from *E.coli* using affinity chromatography (Fig. 5.6 D).

A.

B.

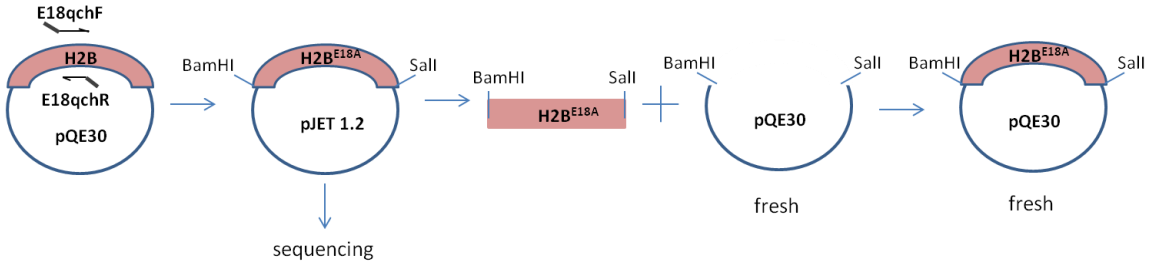

C.

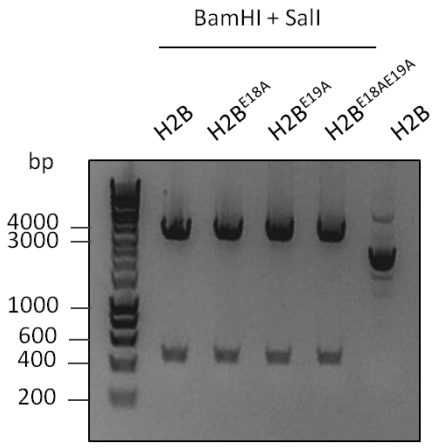

D.

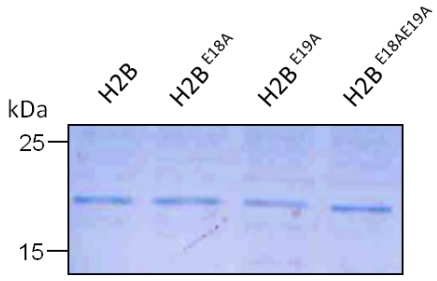

Figure 5.6. Expression and purification of recombinant 6xHis $H2B^{E18A}$, $H2B^{E19A}$ and $H2B^{E18AE19A}$. A. Amino acid sequence alignment of N-terminal region of H2B from *Dictyostelium* and other eukaryotes. Protein sequences were obtained from UniProt, sequence alignment was performed using MUSCLE online service. Amino acids aligned with E18 and E19 in *Dictyostelium* as well as E2 in *H.sapiens* are indicated. B. A schematic representation of the generation of the $H2B^{EtoA}$ expression vectors. The *h2b* coding sequence was amplified by PCR from the pQE30-H2B vector using the QuikChange PCR kit and primer E18qchF and E18qchR containing desired point mutation(s) (E19qchF, E19qchR; E18-19qchF, E18-19qchR). After confirmation of the alteration and the integrity of the remaining coding sequence by sequencing, the fragment containing the *h2b* coding sequence was excised from the vector using BamHI and SalI restriction endonucleases. The fragment was then cloned into fresh pQE30 vector pre-digested with the same enzymes. Positive clones were confirmed by digestion analysis using BamHI and SalI and sequencing C. Final pQE30-$H2B^{EtoA}$ vectors were digested with BamHI and SalI restriction endonucleases and samples were resolved on a 1% agarose gel and visualised following staining with ethidium bromide. The last lane (H2B) contains uncut pQE30-H2B vector. The expected $h2b^{EtoA}$ fragment size is 465bp. D. *E.coli* M15 cells were transfected with pQE30-$H2B^{EtoA}$ vectors and affinity column purification was performed as described in Methods. 6xHis-tagged proteins were resolved by 15% SDS-PAGE and visualized by staining with Coomassie blue.

The ADP-ribosylation of 6xHis-H2B^{E18A}, H2B^{E19A} and H2B^{E18AE19A} proteins by Adprt1a *in vitro* was assessed (Fig. 5.7 A). 6xHis-H2B^{E19A} protein was more efficiently modified in comparison to wild-type 6xHis-H2B suggesting that E19 is not a major acceptor site *in vitro* but potentially serves as a regulator of ADP-ribosylation of neighbouring E18 or other sites. The 6xHis-H2B^{E18A} and 6xHis-H2B^{E18AE19A} proteins both showed reduced modification signal compared to wild-type H2B. Quantification showed that ADP-ribosylation signal of both 6xHis-H2B^{E18A} and 6xHis-H2B^{E18AE19A} proteins was at least 50% lower than that of wild type H2B and the H2B^{E19A} modification was in turn four times higher (Fig. 5.7 B). Interestingly, the decrease in the modification signal of 6xHis-H2B^{E18A} and 6xHis-H2B^{E18AE19A} was to a comparable level to that of the 6xHis-Δ25H2B mutant suggesting that observed effect of the modification loss in 6xHis-Δ25H2B could be due to the removal of these glutamic acids. Taken together, these data suggest E18 to be a predominant acceptor site of ADP-ribosylation by Adprt1a of histone H2B *in vitro*.

A.

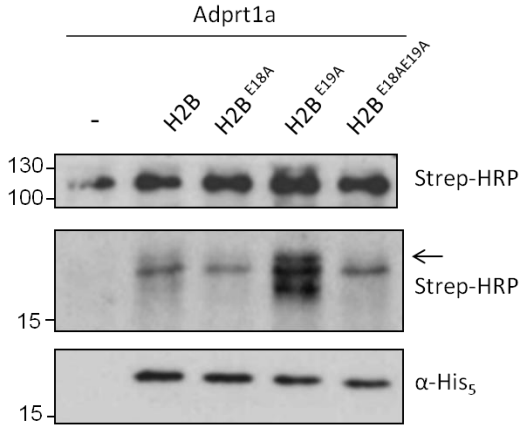

B.

Protein	Signal relative to H2B, %	Standard deviation, %
H2B	100	0
$H2B^{E18A}$	47	34
$H2B^{E19A}$	416	385
$H2B^{E18AE19A}$	45	10

Figure 5.7. Recombinant histone 6xHis-$H2B^{E18A}$, $H2B^{E19A}$ and $H2B^{E18AE19A}$ *in vitro* ADP-ribosylation by Adprt1a. A. Recombinant 6xHis-H2B and 6xHis-$H2B^{EtoA}$ proteins (100ng) were incubated for 30 min either with 6xHis-Adprt1a (100ng) in the presence of Biotin-NAD^+. Samples were then resolved by18% SDS-PAGE and the ADP-ribosylation signal was visulaised by Western blot using Streptavidin-HRP. H2B modification is indicated with arrow. A representative of at least three experiments is shown. B. Quantification of the 6xHis-H2B and $H2B^{EtoA}$ ADP-ribosylation signal. The signal from three independent experiments, as shown in A, was quantified by comparison of relative signal intensities using ImageJ and the average is shown.

5.3 Discussion

Histones were long ago proposed to be acceptors of ADP-ribosylation in response to DNA damage (Burzio et al., 1979). Among others, several studies suggested nucleosomal H2B to be ADP-ribosylated *in vitro* and also modified in the context of H1 depleted chromatin (Huletsky et al., 1989; Huletsky et al., 1985). Consistent with this, among all recombinant *Dictyostelium* histones tested histone 6xHis-H2Bv3 (H2B) is the major acceptor of ADP-ribosylation by recombinant Adprt1a *in vitro*. It was shown that this modification is dependent on the presence of DNA and depends on enzymatic activity of Adprt1a. Additionally, the H2B ADP-ribosylation signal was only detectable using anti-pan-ADP-ribose binding reagent that recognises both single and poly-ADP-ribose units whereas neither anti-poly-ADP-ribose binding reagent nor α-PAR antibody were able to detect the signal, suggesting H2B to be mono-ADP-ribosylated by Adprt1a *in vitro*. This is consistent with earlier findings where H2B isolated from rat liver nuclei and incubated with ^{14}C-labelled NAD^+ has been shown to have only one ADP-ribose unit attached by PEI-cellulose chromatography (Burzio et al., 1979).

Some potential sites of histone H2B ADP-ribosylation have been proposed. Glutamic acid E2 on the N-terminal tail of H2B was proposed to be an acceptor of radioactively labelled NAD^+ and lysine K30 was identified to be ADP-ribosylated using electron transfer dissociation mass-spectrometry of PARP1modified synthetic peptides from the H2B N-terminal tail (Messner et al., 2010; Ogata et al., 1980a). However, these modifications are not yet confirmed by point mutation analysis of full-length protein or by mass-spectrometry in case of E2. Interestingly, recombinant mammalian histone H2B mutated at position E2 to alanine has recently been shown to retain the majority of ADP-ribosylation

by PARP1 *in vitro* suggesting that this is either not the correct site or the presence of more modification sites on this histone protein (Messner et al., 2010).

In this study I propose that *Dictyostelium* histone H2B is ADP-ribosylated on glutamic acid E18 on the N-terminal tail by Adprt1a *in vitro*. It was demonstrated here that H2B ADP-ribosylation by Adprt1a *in vitro* decreases dramatically following deletion of the first 25 amino-acids of the N-terminal tail and signal reduction was observed when E18 was mutated to alanine in the full-length recombinant protein. A similar reduction was observed when both glutamic acids (E18 and E19), which are the only two acidic residues located in the first 25 amino acid region, were mutated (Fig. 5.6 A). Interestingly, mutation of E19 resulted in an increase of the H2B ADP-ribosylation signal suggesting a potential role in negative regulation of the modification. It has been shown that arginine R17 located next to ADP-ribosylated lysine K16 of histone H4 was important for interaction of H4 with PARP1 (Messner et al., 2010). Molecular modelling of the binding mode of PARP1 and H4 revealed a stable interaction between the guanidinium group of histone H4 arginine 17 and a carboxyl group of glutamate found in the PARP1 catalytic centre. In *Dictyostelium* histone H2Bv3 sequence the two glutamic acids E18 and E19 are followed by lysine K20. Potentially, mutation of the acidic residue E19 alters the conformation of the histone-Adprt1a complex and exposes the amino group of lysine K20 or other lysines for interaction with acidic residues of Adprt1a located at the catalytic centre. Although no post-translational modifications of E19 have been reported it would be interesting to investigate whether modification could potentially serve as a regulator of E18 ADP-ribosylation. For example methylation could neutralise the negative charge of the glutamic acid carboxyl group (Sprung et al., 2008).

However, not all the ADP-ribosylation signal was removed by mutating E18 or both E18 and E19 residues suggesting the presence of more potential sites of ADP-ribosylation sites on H2B. There are two more glutamic acids located at positions E34 and E37, for example, that could also be modified. Furthermore, there are several lysines in the H2B N-terminal tail including K30 that could also be taken in consideration. In collaboration with Prof. K. Caldecott group we are now trying to confirm ADP-ribosylation of E18 and reveal further H2B ADP-ribosylation sites by performing mass-spectrometry analysis of recombinant H2B modified by Adprt1a *in vitro*. Also, further investigation of ADP-ribosylation acceptor sites on H2B by more extensive deletion and point mutation analysis is required. Moreover not only H2B but other core *Dictyostelium* histones were shown to be ADP-ribosylated although to a lower extent. This also requires further verification by performing ADP-ribosylation analysis of each of the found histones similarly to the H2B modification verification. Additionally, only one of each type of histone was chosen for this work whereas other less abundant variants could also be modified and thus have a special function related to the selective modification.

6 Histone H2B ADP-ribosylation in *Dictyostelium in vivo*

6.1 Introduction

Having identified ADP-ribosylation of *Dictyostelium* histone H2B *in vitro*, it is of great interest to investigate if H2B is ADP-ribosylated in the living cell and what consequences these modification has for cellular processes. ADP-ribosylation of cellular proteins has been long known to occur in cells in a normal state as well as in response to different stresses. Initially, proteins were shown to be ADP-ribosylated in living cells in response to different types of DNA damage (Berger et al., 1978; Jacobson et al., 1983; Jump et al., 1979; Kreimeyer et al., 1984). Interestingly, among nuclear proteins histones as well as PARPs themselves were thought to be ADP-ribosylated to the greatest extent as the histone fraction contained most of the radioactive signal from isolated nuclei incubated with radioactively labelled NAD^+ or were present in samples made by enrichment of the ADP-ribosylated proteins from cellular lysates by aminophenylborate chromatography (Krupitza and Cerutti, 1989; Ogata et al., 1981; Wong et al., 1977). However, there was no direct evidence for modification of particular histone proteins or histone variants and no established system for *in vivo* modification identification and investigation of functionality of such modifications. More recently with the development of new techniques and detection methods a more extensive ADP-ribosylation proteome has started to be established. Using optimised enrichment of ADP-ribosylated proteins from cells after DNA damage induction using ADP-ribosyl binding motifs or α-PAR antibodies, samples were analysed by liquid chromatography tandem with mass-spectrometry (Dani et al., 2009). Different protein modification and interaction targets were found using this approach including histones and other chromatin associated proteins, DNA repair proteins such as Ligase III, XRCC1 and 4, and also factors involved in transcription and RNA metabolism (Gagne et al., 2012; Isabelle et al., 2012; Jungmichel et al., 2013). However,

only a small proportion of cellular proteins was modified which made it difficult to detect the ADP-ribosylation signal of purified fractions and required enrichment steps in non-denaturing conditions that could affect the endogenous ADP-ribosylation both by modification induction as well as its reversal during sample preparation. Furthermore, even when decreasing the possibility of affecting protein ADP-ribosylation during sample preparation by adding PARP and PARG inhibitors, these detection methods also require the treatment of modified proteins with PAR degrading enzymes, making it possible forproteins to interact with free PAR fragments and be mistaken for covalently modified proteins (Daniels et al., 2014; Jungmichel et al., 2013). Currently mass-spectrometry based methods of ADP-ribosylated protein identification are being further optimised by utilising PARG-knockdown cells for intracellular ADP-ribosylation signal enrichment and using PAR degrading enzymes for prevention of sample contamination with free PAR chains (Palazzo et al., 2015; Zhang et al., 2013). Additionally, treatment of isolated ADP-ribosylated peptides by hydroxylamin allows mass-spectrometry analysis to serve as a potential method of mapping the exact acidic sites of protein ADP-ribosylation *in vivo* (Gagne et al., 2015; Zhang et al., 2013).

At the same time other studies suggest additional proteins to be directly modified by PARP1 *in vivo*. Thus, BRCA1 has been shown to both interact with and be modified by PARP1 *in vivo* by performing co-immunoprecipitation of ADP-ribosylated protein from DNA damage induced HeLa cells using an α-PAR antibody (Hu et al., 2014). This modification has also been confirmed *in vitro* and the modification domain has been identified. Furthermore, p53 that was previously shown to be ADP-ribosylated *in vitro* (Wesierska-Gadek et al., 1996) and has recently been shown to be modified by PARP1 *in vivo* by overexpressing GFP-tagged p53 protein in p53-null mice (Kanai et al., 2007). Together with showing GFP-p53 ADP-ribosylation was dependent on the presence of

PARP1 in cells, ADP-ribosylation sites were mapped by deletion and point mutation analysis *in vitro* and their functionality was shown by overexpressing the mutated GFP-p53 in the p53-null background. The significance of the p53 ADP-ribosylation was demonstrated as ADP-ribosylated p53 could not be targeted by the nuclear export machinery, promoting its DNA damage dependent nuclear accumulation.

Thus, despite the advantages of mass-spectrometry based methods, the traditional approach of the investigation of ADP-ribosylation substrates *in vivo* allows the identification of additional proteins and enables the investigation of functional significance of found modification. In this study, the ADP-ribosylation sites of *Dictyostelium* histone H2B by Adprt1a were identified *in vitro*. The functionality and significance of these mapped sites of H2B in living cells are of interest. As mentioned before, as well as being a haploid organism, *Dictyostelium* contains only a single copy of the gene encoding the histone H2Bv3 variant, making it possible to investigate its ADP-ribosylation status *in vivo* performing genetic manipulations that are well established in *Dictyostelium* (Couto et al., 2011; Hsu et al., 2011). Thus, *in vivo* H2B ADP-ribosylation is investigated in this chapter.

6.2 Results

6.2.1 Core histone ADP-ribosylation *in vivo*

First the ability of core histones to be ADP-ribosylated in *Dictyostelium in vivo* was investigated. To do this, AX2 *Dictyostelium* cells were treated with DNA double-strand break inducing agent phleomycin. Chromatin-enriched samples were then analysed by Western blot using polyclonal α-PAR antibody (data of Dr.Seiji Ura Fig. 6.1 A). Many proteins are shown to be ADP-ribosylated in response to DNA damage, however there is a clear signal of ADP-ribosylation in the area between 15 and 25kDa where *Dictyostelium*

core histones resolve on the gel. Interestingly, the signal in this area is decreased dramatically in cells lacking *adprt1a* and *adprt2* (data of Dr.Seiji Ura Fig. 6.1 B), the major ARTs shown to be involved in DSB-induced protein ADP-ribosylation as assessed by nuclear focus formation (Couto et al., 2011). These observations suggest DNA damage induced ADP-ribosylation of chromatin-associated proteins in the molecular weight range of histones and that this modification is dependent on Adprt1a and/or Adprt2.

Next we wanted to further confirm that observed signal was due to histone modification by analysing the acid extracted protein fraction, enriched in histones, isolated from phleomycin treated AX2 cells (data of Dr. H.Y. Wang Fig. 6.1 C). Interestingly, the signal observed was less intense and ran at a slightly lower molecular weight than the chromatin samples but was still in the area of core histones. This data is consistent with the suggestion that core histones are a potential target of ADP-ribosylation in *Dictyostelium in vivo*.

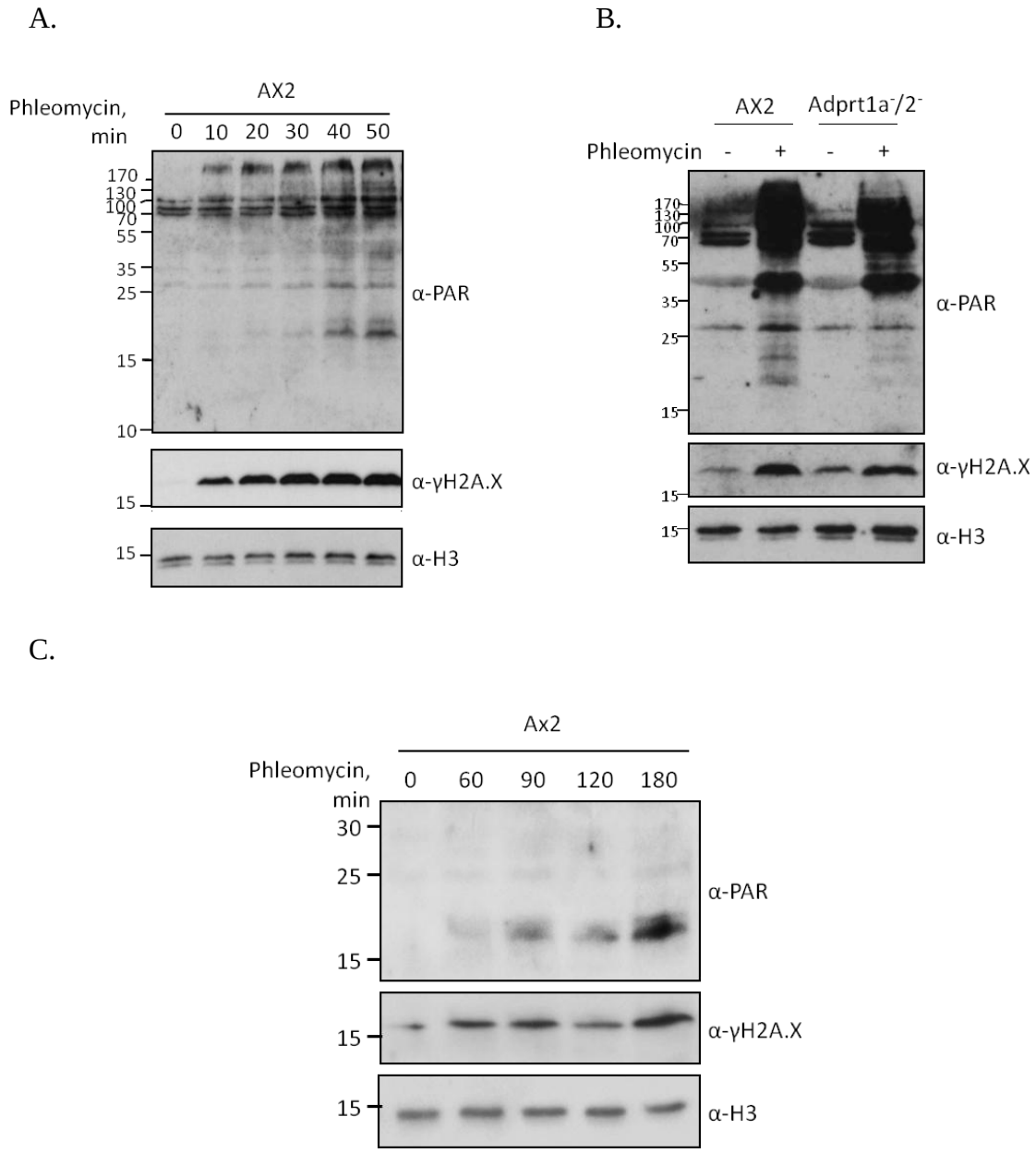

Figure 6.1. Protein ADP-ribosylation in *Dictyostelium*. A. AX2 cells were treated with 300μg/ml phleomycin for the indicated time periods. Chromatin extracts were prepared as described in methods and samples were separated by 15% SDS-PAGE followed by Western Blot analysis with indicated antibodies. B. AX2 and *adprt1a/adprt2*$^{-/-}$ cells were treated with 300μg/ml phleomycin or mock treated and then were analysed as described in A. C. AX2 cells were treated with 300μg/ml phleomycin for the indicated times. Acid extraction for histone enrichment was carried as described in Methods, samples were separated by 12% SDS-PAGE and then analysed by Western blot using indicated primary antibodies.

6.2.2 Introduction of an HA-tag to the endogenous H2B.

6.2.2.1 Construct generation

Previously in chapter 5 histone H2B was shown to be a major acceptor of ADP-ribosylation by Adprt1a *in vitro* among all *Dictyostelium* core histones. The next step was to see if H2B is similarly modified *in vivo* in the living cell. One approach for this is to introduce an epitope tag into the endogenous H2B to make it possible to observe the changes in modification in the living cell following immunoprecipitation. A gene replacement construct for introduction of an N-terminal HA tag into endogenous H2B was constructed. The initial vector design strategy included four steps (Fig. 6.2 A). The *h2b* coding sequence, including flanking regions of more than 1000 bp on each side, was amplified by PCR from *Dictyostelium* genomic DNA (Fig. 6.2 B). Primers for this PCR were designed to cover two restriction endonuclease recognition sites found in the sequences flanking the endogenous *h2b* gene, PvuI at the 5' end and BstEII at the 3' end. Next these sites were used to clone the PCR product into the intermediate pJET1.2 vector. Resulting clones were verified by sequencing. The BSR cassette was introduced into this construct, excising it from the pLPBLP vector using SmaI restriction endonuclease recognition sites on both sides and ligating the blunt-ended fragment into the single BsrGI restriction endonuclease site downstream of the *h2b* gene. The resulting construct contained the *h2b* gene with flanking regions as well as the BSR cassette downstream of the *h2b* coding region. Correct insertion was confirmed by digestion with HindIII and EcoRV restriction endonucleases (Fig. 6.2 C).

A.

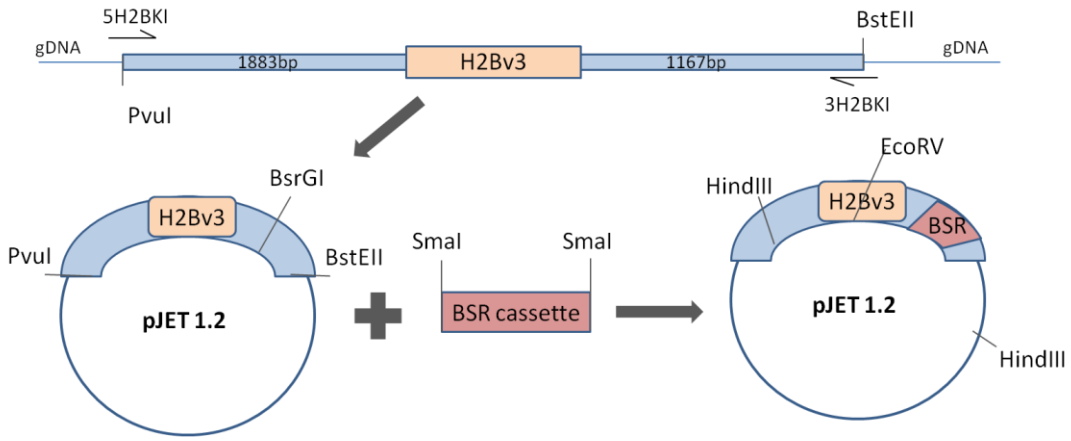

B.

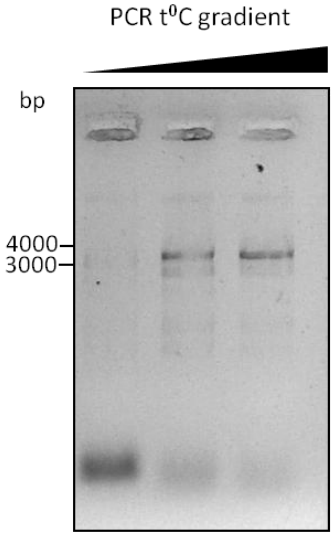

C.

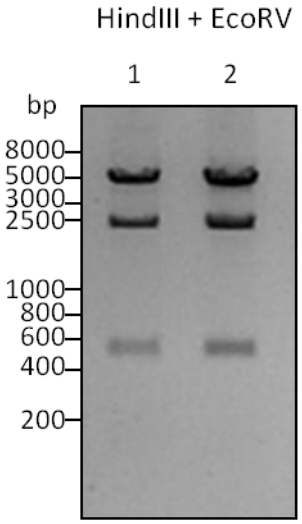

Figure 6.2. Generation of an H2Bv3 gene replacement vector. A. A schematic representation of the cloning strategy. The *h2b* coding sequence, including 3' and 5' flanking regions, was PCRed from genomic DNA. The fragment was then inserted to the pJET1.2 vector followed by introduction of the BSR cassette at the BsrGI site foun in the 3' noncoding region downstream of the *h2b* gene. B. PCR of AX2 genomic DNA using primers 5H2BKI and 3H2BKI was carried out at different annealing temperatures and the product was resolved on a 1% agarose gel. Expected length of the product is 3515bp. C. pJET1.2 vector including the PCR fragment as well as BSR cassette was verified by HindIII and EcoRV restriction endonuclease digestion. Samples were resolved on a 1% agarose gel. Expected fragment sizes are 556, 2420 and 5024bp. Two representative colonies are shown.

The final step was to insert the coding sequence for an HA tag at the N-terminus (Fig. 6.3 A). The HA tag sequence contains an internal NdeI restriction site. This fact was used to PCR the tag in two different parts. The first part was amplified by PCR using primers covering an AfeI site in the 5' flanking region of the *h2b* gene and a reverse primer complementary to the region upstream of the start codon of *h2b* and containing a new start codon as well as part of the HA-tag sequence including the NdeI site. The second part was amplified by PCR using a forward primer containing the HA-tag coding sequence and the first part of the *h2b* gene and the reverse primer was designed to cover a HincII site in the 3' flanking region and also to contain an artificial XbaI site for subsequent cloning steps (Fig. 6.3 A). Each PCR product was cloned into the intermediate pJET1.2 vector following by digestion analysis with indicated restriction endonucleases and sequence confirmation (Fig. 6.3 B, C). The C-terminal fragment was cut from the intermediate vector using the NdeI and XbaI sites and was ligated to the other in the respective pJET1.2 vector forming a fragment containing a full HA tag, part of the *h2b* gene and its 5' flanking region. Positive clones were checked by digestion analysis and sequencing. The final fragment was then cut out from the vector using AfeI and HincII restriction sites and cloned into the initial backbone pJET1.2 vector containing the full *h2b* gene sequence and BSR cassette, cut with the same restriction endonucleases (Fig. 6.3 A). The final pJET1.2-HA-H2B-BSR construct was confirmed by digestion analysis with NdeI enzyme (Fig. 6.3 D). For further experiments the HA-H2B-BSR construct with 5' and 3' flanking regions was cut out using PvuI and BstEII restriction endonucleases.

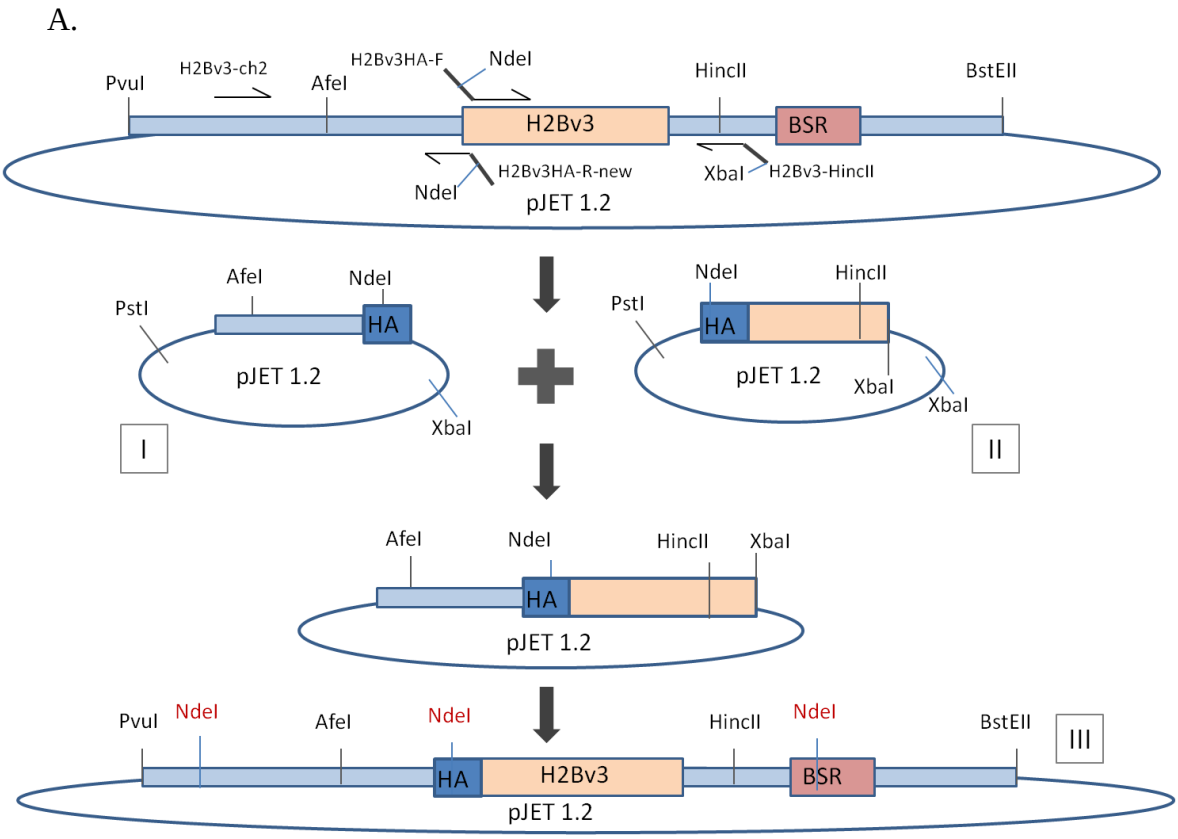
A.
PvuI
H2Bv3-ch2
AfeI
H2Bv3HA-F
NdeI
HincII
BstEII
H2Bv3
BSR
NdeI
H2Bv3HA-R-new
XbaI
H2Bv3-HincII
pJET 1.2
AfeI
NdeI
PstI
HA
pJET 1.2
XbaI
I
NdeI
HincII
PstI
HA
pJET 1.2
XbaI
XbaI
II
AfeI
NdeI
HincII
XbaI
HA
pJET 1.2
PvuI
NdeI
AfeI
NdeI
HincII
NdeI
BstEII
III
HA
H2Bv3
BSR
pJET 1.2

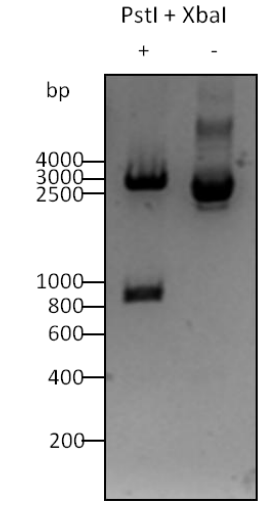
B.
PstI + XbaI
+
-
bp
4000
3000
2500
1000
800
600
400
200

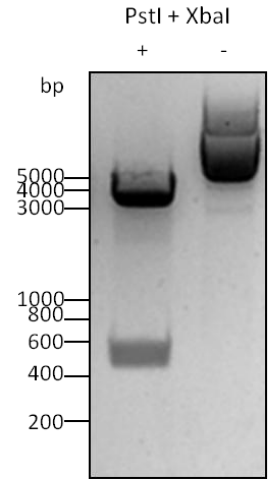
C.
PstI + XbaI
+
-
bp
5000
4000
3000
1000
800
600
400
200

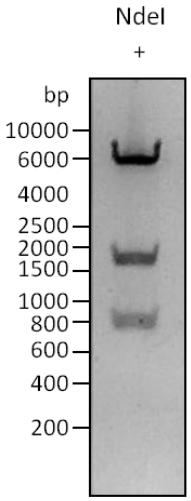
D.
NdeI
+
bp
10000
6000
4000
2500
2000
1500
1000
800
600
400
200

Figure 6.3. Introduction of a sequence encoding an HA tag into the N-terminus of H2Bv3. A. The HA tag was amplified by PCR in two pieces. The first piece was amplified using primers H2Bv3-ch2 and H2Bv3HA-F and then cloned into pJET1.2 (I). The second fragment was amplified using H2Bv3HA-R-new and H2Bv3-HincII primers and also cloned into a separate pJET1.2 (II). After sequence confirmation the second fragment was cut out using NdeI and XbaI restriction endonucleases and ligated to the pJET1.2 vector carrying the first piece (I) digested with NdeI. The final construct was made by cutting out the desired HA-*h2b* fragment with AfeI and HincII restriction enzymes and ligating into the initial vector, pre digested with the same endonucleases (III). B. Plasmid DNA from the ampicillin resistant colonies carrying vector I was verified by digestion analysis using PstI and XbaI restriction endonucleases and resolved on a 1% agarose gel. Expected fragment sizes are 931bp and 2822bp. One representative colony is shown. C. Plasmid DNA from ampicillin resistant colonies carrying vector II was verified by digestion analysis using PstI and XbaI restriction endonucleases. Expected fragment sizes are 502bp and 3451bp. One representative colony is shown. C. The final vector construct was verified by digestion analysis using NdeI endonuclease which has recognition sites in the HA-tag, BSR cassette and in the *h2b* flanking region. Expected fragment sizes are 809, 1609 and 5609 bp.

6.2.2.2 HA-tagged H2B expression, strain analysis

In order to generate a strain with an HA tag inserted into the endogenous *h2b* gene, the fragment containing the *h2b* gene and its flanking regions, N-terminal HA-tag and blasticidin resistance cassette was excised using PvuI and BstEII restriction endonucleases and electroporated into *Dictyostelium* AX2 cells. After two weeks incubation with blasticidin, more than 150 antibiotic resistant clones were picked for subsequent analysis. Resistant clones were pooled and the presence of the BSR cassette in the pooled colonies was checked by performing colony PCR using primers complimentary to the BSR cassette and either the 3' flanking region in the inserted fragment or the genomic DNA outside of the 3' *h2b* gene flanking region used for cloning (Fig. 6.4 A). 18 positive pools were identified as containing correct integration at the 3' end. However, only five of these were positive in the screen of individual colonies using the same PCR conditions (Fig. 6.4 B). This screening step indicated that the selected colonies contain clones with integration or at least partial integration of the gene replacement construct at the endogenous *h2b* locus. All five positive colonies and one negative control colony were expanded for further screening. The next step was to check if the selected colonies contained clones with the HA-tag integrated. To do this, PCR was performed using sets of primers located on both sides of the *h2b* N-terminal region (Ch2.1 and Ch3) or HA-tag primer (screenHA) and 5' *h2b* flanking region primer (Ch3) (Fig. 6.4 C). Only two out of five colonies gave a band of the correct size when using the HA-tag primer indicating that only in these two cases the construct was correctly integrated at both ends (Fig. 6.4 D upper panel). However, PCR amplification across the HA tag insertion site revealed the presence of two bands using genomic DNA from both of those positive samples (Fig. 6.4 D lower panel). Band sizes are consistent with the presence of *h2b* sequences both with and without the sequences encoding the HA tag. These data could suggest the presence of a mixed population of cells with and without full construct integration in i1 and i2 cultures so another round of

individual clone selection was carried out. Unfortunately, any attempts to isolate individual clones containing the full construct integration derived from i1 or i2 cells were unsuccessful (see Appendix 2 for more detail). Taken together, all these data suggest that the introduction of an HA-tag to the N-terminus of endogenous H2B histone was not successful and the strategy might be lethal for *Dictyostelium* cells.

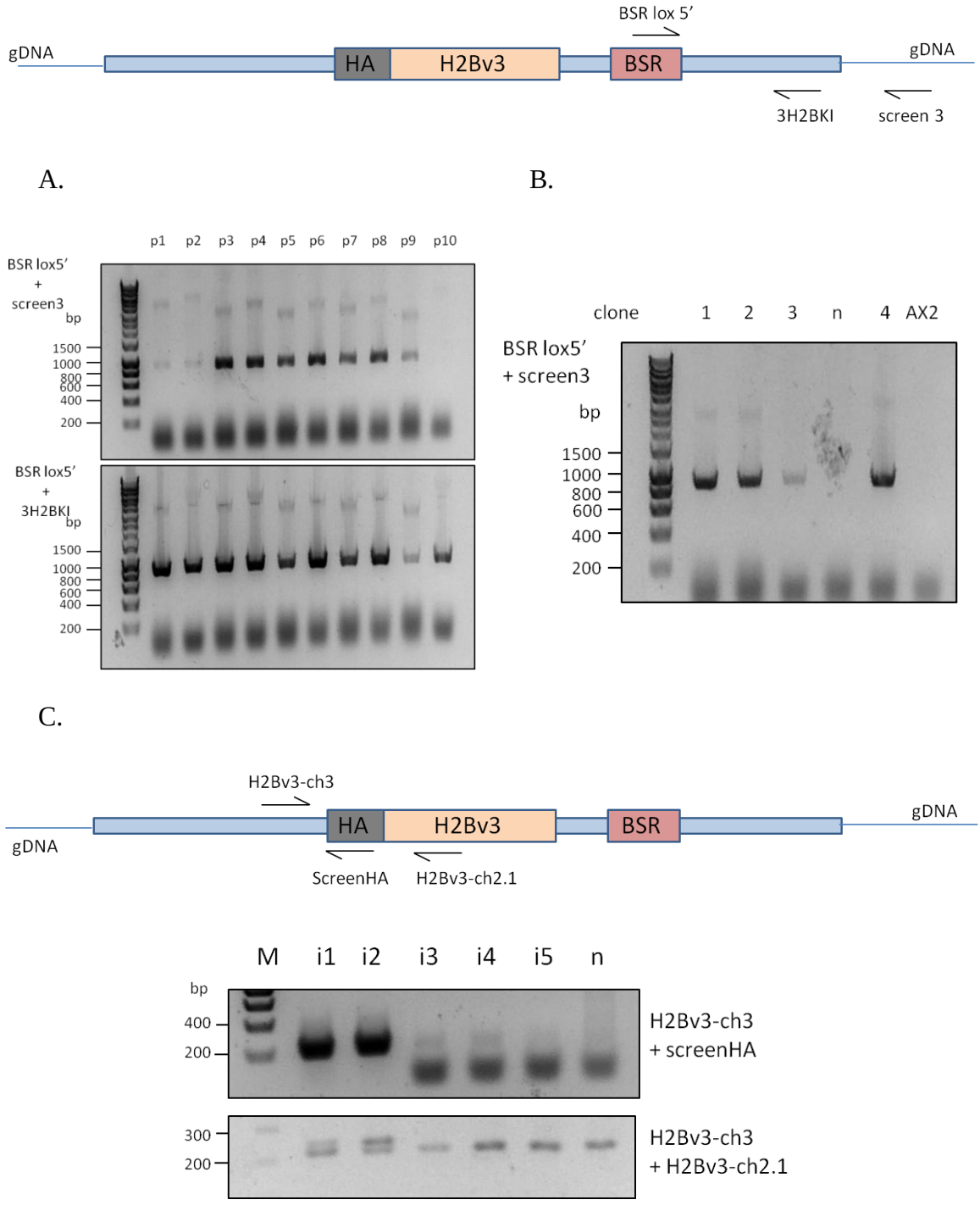

Figure 6.4. Verification of insertion of sequences encoding HA tag into the endogenous *h2b* gene. A. A representative gel of PCR screen using BSRlox5 and either H2Bv3KI or H2Bscreen3 primers. Samples were resolved on a 1% agarose gel. Expected fragment sizes is 832bp C. PCR screen of the individual colonies using BSRlox5 and screen3 primers. Samples were resolved on the 1% agarose gel. 5 out of 18 colonies tested are shown. Expected fragment sizes is 971bp D. Genomic DNA from individual colonies were screened by PCR using H2Bv3-ch3 and either screenHA (upper panel) or H2Bv3-ch2.1 (lower panel) primers. Samples were resolved on 1% and 2% agarose gels respectively. Expected fragment sizes are 228bp in the absence of the sequences encoding the tag, and 255bp in its presence.

6.2.3 Generation of strains expressing epitope-tagged H2B

Since the introduction of the HA tag to the endogenous *Dictyostelium* H2B histone was not successful, it was decided to generate strains overexpressing a tagged version of H2B in addition to the endogenous H2B protein. Three H2B overexpression vectors were obtained from the lab of Prof. Wolfgang Nellen: two extrachromosomal vectors introducing C-terminal 3xFlag or 6xMyc tags to H2B (pDBSRXP-H2B-3xFlag and pDBSRXP-H2B-6xMyc) carrying the blasticidin resistance cassette and an integrating vector with N-terminal 6xMyc tag (pDneo-6xMyc-H2B) carrying resistance to G418 (Dubin and Nellen, 2010). All three vectors were electroporated separately into *Dictyostelium* AX2 cells, followed by selection with blasticidin or G418, and the expression of the tagged histones was investigated in the antibiotic resistant pools by lysing cells and analyzing whole cell extracts by Western Blot using antibodies against the respective tags (Fig. 6.5 A). Interestingly, only the C-terminal tagged histones were found to be detectably expressed in the cells but not the N-terminal 6xMyc tagged H2B, although cells containing the vector were resistant to G418 indicating that the vector was integrated into the *Dictyostelium* genome. These data are consistent with the previously found inability to detect expression of the N-terminal HA-tagged H2B histone from the integrated construct (section 6.2.2).

It was then tested whether the C-terminally tagged H2B histones were incorporated into chromatin. For this, chromatin fractions were extracted from cells overexpressing tagged H2B and the presence of the respective tags investigated by Western blot (Fig. 6.5 B). Again, both 3xFlag-tagged and 6xMyc-tagged histones were presented in the chromatin fraction indicating their integration into chromatin in cells. However, gel mobility of the 6xMyc-tagged H2B histone was different from predicted. It ran at approximately 33kDa whereas the predicted molecular weight is 18.3kDa. Similar observations have been made for other proteins expressed using this expression vector (L. Mathews personal

communication). Therefore, it was decided to use the pDBSR-H2B-3xFlag extrachromosomal overexpression construct for further experiments.

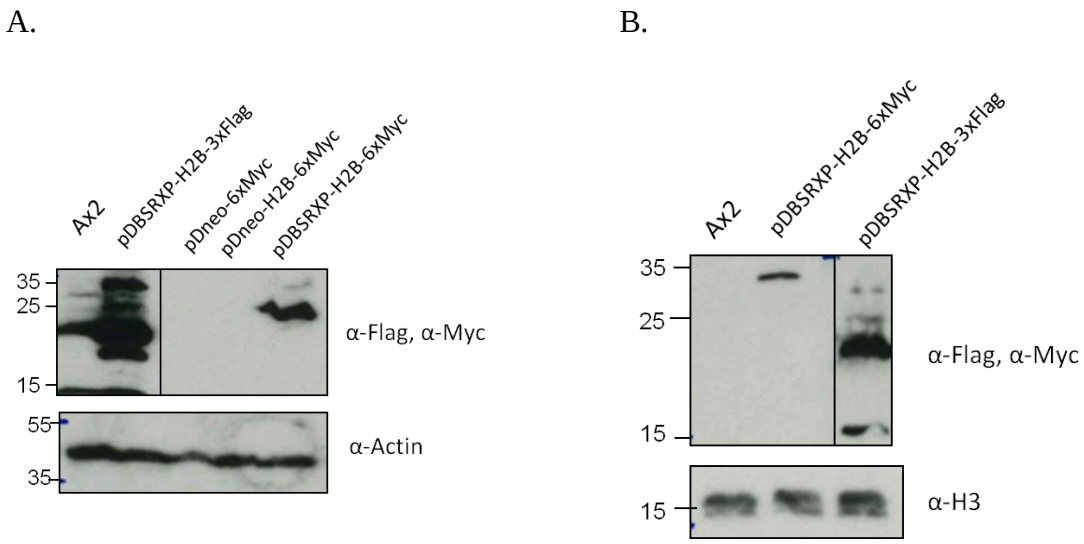

Figure 6.5. Expression of epitope-tagged H2B. A. Ax2 cells were transfected with the indicated vectors and selected for 10 days with respective antibiotics. Pools of resistant cells were then expanded in shaking suspension. Whole cell extracts were separated by 15% SDS-PAGE and analysed by Western blot using relevant primary antibodies. B. Selected AX2 cells described in A. were fractionated as described in methods to obtain a chromatin-enriched fraction and samples were analysed by Western blot using relevant primary antibodies.

6.2.4 Overexpressed histone H2B-3xFlag is ADP-ribosylated *in vivo*

Overexpressed H2B-3xFlag histones are expressed and incorporated into chromatin in AX2 cells. The next step was to see if this tagged histone could be ADP-ribosylated in response to DNA damage in living cells. To investigate this, an initial experiment was carried out in which AX2 cells overexpressing H2B-3xFlag or containing empty 3XFlag-tag vector were treated with DNA double-strand break inducing agent phleomycin for 1h followed by chromatin fraction purification. Chromatin extracts were then analysed by Western blot using polyclonal α-PAR antibody (Fig. 6.6 A) that has been used in the lab previously for *in vivo* ADP-ribosylation signal detection (see section 6.2.1). Unfortunately, the area where the H2B-3xFlag modification signal was expected had a high background signal and no specific signal was detected. In order to enrich for H2B-3xFlag histones, acid extraction procedure was carried out from H2B-3xFlag and 3xFlag expressing cells treated with phleomycin but this also did not reveal any signal corresponding to H2B-3xFlag (data not shown).

Polyclonal α-PAR antibody has been shown to not be suitable for detection of the H2B ADP-ribosylation by Adprt1a *in vitro*. By contrast, H2B ADP-ribosylation signal can be robustly detected using anti-pan-ADP-ribose binding reagent (see chapter 5, section 5.2.2). Therefore detection of the *in vivo* modification of H2B-3xFlag using this anti-pan-ADP-ribose binding reagent was carried out (Fig. 6.6 B). Cells overexpressing H2B-3xFlag or empty vector control were treated with phleomycin and chromatin-enriched fractions were analysed by Western blot (Fig. 6.6 B). Although the signal in the area of H2B-3xFlag was clearer than that of α-PAR antibodies there were still no apparent difference in the samples from control cells and cells expressing tagged H2B with many bands in this area.

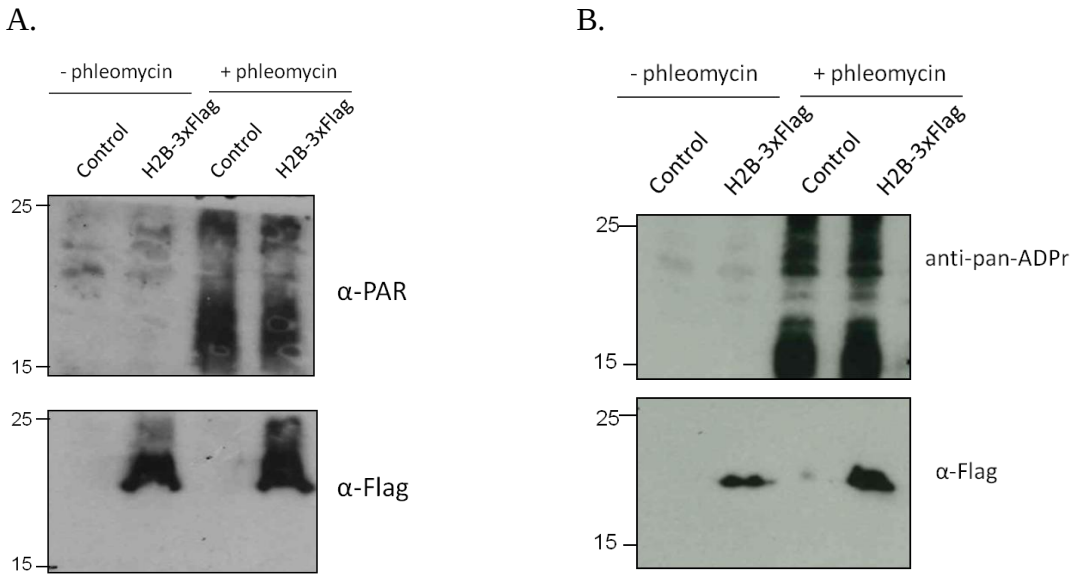

Figure 6.6. No evidence for poly-ADP-ribosylation of H2B-3xFlag *in vivo*. A. AX2 cells overexpressing 3xFlag-tagged H2B or 3xFlag-tag were treated with 300μg/ml phleomycin for 1h or mock treated and then chromatin fractions were extracted. Chromatin samples were resolved on an 18% SDS polyacrylamide gel for 10h and analysed by Western blot using polyclonal α-PAR antibodies. A representative gel of at least three experiments is shown. B. AX2 cells overexpressing H2B-3xFlag were treated with 300μg/ml phleomycin for 1h or mock treated and then chromatin fractions were extracted. Chromatin samples were resolved by 18% SDS-PAGE for 10h and analysed by Western blot using anti-pan-ADP-ribose binding reagent. A representative gel of at least three experiments is shown. Stripping and reprobing the blots with anti-Flag antisera confirmed the presence of H2B-3xFlag.

In order to enrich for the H2B-3xFlag immunoprecipitation was performed following chromatin enrichment using α-Flag antibody and precipitates were analysed using anti-pan-ADP-ribose binding reagent (Fig. 6.7 A). A clear signal of ADP-ribosylation at the expected size of H2B-3xFlag was apparent in the cells overexpressing H2B-3xFlag but not in the controls. This suggests that H2B-3xFlag is ADP-ribosylated in chromatin following DNA double-strand break induction *in vivo*.

This was confirmed by analysing acid extracts which are enriched in histones, isolated from cells overexpressing H2B-3xFlag with or without treatment with phleomycin, and using the anti-pan-ADP-ribose binding reagent to detect the modification (Fig. 6.7 B). The ADP-ribosylation of H2B-3xFlag was detected in the phleomycin treated sample but was absent in the control cells containing empty vector or in the absence of DNA damage. The signal ran at same position as H2B-3xFlag judged by the α-Flag blot obtained by stripping and re-probing the same membrane. Additionally, H2B-3xFlag ADP-ribosylation signal was only recognised by anti-pan but not anti-poly-ADP-ribose reagent (Fig. 6.7 C). Together these findings show that H2B-3xFlag can be overexpressed and incorporated into chromatin in *Dictyostelium* cells and is ADP-ribosylated in response to phleomycin treatment. The ability of the anti-pan-ADP-ribose binding reagent to detect the signal which could not be detected by the anti-poly-ADP-ribose binding reagent or the α-PAR antibody is consistent with this modification being due to mono or short chain ADP-ribosylation. This is the first evidence that histone H2B is ADP-ribosylated in response to DNA damage in *Dictyostelium in vivo*.

A.

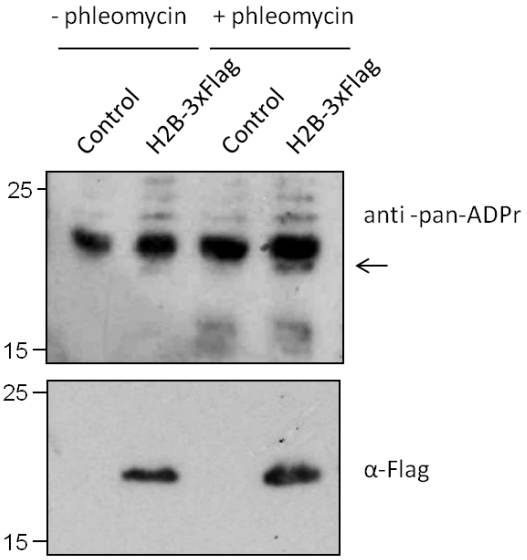
- phleomycin
+ phleomycin
Control
H2B-3xFlag
Control
H2B-3xFlag
25
15
anti -pan-ADPr
25
15
α-Flag

B.

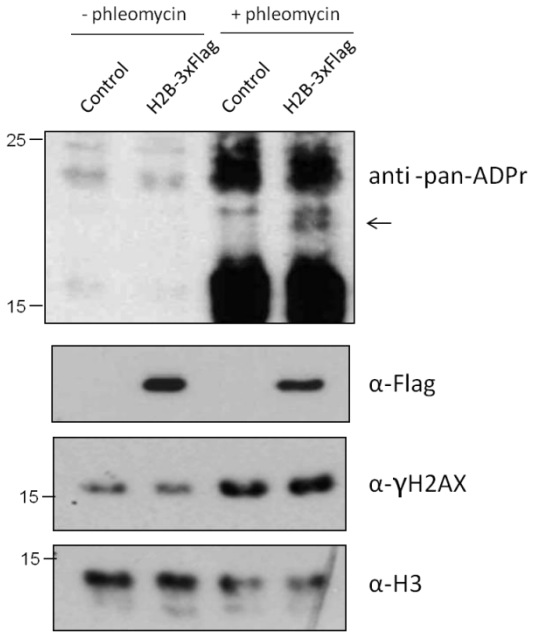
- phleomycin
+ phleomycin
Control
H2B-3xFlag
Control
H2B-3xFlag
25
15
anti -pan-ADPr
α-Flag
15
α-γH2AX
15
α-H3

C.

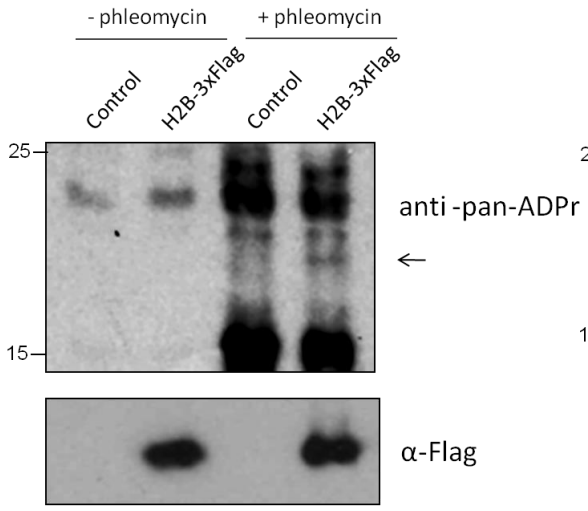
- phleomycin
+ phleomycin
Control
H2B-3xFlag
Control
H2B-3xFlag
25
15
anti -pan-ADPr
α-Flag

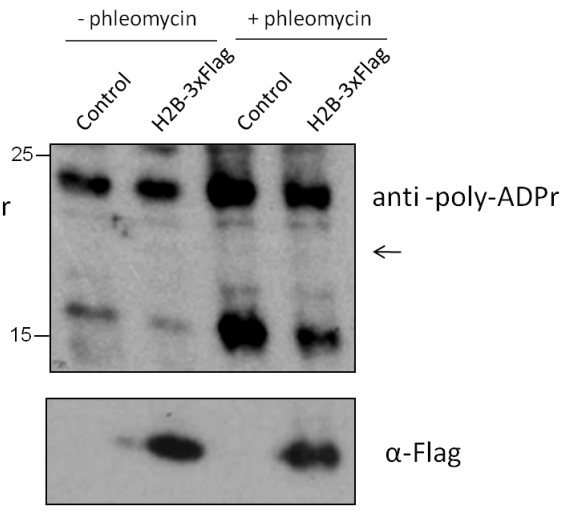
- phleomycin
+ phleomycin
Control
H2B-3xFlag
Control
H2B-3xFlag
25
15
anti -poly-ADPr
α-Flag

Figure 6.7. *In vivo* ADP-ribosylation of H2B-3xFlag A. AX2 cells overexpressing H2B-3xFlag or control cells containing empty vector were treated with 300μg/ml phleomycin for 1h or mock treated and then chromatin fraction was extracted. Proteins were then released from chromatin by boiling in 4% SDS. Following dilution, immunoprecipitation was then carried out using α-Flag antibody as described in Methods. Immunoprecipitation samples were analysed by Western blot using α-pan-ADP-ribose binding reagent. Blots were stripped and reprobed using α-Flag antibody to confirm the presence of H2B-3xFlag. H2B modification is indicated with arrow B. AX2 cells overexpressing H2B-3xFlag or control cells containing empty vector were treated with 300μg/ml phleomycin for 1h or mock treated and then histones were enriched by acid extraction as described in Methods. Samples were then resolved by 18% SDS-PAGE for 10h and analysed by Western blot using indicated antibodies. H2B modification is indicated with arrow A representative gel of at least three experiments is shown. Blots were stripped and reprobed using α-Flag antibody to confirm the presence of H2B-3xFlag. The same samples were probed using α-H2AX to confirm the presence of DNA damage and α-H3 to confirm equal loading of histones. C. AX2 cells overexpressing H2B-3xFlag or control cells containing empty vector were treated with 300μg/ml phleomycin for 1h or mock treated and then histones were enriched by acid extraction as described in Methods. Samples were then resolved by 18% SDS-PAGE for 10h and analysed by Western blot using either anti-pan or anti-poly-ADP-ribose binding reagent. Expected areaof H2B modification signal is indicated with arrow. Blots were stripped and reprobed using α-Flag antibody to confirm the presence of H2B-3xFlag.

6.2.5 ADP-ribosylation of H2B E to A point mutants *in vivo*

6.2.5.1 Generation of vectors to drive overexpression of H2B E to A point mutant proteins in Dictyostelium

After showing that H2B can be ADP-ribosylated in *Dictyostelium in vivo* I wanted to determine if the modification sites identified for Adprt1a ADP-ribosylation of H2B by *in vitro* point mutation analysis (chapter 5) were modified in living cells. To do this extrachromosomal vector constructs were made for overexpression of H2B-3xFlag with glutamate residues E18, E19 or both E18 and E19 mutated to alanine. The coding sequences of the *h2b* gene with point mutations were already available in pQE30 expression vectors (described in chapter 5 section 5.2.4). To incorporate these mutations into the *Dictyostelium* extrachromosomal vector the H2B coding region, including the start but not stop codon was amplified by PCR from each of the pQE30-H2B constructs using primers introducing PstI and BamHI restriction endonuclease sites at the 5' and 3' ends respectively for further cloning (Fig. 6.8 A). The PCR products were then cloned into intermediate pJET1.2 vectors and confirmed by sequencing. The H2B coding sequence was then excised using PstI and BamHI endonucleases and cloned into the pDBSRXP-3xFlag backbone cut with the same enzymes. Final clones were confirmed by digestion analysis with HindIII and sequencing (Fig. 6.8 B).

A.

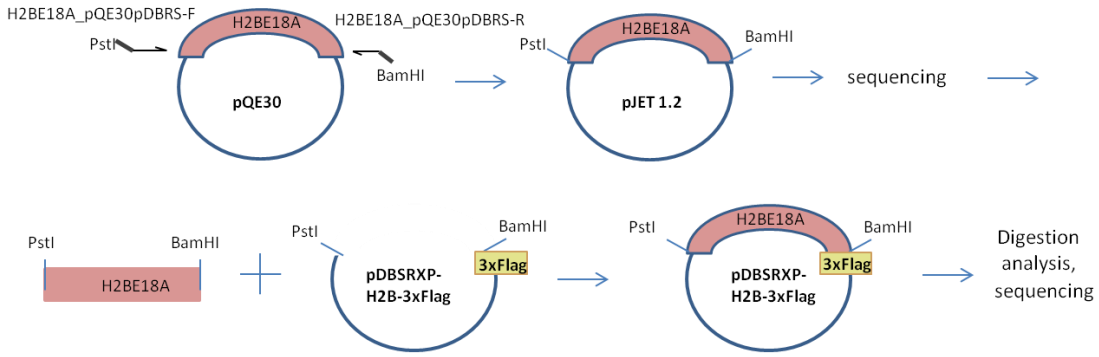

B.

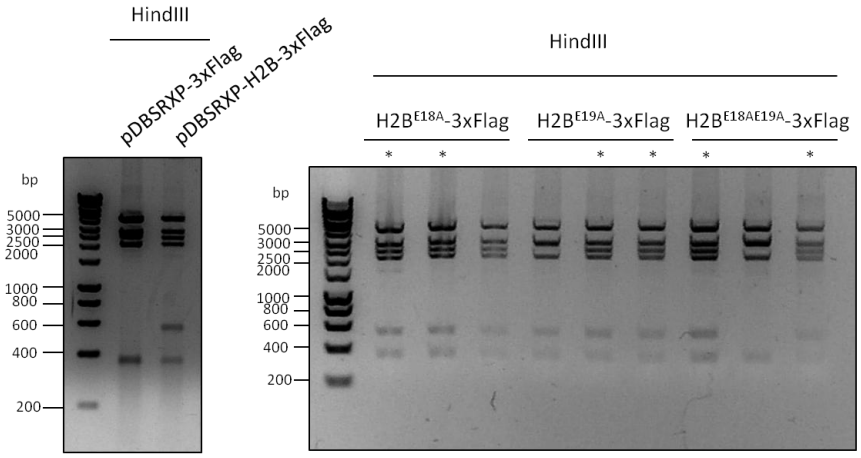

Figure 6.8. Generation of H2B-3xFlag E to A *Dictyostelium* overexpression vectors. A. A schematic representation of the cloning strategy. H2B E to A coding regions were amplified by PCR from the relevant pQE30-H2B^{EtoA} vector using H2BE18A_pQE30pDBSR_F and H2BE18A_pQE30pDBSR_F primers and cloned into pJET1.2. The coding fragment was then excised using PstI and BamHI restriction endonucleases and was ligated into the pDBSRXP-3xFlag backbone cut with the same enzymes. B. The final constructs were verified by restriction digestion by HindIII. The required fragment pattern is shown by comparison to the original unmutated pDBSRXP-H2B-3xFlag vector. Two colonies were selected for each mutant for further analysis (marked with stars).

6.2.5.2 In vivo ADP-ribosylation of overexpressed H2B-3xFlag E18A, E19A and E18E19A proteins

As for the wild-type H2B-3xFlag, the ability of $H2B^{EtoA}$-3xFlag proteins to be expressed and incorporated into chromatin in living cells was determined. For this pDBSRXP-$H2B^{EtoA}$-3xFlag constructs were electroporated into *Dictyostelium* AX2 cells, selected with blasticidin and then whole cells extracts were made from pools of resistant cells. Expression of the desired proteins was judged by Western blot using the α-Flag antibody (Fig. 6.9 A). All H2B-3xFlag histones were overexpressed at similar levels in AX2 cells. Then the ability of the proteins to incorporate into chromatin was investigated. To do this, chromatin fractions were purified from the cells overexpressing wild type H2B-3xFlag and its E to A mutants and chromatin extracts were analysed by Western blot (Fig. 6.9 B). In this case also all $H2B^{EtoA}$-3xFlag mutants as well as unmutated H2B were present in the chromatin fraction to an equal extent suggesting the ability to incorporate into chromatin was not affected by the introduced mutations.

The proportion of the overexpressed histones in chromatin relative to the endogenous H2B was investigated. To do this a *Dictyostelium* α-H2B antibody generated in our laboratory (Dr. Seiji Ura, personal communication) was used to detect both the endogenous and tagged H2B histones in the chromatin samples (Fig. 6.9 B). For all of the Flag-tagged H2B proteins the expression was much less than that of the endogenous H2B histone. This proportion remained the same in different sets of transfections and didn't depend on the transfection conditions (data not shown).

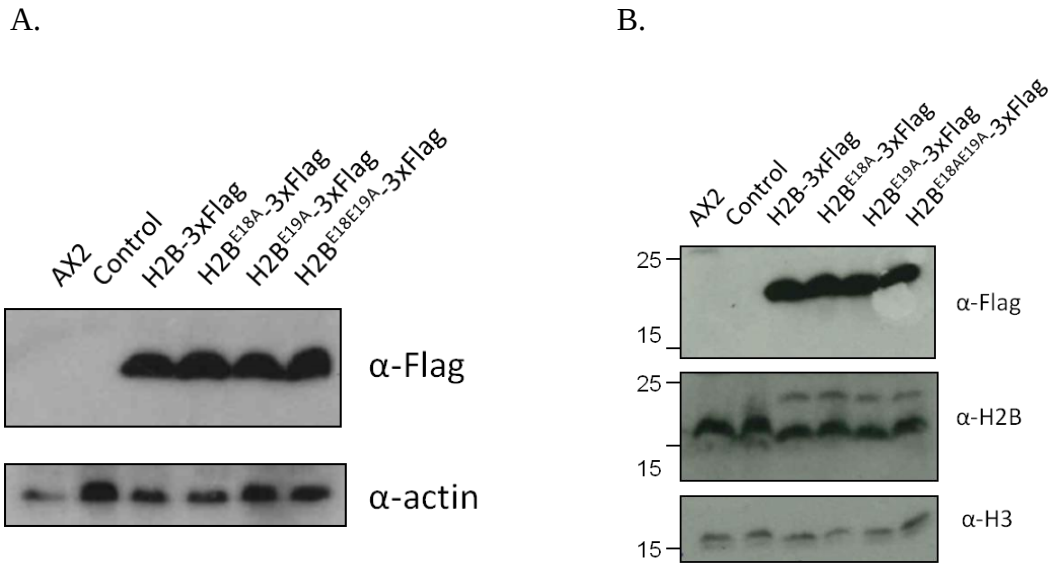

Figure 6.9. Characterisation of strains overexpressing H2B-3xFlag E to A point mutations. A. Ax2 cells were transfected with the indicated vectors and selected for 10 days with blasticidin. Surviving cells were then expanded in pools in shaking suspension and lysed as described in methods. Whole cells extracts were then separated by 18% SDS-PAGE and analysed by Western blot using α-Flag primary antibodies. The blot was stripped and reprobed with actin to confirm equal loading. B. Pools described in A. were fractionated as described in methods to obtain chromatin fractions and samples were analysed by Western blot using the indicated primary antibodies. Probing with a-H3 confirmed equal loading.

Next the ADP-ribosylation status of $H2B^{E18A}$-3xFlag, $H2B^{E19A}$-3xFlag and $H2B^{E18AE19A}$-3xFlag proteins was investigated. Overexpression pools were treated with phleomycin, histone-enriched fractions were obtained using the acid extraction method and then the extracts were analysed by Western blot using α-pan-ADP-ribose binding reagent (Fig. 6.10). The level of ADP-ribosylation of $H2B^{E19A}$-3xFlag protein was comparable to that of H2B-3xFlag. The $H2B^{E18A}$-3xFlag showed a slight decrease in the modification signal, but $H2B^{E18A\text{-}E19A}$-3xFlag double-mutant ADP-ribosylation was reduced to a greater extent compared to the wild type H2B-3xFlag.

Taken together these results show that the mutated versions of H2B-3xFlag are overexpressed and incorporated into chromatin to a similar extent as the wild-type protein. The H2B-3xFlag protein lacking both predicted ADP-ribosylation target residues glutamate E18 and E19 is modified to a lesser extent than the wild-type H2B-3xFlag, although replacing just one of the sites does not have a large effect on the extent of ADP-ribosylation.

A.

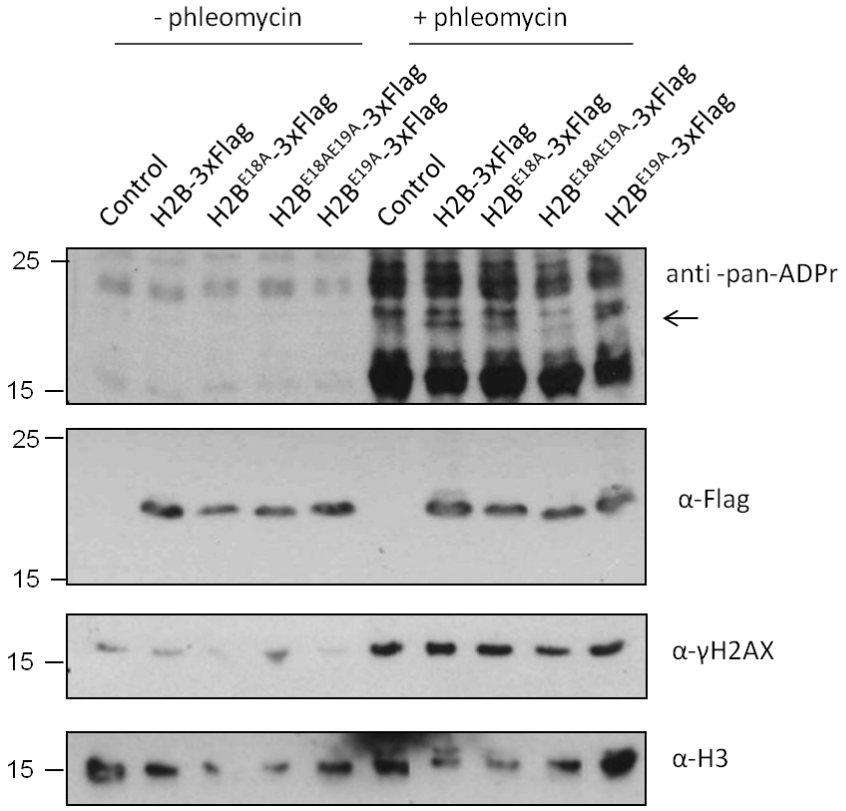
- phleomycin
+ phleomycin
Control
H2B-3xFlag
H2B^E18A-3xFlag
H2B^E18AE19A-3xFlag
H2B^E19A-3xFlag
Control
H2B-3xFlag
H2B^E18A-3xFlag
H2B^E18AE19A-3xFlag
H2B^E19A-3xFlag
25
15
anti -pan-ADPr
25
15
α-Flag
15
α-γH2AX
15
α-H3

B.

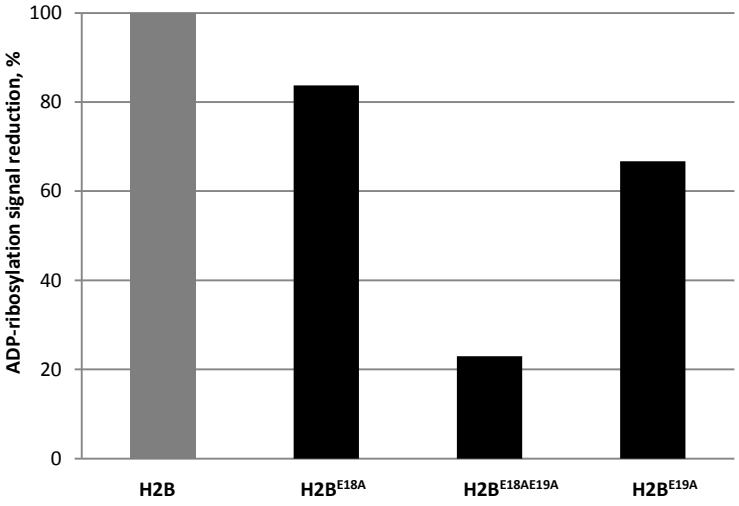
ADP-ribosylation signal reduction, %
100
80
60
40
20
0
H2B
H2B^E18A
H2B^E18AE19A
H2B^E19A

Figure 6.10. *In vivo* ADP-ribosylation of $H2B^{E18A}$-3xFlag, $H2B^{E19A}$-3xFlag and $H2B^{E18AE19A}$-3xFlag proteins. A. AX2 cells overexpressing H2B-3xFlag or point mutated versions as indicated were treated with 300μg/ml phleomycin for 1h or mock treated and then histones were enriched by acid extraction as described in methods. Samples were then resolved by 18% SDS-PAGE for 10h and analysed by Western blot using indicated antibodies. H2B modification is indicated with arrow. A representative gel of two experiments is shown. B. Quantification of the ADP-ribosylation signal for overexpressed H2B-3xFlag, $H2B^{E18A}$-3xFlag, $H2B^{E19A}$-3xFlag and $H2B^{E18AE19A}$-3xFlag proteins. ADP-ribosylation carried out as in A was quantified by comparison of relative signal intensities using ImageJ. Signal reduction relative to H2B-3xFlag is shown.

Only a small proportion of the H2B histone in chromatin fractions is H2B-3xFlag protein with the majority being endogenous H2B protein. This means that it is unlikely that any phenotypic difference in the cells overexpressing these mutated versions of H2B would be observed. However, retention of Ku70/80 on chromatin following DNA damage was investigated in these strains. In our laboratory it has been shown previously that *Dictyostelium* cells lacking the Adprt1a ADP-ribosyl transferase are deficient in NHEJ and specifically have a deficiency in the recruitment or retention of Ku70/80 on chromatin following DSB induction (Couto et al., 2011). Since in this work Adprt1a was shown to ADP-ribosylate histone H2B *in vitro* I hypothesised that this modification has a role in NHEJ and in retention of NHEJ factors on chromatin including the Ku70/80 heterodimer. To investigate this, H2B-3xFlag overexpressing strains were treated with phleomycin for 1h and then chromatin fractions were analysed by Western blot using *Dictyostelium* α-Ku80 antibody (Fig. 6.11). Treatment with Phleomycin caused an increased association of Ku80 with the chromatin fraction, as previously observed (Couto et al., 2011) but there was no difference observed in the amount of Ku80 in the chromatin fractions from cells expressing any $H2B^{EtoA}$-3xFlag proteins compared to the wild-type H2B-3xFlag strains or strains transfected with empty vector. Probing the blots with a-Flag and a-H2B antibodies confirmed the incorporation of the proteins in to chromatin, with H3 confirmed equal loading.

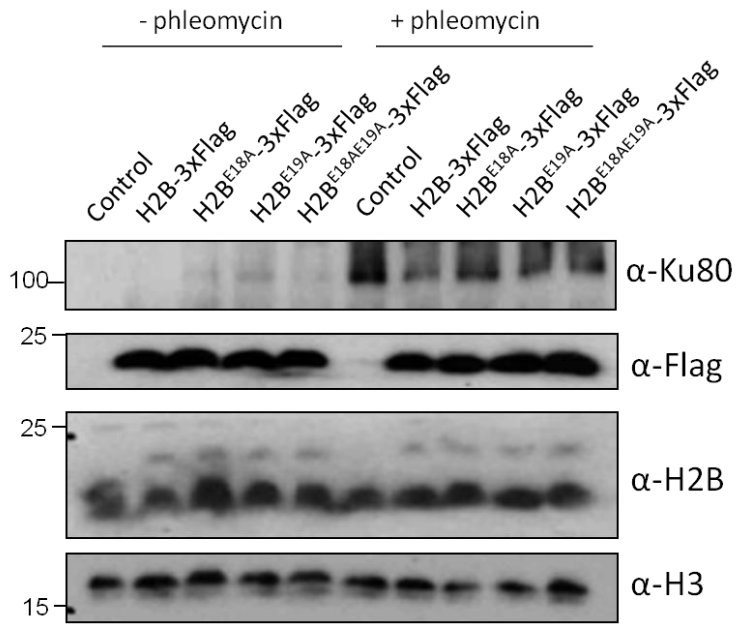

Figure 6.11. Recruitment of Ku80 to chromatin following double strand breaks in strains overexpressing $H2B^{EtoA}$-3xFlag proteins. AX2 cells overexpressing H2B-3xFlag or its point mutant derivatives were treated with 300μg/ml phleomycin for 1h or mock treated and then chromatin fractions extracted. Chromatin samples were resolved on an 18% polyacrylamide gel for 10h and analysed by Western blot using indicated antibodies.

6.3 Discussion

In this chapter the ADP-ribosylation of histone H2B *in vivo* in *Dictyostelium* was addressed. An attempt was made to introduce an N-terminal HA-tag into the endogenous H2B but was unsuccessful. This could be due to the size of the tag or to its location at the N-terminus. Although there are several studies utilising both N- and C-terminally tagged histone overexpression models for live cell histone tracking and investigating histone function in cellular processes (Benson et al., 2006; Conn et al., 2011; Harada et al., 2015; Kimura and Cook, 2001; Schaniel and Moore, 2009), the presence of the tag on the N-terminal end of endogenous H2B histone could affect post-translational modifications known to occur on the N-terminal tail (Stevense et al., 2011), prevent interaction with its chaperone and be detrimental to cell growth in the absence of any untagged protein. It is possible that the presence of a C-terminal tag on the endogenous H2B could be less harmful for the cells and it would be possible to attempt to introduce a tag into the endogenous protein in this position; however there are still post-translational modification sites located on that end that could also affect the cell viability (Stevense et al., 2011). Additionally, introduction of the BSR cassette into the genome could affect the expression of the gene located downstream of the *h2b* coding sequence although the function of the gene is unknown (dictyBase).

Next the expression of the C-terminal Flag-tagged H2B, driven from an extrachromosomal overexpression vector, and its incorporation into chromatin was shown. Moreover H2B-3xFlag was demonstrated to be ADP-ribosylated in response to DSBs. ADP-ribosylated H2B-3xFlag was immunoprecipitated from the chromatin enriched fraction and was present in histone-enriched acid extracts following the exposure of cells to phleomycin. The ability of the anti-pan-ADP-ribose binding reagent to detect the signal

corresponding to tagged H2B which could not be detected by the anti-poly-ADP-ribose binding reagent or the α-PAR antibody is consistent with H2B modification being mono- or short chain ADP-ribosylation. Interestingly, both anti-pan- and anti-poly-ADP-ribose binding reagents, as well as the α-PAR antibody, revealed a strong signal of ADP-ribosylation in both chromatin and histone-enriched samples in the area where core histones are resolved suggesting the possibility of other core histone being mono- or poly-ADP-ribosylated. This observation is in agreement with the potential ADP-ribosylation of histone H2A, H3b and H4 detected in *in vitro* analysis (chapter 5, section 5.2.2). Therefore it would be interesting to investigate the ADP-ribosylation status of these histones *in vitro* and its validity in cells.

Furthermore, the validity of the H2B ADP-ribosylation sites mapped *in vitro* was investigated. H2B-3xFlag histone in which both E18 and E19 have been mutated to alanine was shown to be modified to a lesser extent than wild-type H2B-3xFlag in cells treated with phleomycin. Interestingly, the E18 residue alone was identified to be the predominant acceptor site of Adprt1a-mediated ADP-ribosylation *in vitro* but changing this residue alone did not lead to a decrease in modification *in vivo*. Similarly, *in vitro* mutation of E19 led to a large increase in ADP-ribosylation by Adprt1a and this increase was not apparent *in vivo*. This could be due the different exposure of the residues in the context of chromatin as opposed to isolated recombinant H2B histone. It would be interesting to investigate the ADP-ribosylation of the $H2B^{EtoA}$ mutated proteins in the context of reconstituted nucleosomes to determine if the pattern is more similar to the *in vivo* findings. It is also possible that Adprt1a is not the ART, or not the only ART, responsible for the modification *in vivo*. It is known that Adprt2 also plays a role in ADP-ribosylation in response to DNA DSBs (Couto et al., 2011). This could be investigated by overexpressing the relevant proteins in cells lacking the genes encoding one or both of these ARTs. A third

possibility is the activity of enzymes which remove ADP-ribosylation which might act differently on the different substrates *in vivo*. The *Dictyostelium* genome contains a number of genes predicted to encode such enzymes (Perina et al., 2014).

The necessity to remove both glutamic acid residues in order to reduce the ADP-ribosylation could also reflect the potential ability of ARTs to modify residues located adjacent to, or in the region of, the main target site. Several studies have reported clusters of glutamate, aspartate and lysine residues to be targets for PARP1 and PARP2 auto-modification and for more recently discovered PARPs involved in different cellular processes (Chapman et al., 2013; Haenni et al., 2008; Vyas et al., 2014). Also, when mapping ADP-ribosylation sites on p53 only deletion of three potential sites located next to each other led to the abolishment of p53 modification by PARP1 while single mutations did not show such a great effect (Kanai et al., 2007). Furthermore, attempts were recently made to map ADP-ribosylation sites on BRCA1 *in vivo* but the modification was found to be present on a region of the DNA binding domain and was not mapped to a single specific site (Hu et al., 2014).

Despite the fact that there is evidence for the ADP-ribosylation of mammalian histones, including H2B, there is still nothing known about the functional role of this modification. Identification of the ADP-ribosylation of H2B in *Dictyostelium,* as well as mapping H2B modification sites, presents an ideal opportunity for investigating the functional significance of this modification in *Dictyostelium*. Therefore, the potential effect of loss of the H2B ADP-ribosylation on the DNA damage response is currently being investigated in our laboratory. As overexpressed H2B-3xFlag histone constituted a small proportion of the overall H2B protein in chromatin the strains described here are not ideal to determine the phenotype of the loss of H2B ADP-ribosylation. Therefore stains carrying E to A point

mutations in H2B that are similar to the ones described in this study but in the endogenous H2B gene have been made by gene replacement (Dr. Seiji Ura). Given the difficulty in introducing the HA-tag to the N-terminus of the endogenous H2B shown here, the point mutations were introduced into untagged H2B histone which can be detected using *Dictyostelium* α-H2B antibody generated in the lab. Interestingly, preliminary results suggest a decrease in ADP-ribosylation level of $H2B^{E18AE19A}$ double mutant compared to wild-type H2B (Dr. Seiji Ura personal communication). These strains will provide a valuable resource to determine the functional significance of this modification.

7 General discussion

Histones variants and histone post-translational modifications have been widely demonstrated to play a role in the cellular response to DNA damage. Histone acetylation, methylation, phosphorylation and ubiquitylation are known to regulate chromatin structure by promoting relaxation or compaction of chromatin, facilitate reorganisation of nucleosomes around the DNA break and promote recruitment of DNA repair factors (Escargueil et al., 2008; House et al., 2014).

In this work I investigate the ADP-ribosylation of core histones and its potential role in the DNA damage response in *Dictyostelium discoideum*. I have shown that, when using isolated recombinant histones as substrates, histone H2B is the major acceptor of ADP-ribosylation by recombinant Adprt1a in the presence of damaged DNA *in vitro*. Auto-modification of Adprt1a is predominantly mono-ADP-ribosylation and evidence is presented that modification of H2B may also be mono-ADP-ribosylation, as it is specifically recognised by a pan-ADP-ribose binding protein, but not one which only recognises poly ADP-ribosylation. I then showed that H2B is also a target of ADP-ribosylation *in vivo* as overexpressed epitope-tagged H2B-3xFlag was incorporated into chromatin and ADP-ribosylated in response to DNA DSB induction as shown both by western blot analysis of acid extracted histones and immunoprecipitation of chromatin associated proteins. Furthermore, glutamates E18 was identified as a site of ADP-ribosylation of recombinant H2B by Adprt1a and a role for this residue and the adjacent E19 was confirmed using overexpressed H2B-3xFlag *in vivo*. The next step will be to investigate the functional significance of these modifications and their role in DNA double-strand break repair pathways.

As for any histone post-translational modification the functional role of H2B ADP-ribosylation could be either direct via recruitment of DNA repair factors to the DNA break or indirect by introducing local changes to the chromatin structure and facilitating access of repair associated factors to the damaged site.

Recently, in mammalian cells PARP3 has been shown to be activated by DNA DSBs and perform mono-ADP-ribosylation of itself and linker histone H1 *in vitro* (Loseva et al., 2010; Rulten et al., 2011). Moreover, PARP3 has been proposed to participate in DSB repair via recruiting the PBZ domain containing protein APLF to the sites of DNA damage. The PBZ domain of APLF has been shown to have strong affinity for PAR chains and also to bind auto-modified PARP3 and ADP-ribosylated histone H1 (Rulten et al., 2008; Rulten et al., 2011). The latter is particularly interesting as this modification has been shown to be predominantly mono-ADP-ribosylation with a low amount of short oligo-ADP-ribosyl chains (Loseva et al., 2010; Rulten et al., 2011) whereas structural studies suggest that PBZ domains bind only polymers of ADP-ribose (Eustermann et al., 2010; Li et al., 2010a). However, it makes it possible to speculate that mono-ADP-ribosylation of H2B by Adprt1a could similarly be recognised by PBZ domain containing proteins in *Dictyostelium.*

In contrast to mammalian cells where only three proteins have been shown to contain PBZ domains (APL, APLF and CHFR), seven putative proteins are predicted to contain a PBZ motif in *Dictyostelium* (Ahel et al., 2008). Two of them, Ku70 and Rad17, are known DNA repair proteins (Morio and Kim, 2008; Parrilla-Castellar et al., 2004). Interestingly, the Ku70/80 heterodimer has already been shown to be recruited to chromatin in an Adprt1a-dependent manner and this recruitment is dependent on the presence of the PBZ domain of Ku70 (Couto et al., 2011). Deletion of the Ku70 PBZ domain also leads to decreased levels

of NHEJ, further confirming the importance of the domain. Since there is no information about the mechanism of the Adprt1a-dependent recruitment of Ku70/80 it could be possible for the recruitment to occur via, or be facilitated by, interaction with ADP-ribosylated H2B. In order to test this hypothesis interaction of Ku70 with ADP-ribosylated H2B should be investigated. Similarly to mammalian APLF, *in vitro* interaction of ADP-ribosylated H2B with Ku70 and Ku70 in which the PBZ domain has been deleted could be addressed by performing slot-blot assays or pull-down assays, detecting interaction by using antibodies against tagged recombinant proteins. The validity of the interaction could also be addressed in cells by looking at chromatin association of Ku70/80 in cells expressing wild-type H2B and $H2B^{E18AE19A}$. If proven, the functional significance of such interaction could be addressed *in vivo* by investigating the NHEJ efficiency of cells carrying $H2B^{E18AE19A}$ mutations in comparison to parental AX2 cells using the REMI assay.

Another DNA repair protein containing a PBZ domain in *Dictyostelium* is Rad17. Rad17 is known to function in ATR-dependent check point signalling by facilitating the loading of the 9-1-1 complex and subsequent activation of the check point kinase 1 (chk1) in response to DNA damage (Parrilla-Castellar et al., 2004). However, it has recently been shown to play a role in DNA DSB repair by homologous recombination by promoting recruitment of NBS1 and therefore MRN complex to the break in an MDC1-independent manner (Wang et al., 2014). This makes it possible to speculate that Rad17 could be recruited to the chromatin in an ART dependent manner in *Dictyostelium* and ADP-ribosylation of H2B could facilitate this recruitment. In this case, similarly to mammalian cells ADP-ribosylation could contribute to the pathway choice between end re-ligation via NHEJ or resection and repair by HR by promoting recruitment of either the Ku70/80 or MRN complex respectively. Unfortunately, to my knowledge neither Rad17 nor chk1-dependent

check-point activation have been studied in *Dictyostelium* although all major components of this pathway are conserved (dictyBase). It would therefore be interesting to look at the presence of this pathway and involvement of ADP-ribosylated H2B by addressing cell cycle progression following DNA damage in Ax2 and $H2B^{E18AE19A}$ cell lines.

Additionally, H2B mono-ADP-ribosylation signal could be recognised by proteins containing macrodomains, especially as these domains are believed to interact with monoADP ribosylated proteins (Karras et al., 2005). The *Dictyostelium* genome encodes six macrodomain containing proteins and three of them are currently annotated (dictyBase, Alasdair Gunn personal communication). Similarly to mammalian ARTs (ARTD7, 8 and 9), one of the predicted proteins containing an ART catalytic domain in *Dictyostelium*, pARTg, also includes a macrodomain (Aguiar et al., 2005). Recently ARTD9 has been reported to be recruited to laser microirradiation-induced DNA damage sites in a PARP1-dependent manner and this recruitment is dependent on the ARTD9 macrodomain (Yan et al., 2013). The PAR-dependent recruitment of ARTD9 then leads to recruitment of its binding partner, B-lymphoma and BAL-associated protein (BBAP) E3-ubiquitin ligase and subsequent recruitment of 53BP1 and BRCA1. pARTg could therefore be similarly recruited to DSBs in response to Aprt1a activity including H2B ADP-ribosylation. Thus, it would be interesting to investigate the chromatin association of the pARTg in the H2B E18AE19A strains.

Additionally, unlike mammals, *Dictyostelium* DNA Ligase III also contains a putative macrodomain suggesting a potential role of the latter in recruitment of Ligase III to DNA breaks. The *in vitro* interaction of ADP-ribosylated H2B and Ligase III, as well as *in vivo* recruitment of the latter to chromatin in $H2B^{E18AE19A}$ cells, could be investigated.

As mentioned earlier a potential role of H2B ADP-ribosylation could also be to alter the local chromatin structure at the site of a DSB caused by the introduction of a negatively charged ADP-ribosyl group. ADP-ribosylation has already been shown to cause chromatin relaxation. First, purified polynucleosomes have been demonstrated to have a more relaxed state when poly-ADP-ribosylated *in vitro* using electron microscopy and such relaxation has later been proposed to be due to the ADP-ribosylation of linker histone H1 (Frechette et al., 1985; Poirier et al., 1982). Later studies however have revealed a dual role for PARP1 itself on the status of chromatin as the binding of unmodified PARP1 leads to a more compact form of chromatin whereas addition of NAD^+ and subsequent PARP1 auto-modification reverses this effect (Kim et al., 2004). Recently, the latter has been confirmed by showing that in human cells decondensation of intact chromatin following DNA damage induced by UV laser microirradiation is dependent on PARP1 activity and is not directly linked to the known DNA damage chromatin remodelers (Izhar et al., 2015). Although the role of core histone ADP-ribosylation has not been identified in these studies, it is still unclear if the DNA damage induced ADP-ribosylation of H2B would further contribute to the chromatin relaxation effect of ARTs.

Interestingly, one of the post-translational modifications of H2B, mono-ubiquitylation (H2Bub1) on lysine K120 in the C-terminal tail, has been found to be actively involved in regulation of chromatin structure by altering local and high-order chromatin compaction (Chandrasekharan et al., 2009). Furthermore, the level of H2Bub1 has been shown to increase rapidly in response to DNA damage independently of transcription and the loss of this mono-ubiquitylation leads to reduced efficiency of both DNA DSB repair pathways (Moyal et al., 2011). H2Bub1 is also found to be required for efficient DNA end resection and recruitment of RAD51 and BRCA2 (Nakamura et al., 2011). Thus, H2B ADP-ribosylation could have a similar role by facilitating local chromatin relaxation at the break

and therefore facilitating access of the repair machinery and/or directly recruiting DNA repair factors via their ADP-ribosyl binding motifs.

In this study I have identified ADP-ribosylation of epitope-tagged H2B *in vivo*, mapped sites of H2B ADP-ribosylation by Adprt1a *in vitro* and shown that mutation of the discovered sites decreases modification of the overexpressed H2B in cells. These findings provide the basis of a mechanistic understanding of the importance of this modification.

Appendix

1. List of Primers used in this work.

Chapter 3. Role of histone H3 variants in DNA damage response in Dictyostelium.

Primer name	Sequence	Location
82409A	GGGGGTAGTGGTGGCGTT	DDB_G0282409
82409B	GGTCGTTGAGTGTATTGAGTT	DDB_G0282409
91974A2 (A)	CGGTAGCAACTGATTTGATTTT	DDB_G0291974
91974C (B)	GGTGAAGAACCTGGTAATGTA	DDB_G0291974
BSR lox 5’	GAGAAATGTTAAATTGATCC	BSR cassette
ARNot1	AGCTTGCGGCCGCA	HindIII site in pLPBLP

Chapter 5. Histone H2B ADP-ribosylation by Adprt1a in vitro

Primer name	Sequence	Location
3NH2B-new	CGACCCGGGTTAGTTTTTGCTTTCAGTTGGATTG	DDB_G0286509 *(h2bv3)*
N25H2B	CCAGGATCCATGACCCCAAAAGTAACCAAAACC	DDB_G0286509
E18qchF	ACTCAATCTGGTGCAGAGAAAACCGCTTCA	DDB_G0286509
E18qchR	TGAAGCGGTTTTCTCTGCACCAGATTGAGT	DDB_G0286509
E19qchF	ACTCAATCTGGTGAAGCGAAAACCG	DDB_G0286509
E19qchR	CGGTTTTCGCTTCACCAGATTGAGT	DDB_G0286509
E18-19qchF	ACTCAATCTGGTGCAGCGAAAACCG	DDB_G0286509
E18-19qchR	CGGTTTTCGCTGCACCAGATTGAGT	DDB_G0286509

Primer name	Sequence	Location
5H2BKI	CTTATACGATCGACTGATGCTGTAACAATAG	Chromosome 4 453224
3H2BKI	CCATATCATGGTGGATATTACCATGG	Chromosome 4 456713
H2Bv3HA-F	CCCTACCCATACGATGTTCCAGATTACGCTGTATTCGTTAAAGG	HA tag DDB_G0286509
H2Bv3HA-R-new	AGCATAATCTGGAACATCATATGGATATTTGAATTATATTAATTGACTATTGCAT	DDB_G0286509 HA tag
H2Bv3-HincII	TCTAGAGGATTGTACTTGTTGACAGCAGTCATACCTTGTAAG	DDB_G0286509
H2Bv3-ch2	GGAATTGACCAAAATTGGAAAGTGT	Chromosome 4 454341
BSR lox 5’	GAGAAATGTTAAATTGATCC	BSR cassette
screen3	GTCATTTATGGTCCACCAGACAC	Chromosome 4 456740
screenHA	AGCATAATCTGGAACATCATATGGATA	HA tag
H2Bv3-ch3	GACTTACCACACCAACTTTTTCG	Chromosome 4 454907
H2Bv3-ch2.1	GCTTTCTTTTGACCTTTAACG	DDB_G0286509
H2BE18A_pQE30 pDBSR_F	AAACTGCAGAAATGGTATTCGTTAAAGGTCAAAAG	DDB_G0286509
H2BE18A_pQE30 pDBSR_R	ACCGGATCCGTTTTTGCTTTCAGTTGGATTG	DDB_G0286509

2. Introduction of HA-tag to endogenous histone H2B. Strain verification.

PCR amplification across the HA tag insertion site using gDNA purified from the positive cultures revealed two cell cultures (i1 and i2) containing two bands at the predicted region and therefore potentially carrying integration of the gene disruption construct (chapter 6 Fig. 6.4). The presence of the two bands could suggest the presence of a mixed population of cells with and without full construct integration in i1 and i2 cultures so individual clone selection was carried out. To do this, the indicated colonies were resuspended in fresh media containing antibiotics, diluted and replated in 96-well plates. Surprisingly, very few colonies appeared after this step. Three individual clones from i1 and i2 cultures were analysed by PCR using the *h2b* N-terminal screen as described above (Fig. I A). Unfortunately, all clones from the i1 colony showed only the wild-type band indicating the absence of integration of the sequence encoding the HA tag. Surprisingly, single clones arising from the i2 culture again showed a double band in the desired area. This finding could either indicate the necessity of the more thorough individual clone selection or it could indicate more complex genomic arrangements, perhaps with duplication of the *h2b* gene before the integration or integration only at the 3'end. Although the desired result was to obtain HA-tagged H2B expressing cells, these possibilities could also meet the requirement of obtaining tagged-H2B expression for analysis of its modification, even if it was co-expressed with untagged H2B histone. Thus, the expression of the HA-tagged H2B was checked by preparing i2-1 and i2-2 cell lysates and analysing them by Western blot using α-HA antibody (Fig. I B). Unfortunately, there was no signal from HA in either of the samples. This could either indicate the inability of *Dictyostelium* cells to express N-terminal HA-tagged H2B or the presence of a high amount of cells without integration of the full construct masking the signal from the target cells. In order to check this, another round of individual clone selection was performed as described above by plating cells on

24-well plates. This time all individual colonies were screened by *h2b* N-terminus screening PCR (Fig. I C). Interestingly, a 15 clones again showed only the wild-type *h2b* band, 6 also gave the doublet but three individual clones showed only the upper band suggesting the presence of only HA-tagged *h2b* histone gene in their genomic DNA.

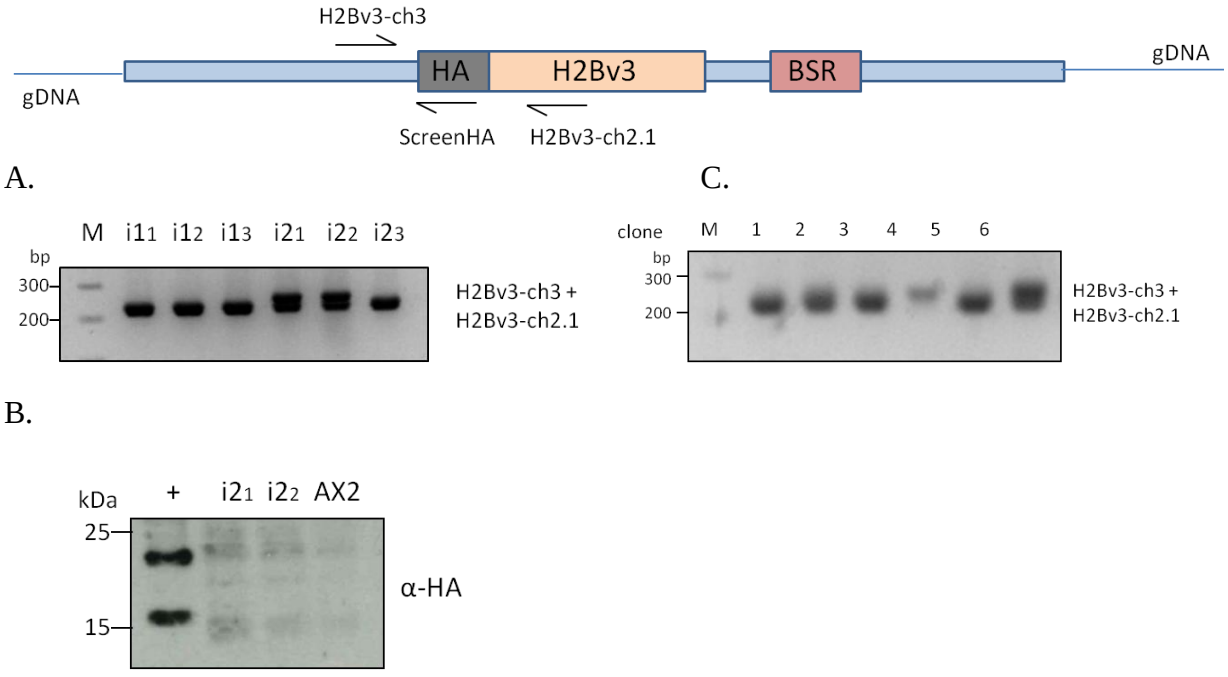

Figure I. Analysis of strains potentially expressing HA-tagged H2B. A.PCR verification of individual colonies obtained from re-cloning and blasticidin selection of i1 and i2 cultures. PCR was carried out using H2Bv3Ch3 and H2Bv3Ch2.1 primers and samples were resolved on a 2% agarose gel. Expected fragment sizes are 228bp in the absence of the sequences encoding the tag, and 255bp in its presence. B. Cells from two positive colonies $i2_1$ and $i2_2$ were lysed and lysates were resolved on 15% SDS-PAGE followed by Western blot analysis using α-HA primary antibody. A lysate from the same number of cells overexpressing an HA-tagged protein of a similar size is shown on the first lane as a positive control. C. Individual clones obtained from re-spreading and blasticidin selection of $i1_1$ and $i1_2$ were screened by PCR as described in A. Representative result of first 6 clones is shown.

Unfortunately, it was impossible to expand these cloned cells as any attempts to transfer the cells to the shaking expansion or SM-agar plates with *Klebsiella* or even 6-well plates resulted in cell death. Furthermore, it was also impossible to expand most of the individual clones from this screen that showed the double band. Eventually, only one clone showed some growth in culture. Western blot analysis was then performed of cell lysate from this to investigate the expression of the HA-tagged histone H2B in these cells. However, as in the previous experiment, there was no signal indicating the expression of any HA-tagged protein (data not shown). Taken together, all these data suggest that the introduction of an HA-tag to the N-terminus of endogenous H2B histone was not successful and the strategy might be lethal for *Dictyostelium* cells.

References

Adachi, N., Suzuki, H., Iiizumi, S., and Koyama, H. (2003). Hypersensitivity of nonhomologous DNA end-joining mutants to VP-16 and ICRF-193: implications for the repair of topoisomerase II-mediated DNA damage. J Biol Chem *278*, 35897-35902.

Adam, S., Polo, S.E., and Almouzni, G. (2013). Transcription recovery after DNA damage requires chromatin priming by the H3.3 histone chaperone HIRA. Cell *155*, 94-106.

Adamietz, P., and Rudolph, A. (1984). ADP-ribosylation of nuclear proteins in vivo. Identification of histone H2B as a major acceptor for mono- and poly(ADP-ribose) in dimethyl sulfate-treated hepatoma AH 7974 cells. J Biol Chem *259*, 6841-6846.

Aguiar, R.C., Takeyama, K., He, C., Kreinbrink, K., and Shipp, M.A. (2005). B-aggressive lymphoma family proteins have unique domains that modulate transcription and exhibit poly(ADP-ribose) polymerase activity. J Biol Chem *280*, 33756-33765.

Ahel, D., Horejsi, Z., Wiechens, N., Polo, S.E., Garcia-Wilson, E., Ahel, I., Flynn, H., Skehel, M., West, S.C., Jackson, S.P., *et al.* (2009). Poly(ADP-ribose)-dependent regulation of DNA repair by the chromatin remodeling enzyme ALC1. Science *325*, 1240-1243.

Ahel, I., Ahel, D., Matsusaka, T., Clark, A.J., Pines, J., Boulton, S.J., and West, S.C. (2008). Poly(ADP-ribose)-binding zinc finger motifs in DNA repair/checkpoint proteins. Nature *451*, 81-85.

Ahel, I., Rass, U., El-Khamisy, S.F., Katyal, S., Clements, P.M., McKinnon, P.J., Caldecott, K.W., and West, S.C. (2006). The neurodegenerative disease protein aprataxin resolves abortive DNA ligation intermediates. Nature *443*, 713-716.

Ahmad, K., and Henikoff, S. (2002). The histone variant H3.3 marks active chromatin by replication-independent nucleosome assembly. Mol Cell *9*, 1191-1200.

Alatwi, H.E., and Downs, J.A. (2015). Removal of H2A.Z by INO80 promotes homologous recombination. EMBO Rep *16*, 986-994.

Ali, A.A., Timinszky, G., Arribas-Bosacoma, R., Kozlowski, M., Hassa, P.O., Hassler, M., Ladurner, A.G., Pearl, L.H., and Oliver, A.W. (2012). The zinc-finger domains of PARP1 cooperate to recognize DNA strand breaks. Nat Struct Mol Biol *19*, 685-692.

Allen, M.D., Buckle, A.M., Cordell, S.C., Lowe, J., and Bycroft, M. (2003). The crystal structure of AF1521 a protein from Archaeoglobus fulgidus with homology to the non-histone domain of macroH2A. J Mol Biol *330*, 503-511.

Altmeyer, M., Messner, S., Hassa, P.O., Fey, M., and Hottiger, M.O. (2009). Molecular mechanism of poly(ADP-ribosyl)ation by PARP1 and identification of lysine residues as ADP-ribose acceptor sites. Nucleic Acids Res *37*, 3723-3738.

Ame, J.C., Rolli, V., Schreiber, V., Niedergang, C., Apiou, F., Decker, P., Muller, S., Hoger, T., Menissier-de Murcia, J., and de Murcia, G. (1999). PARP-2, A novel

mammalian DNA damage-dependent poly(ADP-ribose) polymerase. J Biol Chem *274*, 17860-17868.

Aravind, L. (2001). The WWE domain: a common interaction module in protein ubiquitination and ADP ribosylation. Trends Biochem Sci *26*, 273-275.

Ashworth, J.M., and Quance, J. (1972). Enzyme synthesis in myxamoebae of the cellular slime mould Dictyostelium discoideum during growth in axenic culture. Biochem J *126*, 601-608.

Audebert, M., Salles, B., and Calsou, P. (2004). Involvement of poly(ADP-ribose) polymerase-1 and XRCC1/DNA ligase III in an alternative route for DNA double-strand breaks rejoining. J Biol Chem *279*, 55117-55126.

Auer, B., Flick, K., Wang, Z.Q., Haidacher, D., Jager, S., Berghammer, H., Kofler, B., Schweiger, M., and Wagner, E.F. (1995). On the biological role of the nuclear polymerizing NAD+: protein(ADP-ribosyl) transferase (ADPRT): ADPRT from Dictyostelium discoideum and inactivation of the ADPRT gene in the mouse. Biochimie *77*, 444-449.

Ayoub, N., Jeyasekharan, A.D., Bernal, J.A., and Venkitaraman, A.R. (2008). HP1-beta mobilization promotes chromatin changes that initiate the DNA damage response. Nature *453*, 682-686.

Bai, P. (2015). Biology of Poly(ADP-Ribose) Polymerases: The Factotums of Cell Maintenance. Mol Cell *58*, 947-958.

Barski, A., Cuddapah, S., Cui, K., Roh, T.Y., Schones, D.E., Wang, Z., Wei, G., Chepelev, I., and Zhao, K. (2007). High-resolution profiling of histone methylations in the human genome. Cell *129*, 823-837.

Beck, C., Boehler, C., Guirouilh Barbat, J., Bonnet, M.E., Illuzzi, G., Ronde, P., Gauthier, L.R., Magroun, N., Rajendran, A., Lopez, B.S., *et al.* (2014). PARP3 affects the relative contribution of homologous recombination and nonhomologous end-joining pathways. Nucleic Acids Res *42*, 5616-5632.

Bekker-Jensen, S., and Mailand, N. (2011). The ubiquitin- and SUMO-dependent signaling response to DNA double-strand breaks. FEBS Lett *585*, 2914-2919.

Benjamin, R.C., and Gill, D.M. (1980). Poly(ADP-ribose) synthesis in vitro programmed by damaged DNA. A comparison of DNA molecules containing different types of strand breaks. J Biol Chem *255*, 10502-10508.

Bennardo, N., Cheng, A., Huang, N., and Stark, J.M. (2008). Alternative-NHEJ is a mechanistically distinct pathway of mammalian chromosome break repair. PLoS Genet *4*, e1000110.

Benson, L.J., Gu, Y., Yakovleva, T., Tong, K., Barrows, C., Strack, C.L., Cook, R.G., Mizzen, C.A., and Annunziato, A.T. (2006). Modifications of H3 and H4 during chromatin replication, nucleosome assembly, and histone exchange. J Biol Chem *281*, 9287-9296.

Berger, N.A., Weber, G., and Kaichi, A.S. (1978). Characterization and comparison of poly(adenosine dephosphoribose) synthesis and DNA synthesis in nucleotide-permeable cells. Biochim Biophys Acta *519*, 87-104.

Block, W.D., and Lees-Miller, S.P. (2005). Putative homologues of the DNA-dependent protein kinase catalytic subunit (DNA-PKcs) and other components of the non-homologous end joining machinery in Dictyostelium discoideum. DNA Repair (Amst) *4*, 1061-1065.

Boehler, C., Gauthier, L., Yelamos, J., Noll, A., Schreiber, V., and Dantzer, F. (2011a). Phenotypic characterization of Parp-1 and Parp-2 deficient mice and cells. Methods Mol Biol *780*, 313-336.

Boehler, C., Gauthier, L.R., Mortusewicz, O., Biard, D.S., Saliou, J.M., Bresson, A., Sanglier-Cianferani, S., Smith, S., Schreiber, V., Boussin, F., *et al.* (2011b). Poly(ADP-ribose) polymerase 3 (PARP3), a newcomer in cellular response to DNA damage and mitotic progression. Proc Natl Acad Sci U S A *108*, 2783-2788.

Bolderson, E., Savage, K.I., Mahen, R., Pisupati, V., Graham, M.E., Richard, D.J., Robinson, P.J., Venkitaraman, A.R., and Khanna, K.K. (2012). Kruppel-associated Box (KRAB)-associated co-repressor (KAP-1) Ser-473 phosphorylation regulates heterochromatin protein 1beta (HP1-beta) mobilization and DNA repair in heterochromatin. J Biol Chem *287*, 28122-28131.

Bork, P., Hofmann, K., Bucher, P., Neuwald, A.F., Altschul, S.F., and Koonin, E.V. (1997). A superfamily of conserved domains in DNA damage-responsive cell cycle checkpoint proteins. Faseb J *11*, 68-76.

Bothmer, A., Robbiani, D.F., Feldhahn, N., Gazumyan, A., Nussenzweig, A., and Nussenzweig, M.C. (2010). 53BP1 regulates DNA resection and the choice between classical and alternative end joining during class switch recombination. J Exp Med *207*, 855-865.

Botuyan, M.V., Lee, J., Ward, I.M., Kim, J.E., Thompson, J.R., Chen, J., and Mer, G. (2006). Structural basis for the methylation state-specific recognition of histone H4-K20 by 53BP1 and Crb2 in DNA repair. Cell *127*, 1361-1373.

Breslin, C., Hornyak, P., Ridley, A., Rulten, S.L., Hanzlikova, H., Oliver, A.W., and Caldecott, K.W. (2015). The XRCC1 phosphate-binding pocket binds poly (ADP-ribose) and is required for XRCC1 function. Nucleic Acids Res.

Bryant, H.E., Petermann, E., Schultz, N., Jemth, A.S., Loseva, O., Issaeva, N., Johansson, F., Fernandez, S., McGlynn, P., and Helleday, T. (2009). PARP is activated at stalled forks to mediate Mre11-dependent replication restart and recombination. Embo J *28*, 2601-2615.

Bryant, H.E., Schultz, N., Thomas, H.D., Parker, K.M., Flower, D., Lopez, E., Kyle, S., Meuth, M., Curtin, N.J., and Helleday, T. (2005). Specific killing of BRCA2-deficient tumours with inhibitors of poly(ADP-ribose) polymerase. Nature *434*, 913-917.

Bunting, S.F., Callen, E., Wong, N., Chen, H.T., Polato, F., Gunn, A., Bothmer, A., Feldhahn, N., Fernandez-Capetillo, O., Cao, L., *et al.* (2010). 53BP1 inhibits homologous recombination in Brca1-deficient cells by blocking resection of DNA breaks. Cell *141*, 243-254.

Burzio, L.O., Riquelme, P.T., and Koide, S.S. (1979). ADP ribosylation of rat liver nucleosomal core histones. J Biol Chem *254*, 3029-3037.

Bussen, W., Raynard, S., Busygina, V., Singh, A.K., and Sung, P. (2007). Holliday junction processing activity of the BLM-Topo IIIalpha-BLAP75 complex. J Biol Chem *282*, 31484-31492.

Caldecott, K.W. (2014). DNA single-strand break repair. Exp Cell Res *329*, 2-8.

Campos, E.I., and Reinberg, D. (2009). Histones: annotating chromatin. Annu Rev Genet *43*, 559-599.

Chandrasekharan, M.B., Huang, F., and Sun, Z.W. (2009). Ubiquitination of histone H2B regulates chromatin dynamics by enhancing nucleosome stability. Proc Natl Acad Sci U S A *106*, 16686-16691.

Chapman, J.D., Gagne, J.P., Poirier, G.G., and Goodlett, D.R. (2013). Mapping PARP-1 auto-ADP-ribosylation sites by liquid chromatography-tandem mass spectrometry. J Proteome Res *12*, 1868-1880.

Chen, H., Lisby, M., and Symington, L.S. (2013). RPA coordinates DNA end resection and prevents formation of DNA hairpins. Mol Cell *50*, 589-600.

Chen, L., Nievera, C.J., Lee, A.Y., and Wu, X. (2008). Cell cycle-dependent complex formation of BRCA1.CtIP.MRN is important for DNA double-strand break repair. J Biol Chem *283*, 7713-7720.

Chida, J., Amagai, A., Tanaka, M., and Maeda, Y. (2008). Establishment of a new method for precisely determining the functions of individual mitochondrial genes, using Dictyostelium cells. BMC Genet *9*, 25.

Chiolo, I., Minoda, A., Colmenares, S.U., Polyzos, A., Costes, S.V., and Karpen, G.H. (2011). Double-strand breaks in heterochromatin move outside of a dynamic HP1a domain to complete recombinational repair. Cell *144*, 732-744.

Cho, S.H., Goenka, S., Henttinen, T., Gudapati, P., Reinikainen, A., Eischen, C.M., Lahesmaa, R., and Boothby, M. (2009). PARP-14, a member of the B aggressive lymphoma family, transduces survival signals in primary B cells. Blood *113*, 2416-2425.

Chou, D.M., Adamson, B., Dephoure, N.E., Tan, X., Nottke, A.C., Hurov, K.E., Gygi, S.P., Colaiacovo, M.P., and Elledge, S.J. (2010). A chromatin localization screen reveals poly (ADP ribose)-regulated recruitment of the repressive polycomb and NuRD complexes to sites of DNA damage. Proc Natl Acad Sci U S A *107*, 18475-18480.

Chubb, J.E., and Rea, S. (2010). Core and linker histone modifications involved in the DNA damage response. Subcell Biochem *50*, 17-42.

Chubb, J.R., Bloomfield, G., Xu, Q., Kaller, M., Ivens, A., Skelton, J., Turner, B.M., Nellen, W., Shaulsky, G., Kay, R.R., *et al.* (2006). Developmental timing in Dictyostelium is regulated by the Set1 histone methyltransferase. Dev Biol *292*, 519-532.

Citarelli, M., Teotia, S., and Lamb, R.S. (2010). Evolutionary history of the poly(ADP-ribose) polymerase gene family in eukaryotes. BMC Evol Biol *10*, 308.

Clapier, C.R., and Cairns, B.R. (2009). The biology of chromatin remodeling complexes. Annu Rev Biochem *78*, 273-304.

Conn, K.L., Hendzel, M.J., and Schang, L.M. (2011). Core histones H2B and H4 are mobilized during infection with herpes simplex virus 1. J Virol *85*, 13234-13252.

Cook, B.D., Dynek, J.N., Chang, W., Shostak, G., and Smith, S. (2002). Role for the related poly(ADP-Ribose) polymerases tankyrase 1 and 2 at human telomeres. Mol Cell Biol *22*, 332-342.

Corda, D., and Di Girolamo, M. (2002). Mono-ADP-ribosylation: a tool for modulating immune response and cell signaling. Sci STKE *2002*, pe53.

Courilleau, C., Chailleux, C., Jauneau, A., Grimal, F., Briois, S., Boutet-Robinet, E., Boudsocq, F., Trouche, D., and Canitrot, Y. (2012). The chromatin remodeler p400 ATPase facilitates Rad51-mediated repair of DNA double-strand breaks. J Cell Biol *199*, 1067-1081.

Coussens, M.A., Wendland, R.L., Deriano, L., Lindsay, C.R., Arnal, S.M., and Roth, D.B. (2013). RAG2's acidic hinge restricts repair-pathway choice and promotes genomic stability. Cell Rep *4*, 870-878.

Couto, C.A., Hsu, D.W., Teo, R., Rakhimova, A., Lempidaki, S., Pears, C.J., and Lakin, N.D. (2013). Nonhomologous end-joining promotes resistance to DNA damage in the absence of an ADP-ribosyltransferase that signals DNA single strand breaks. J Cell Sci *126*, 3452-3461.

Couto, C.A., Wang, H.Y., Green, J.C., Kiely, R., Siddaway, R., Borer, C., Pears, C.J., and Lakin, N.D. (2011). PARP regulates nonhomologous end joining through retention of Ku at double-strand breaks. J Cell Biol *194*, 367-375.

Cowell, I.G., Sunter, N.J., Singh, P.B., Austin, C.A., Durkacz, B.W., and Tilby, M.J. (2007). gammaH2AX foci form preferentially in euchromatin after ionising-radiation. PLoS One *2*, e1057.

Cruz-Garcia, A., Lopez-Saavedra, A., and Huertas, P. (2014). BRCA1 accelerates CtIP-mediated DNA-end resection. Cell Rep *9*, 451-459.

D'Amours, D., Desnoyers, S., D'Silva, I., and Poirier, G.G. (1999). Poly(ADP-ribosyl)ation reactions in the regulation of nuclear functions. Biochem J *342 (Pt 2)*, 249-268.

Dahle, J., and Kvam, E. (2003). Induction of delayed mutations and chromosomal instability in fibroblasts after UVA-, UVB-, and X-radiation. Cancer Res *63*, 1464-1469.

Dani, N., Stilla, A., Marchegiani, A., Tamburro, A., Till, S., Ladurner, A.G., Corda, D., and Di Girolamo, M. (2009). Combining affinity purification by ADP-ribose-binding macro domains with mass spectrometry to define the mammalian ADP-ribosyl proteome. Proc Natl Acad Sci U S A *106*, 4243-4248.

Daniels, C.M., Ong, S.E., and Leung, A.K. (2014). Phosphoproteomic approach to characterize protein mono- and poly(ADP-ribosyl)ation sites from cells. J Proteome Res *13*, 3510-3522.

De Bont, R., and van Larebeke, N. (2004). Endogenous DNA damage in humans: a review of quantitative data. Mutagenesis *19*, 169-185.

de Wit, E., and van Steensel, B. (2009). Chromatin domains in higher eukaryotes: insights from genome-wide mapping studies. Chromosoma *118*, 25-36.

Dictybase www.dictybase.org

DictyExpress www.dictyexpress.biolab.si

Dion, M.F., Kaplan, T., Kim, M., Buratowski, S., Friedman, N., and Rando, O.J. (2007). Dynamics of replication-independent histone turnover in budding yeast. Science *315*, 1405-1408.

Doil, C., Mailand, N., Bekker-Jensen, S., Menard, P., Larsen, D.H., Pepperkok, R., Ellenberg, J., Panier, S., Durocher, D., Bartek, J., *et al.* (2009). RNF168 binds and amplifies ubiquitin conjugates on damaged chromosomes to allow accumulation of repair proteins. Cell *136*, 435-446.

Downs, J.A., and Jackson, S.P. (2004). A means to a DNA end: the many roles of Ku. Nat Rev Mol Cell Biol *5*, 367-378.

Dubin, M., Fuchs, J., Graf, R., Schubert, I., and Nellen, W. (2010). Dynamics of a novel centromeric histone variant CenH3 reveals the evolutionary ancestral timing of centromere biogenesis. Nucleic Acids Res *38*, 7526-7537.

Dubin, M., and Nellen, W. (2010). A versatile set of tagged expression vectors to monitor protein localisation and function in Dictyostelium. Gene *465*, 1-8.

Duriez, P.J., Desnoyers, S., Hoflack, J.C., Shah, G.M., Morelle, B., Bourassa, S., Poirier, G.G., and Talbot, B. (1997). Characterization of anti-peptide antibodies directed towards the automodification domain and apoptotic fragment of poly (ADP-ribose) polymerase. Biochim Biophys Acta *1334*, 65-72.

Eichinger, L., Pachebat, J.A., Glockner, G., Rajandream, M.A., Sucgang, R., Berriman, M., Song, J., Olsen, R., Szafranski, K., Xu, Q., *et al.* (2005). The genome of the social amoeba Dictyostelium discoideum. Nature *435*, 43-57.

Escargueil, A.E., Soares, D.G., Salvador, M., Larsen, A.K., and Henriques, J.A. (2008). What histone code for DNA repair? Mutat Res *658*, 259-270.

Escribano-Diaz, C., Orthwein, A., Fradet-Turcotte, A., Xing, M., Young, J.T., Tkac, J., Cook, M.A., Rosebrock, A.P., Munro, M., Canny, M.D., *et al.* (2013). A cell cycle-dependent regulatory circuit composed of 53BP1-RIF1 and BRCA1-CtIP controls DNA repair pathway choice. Mol Cell *49*, 872-883.

Eustermann, S., Brockmann, C., Mehrotra, P.V., Yang, J.C., Loakes, D., West, S.C., Ahel, I., and Neuhaus, D. (2010). Solution structures of the two PBZ domains from human APLF and their interaction with poly(ADP-ribose). Nat Struct Mol Biol *17*, 241-243.

Eustermann, S., Videler, H., Yang, J.C., Cole, P.T., Gruszka, D., Veprintsev, D., and Neuhaus, D. (2011). The DNA-binding domain of human PARP-1 interacts with DNA single-strand breaks as a monomer through its second zinc finger. J Mol Biol *407*, 149-170.

Fahrer, J., Kranaster, R., Altmeyer, M., Marx, A., and Burkle, A. (2007). Quantitative analysis of the binding affinity of poly(ADP-ribose) to specific binding proteins as a function of chain length. Nucleic Acids Res *35*, e143.

Falk, M., Lukasova, E., and Kozubek, S. (2008). Chromatin structure influences the sensitivity of DNA to gamma-radiation. Biochim Biophys Acta *1783*, 2398-2414.

Farmer, H., McCabe, N., Lord, C.J., Tutt, A.N., Johnson, D.A., Richardson, T.B., Santarosa, M., Dillon, K.J., Hickson, I., Knights, C., *et al.* (2005). Targeting the DNA repair defect in BRCA mutant cells as a therapeutic strategy. Nature *434*, 917-921.

Feijs, K.L., Forst, A.H., Verheugd, P., and Luscher, B. (2013). Macrodomain-containing proteins: regulating new intracellular functions of mono(ADP-ribosyl)ation. Nat Rev Mol Cell Biol *14*, 443-451.

Fekairi, S., Scaglione, S., Chahwan, C., Taylor, E.R., Tissier, A., Coulon, S., Dong, M.Q., Ruse, C., Yates, J.R., 3rd, Russell, P., *et al.* (2009). Human SLX4 is a Holliday junction resolvase subunit that binds multiple DNA repair/recombination endonucleases. Cell *138*, 78-89.

Flynn, R.L., and Zou, L. (2010). Oligonucleotide/oligosaccharide-binding fold proteins: a growing family of genome guardians. Crit Rev Biochem Mol Biol *45*, 266-275.

Forst, A.H., Karlberg, T., Herzog, N., Thorsell, A.G., Gross, A., Feijs, K.L., Verheugd, P., Kursula, P., Nijmeijer, B., Kremmer, E., *et al.* (2013). Recognition of mono-ADP-ribosylated ARTD10 substrates by ARTD8 macrodomains. Structure *21*, 462-475.

Frechette, A., Huletsky, A., Aubin, R.J., de Murcia, G., Mandel, P., Lord, A., Grondin, G., and Poirier, G.G. (1985). Poly(ADP-ribosyl)ation of chromatin: kinetics of relaxation and its effect on chromatin solubility. Can J Biochem Cell Biol *63*, 764-773.

Frey, A., Listovsky, T., Guilbaud, G., Sarkies, P., and Sale, J.E. (2014). Histone H3.3 is required to maintain replication fork progression after UV damage. Curr Biol *24*, 2195-2201.

Friesner, J.D., Liu, B., Culligan, K., and Britt, A.B. (2005). Ionizing radiation-dependent gamma-H2AX focus formation requires ataxia telangiectasia mutated and ataxia telangiectasia mutated and Rad3-related. Mol Biol Cell *16*, 2566-2576.

Gagne, J.P., Ethier, C., Defoy, D., Bourassa, S., Langelier, M.F., Riccio, A.A., Pascal, J.M., Moon, K.M., Foster, L.J., Ning, Z., *et al.* (2015). Quantitative site-specific ADP-ribosylation profiling of DNA-dependent PARPs. DNA Repair (Amst) *30*, 68-79.

Gagne, J.P., Isabelle, M., Lo, K.S., Bourassa, S., Hendzel, M.J., Dawson, V.L., Dawson, T.M., and Poirier, G.G. (2008). Proteome-wide identification of poly(ADP-ribose) binding proteins and poly(ADP-ribose)-associated protein complexes. Nucleic Acids Res *36*, 6959-6976.

Gagne, J.P., Pic, E., Isabelle, M., Krietsch, J., Ethier, C., Paquet, E., Kelly, I., Boutin, M., Moon, K.M., Foster, L.J., *et al.* (2012). Quantitative proteomics profiling of the poly(ADP-ribose)-related response to genotoxic stress. Nucleic Acids Res *40*, 7788-7805.

Galande, S., and Kohwi-Shigematsu, T. (1999). Poly(ADP-ribose) polymerase and Ku autoantigen form a complex and synergistically bind to matrix attachment sequences. J Biol Chem *274*, 20521-20528.

Garvin, A.J., Densham, R.M., Blair-Reid, S.A., Pratt, K.M., Stone, H.R., Weekes, D., Lawrence, K.J., and Morris, J.R. (2013). The deSUMOylase SENP7 promotes chromatin relaxation for homologous recombination DNA repair. EMBO Rep *14*, 975-983.

Giri, C.P., West, M.H., and Smulson, M. (1978). Nuclear protein modification and chromatin substructure. 1. Differential poly(adenosine diphosphate) ribosylation of chromosomal proteins in nuclei versus isolated nucleosomes. Biochemistry *17*, 3495-3500.

Goodarzi, A.A., Jeggo, P., and Lobrich, M. (2010). The influence of heterochromatin on DNA double strand break repair: Getting the strong, silent type to relax. DNA Repair (Amst) *9*, 1273-1282.

Goodarzi, A.A., Kurka, T., and Jeggo, P.A. (2011). KAP-1 phosphorylation regulates CHD3 nucleosome remodeling during the DNA double-strand break response. Nat Struct Mol Biol *18*, 831-839.

Gottschalk, A.J., Timinszky, G., Kong, S.E., Jin, J., Cai, Y., Swanson, S.K., Washburn, M.P., Florens, L., Ladurner, A.G., Conaway, J.W., *et al.* (2009). Poly(ADP-ribosyl)ation directs recruitment and activation of an ATP-dependent chromatin remodeler. Proc Natl Acad Sci U S A *106*, 13770-13774.

Gottschalk, A.J., Trivedi, R.D., Conaway, J.W., and Conaway, R.C. (2012). Activation of the SNF2 family ATPase ALC1 by poly(ADP-ribose) in a stable ALC1.PARP1.nucleosome intermediate. J Biol Chem *287*, 43527-43532.

Grawunder, U., Zimmer, D., Kulesza, P., and Lieber, M.R. (1998). Requirement for an interaction of XRCC4 with DNA ligase IV for wild-type V(D)J recombination and DNA double-strand break repair in vivo. J Biol Chem *273*, 24708-24714.

Gu, J., Lu, H., Tsai, A.G., Schwarz, K., and Lieber, M.R. (2007). Single-stranded DNA ligation and XLF-stimulated incompatible DNA end ligation by the XRCC4-DNA ligase IV complex: influence of terminal DNA sequence. Nucleic Acids Res *35*, 5755-5762.

Guenther, M.G., Levine, S.S., Boyer, L.A., Jaenisch, R., and Young, R.A. (2007). A chromatin landmark and transcription initiation at most promoters in human cells. Cell *130*, 77-88.

Haenni, S.S., Hassa, P.O., Altmeyer, M., Fey, M., Imhof, R., and Hottiger, M.O. (2008). Identification of lysines 36 and 37 of PARP-2 as targets for acetylation and auto-ADP-ribosylation. Int J Biochem Cell Biol *40*, 2274-2283.

Haince, J.F., McDonald, D., Rodrigue, A., Dery, U., Masson, J.Y., Hendzel, M.J., and Poirier, G.G. (2008). PARP1-dependent kinetics of recruitment of MRE11 and NBS1 proteins to multiple DNA damage sites. J Biol Chem *283*, 1197-1208.

Hake, S.B., Garcia, B.A., Duncan, E.M., Kauer, M., Dellaire, G., Shabanowitz, J., Bazett-Jones, D.P., Allis, C.D., and Hunt, D.F. (2006). Expression patterns and post-translational modifications associated with mammalian histone H3 variants. J Biol Chem *281*, 559-568.

Happel, N., and Doenecke, D. (2009). Histone H1 and its isoforms: contribution to chromatin structure and function. Gene *431*, 1-12.

Harada, A., Maehara, K., Sato, Y., Konno, D., Tachibana, T., Kimura, H., and Ohkawa, Y. (2015). Incorporation of histone H3.1 suppresses the lineage potential of skeletal muscle. Nucleic Acids Res *43*, 775-786.

Hassa, P.O., Haenni, S.S., Elser, M., and Hottiger, M.O. (2006). Nuclear ADP-ribosylation reactions in mammalian cells: where are we today and where are we going? Microbiol Mol Biol Rev *70*, 789-829.

Hauser, L.J., Dhar, M.S., and Olins, D.E. (1995). Dictyostelium discoideum contains a single-copy gene encoding a unique subtype of histone H1. Gene *154*, 119-122.

He, F., Tsuda, K., Takahashi, M., Kuwasako, K., Terada, T., Shirouzu, M., Watanabe, S., Kigawa, T., Kobayashi, N., Guntert, P., *et al.* (2012). Structural insight into the interaction of ADP-ribose with the PARP WWE domains. FEBS Lett *586*, 3858-3864.

Hicks, W.M., Yamaguchi, M., and Haber, J.E. (2011). Real-time analysis of double-strand DNA break repair by homologous recombination. Proc Natl Acad Sci U S A *108*, 3108-3115.

Hochegger, H., Dejsuphong, D., Fukushima, T., Morrison, C., Sonoda, E., Schreiber, V., Zhao, G.Y., Saberi, A., Masutani, M., Adachi, N., *et al.* (2006). Parp-1 protects homologous recombination from interference by Ku and Ligase IV in vertebrate cells. Embo J *25*, 1305-1314.

Hoeijmakers, J.H. (2007). Genome maintenance mechanisms are critical for preventing cancer as well as other aging-associated diseases. Mech Ageing Dev *128*, 460-462.

Hoeijmakers, J.H. (2009). DNA damage, aging, and cancer. N Engl J Med *361*, 1475-1485.

Holloman, W.K. (2011). Unraveling the mechanism of BRCA2 in homologous recombination. Nat Struct Mol Biol *18*, 748-754.

Hottiger, M.O. (2015). Nuclear ADP-Ribosylation and Its Role in Chromatin Plasticity, Cell Differentiation, and Epigenetics. Annu Rev Biochem *84*, 227-263.

Hottiger, M.O., Hassa, P.O., Luscher, B., Schuler, H., and Koch-Nolte, F. (2010). Toward a unified nomenclature for mammalian ADP-ribosyltransferases. Trends Biochem Sci *35*, 208-219.

Hough, C.J., and Smulson, M.E. (1984). Association of poly(adenosine diphosphate ribosylated) nucleosomes with transcriptionally active and inactive regions of chromatin. Biochemistry *23*, 5016-5023.

House, N.C., Koch, M.R., and Freudenreich, C.H. (2014). Chromatin modifications and DNA repair: beyond double-strand breaks. Front Genet *5*, 296.

Hsu, D.W., Chubb, J.R., Muramoto, T., Pears, C.J., and Mahadevan, L.C. (2012). Dynamic acetylation of lysine-4-trimethylated histone H3 and H3 variant biology in a simple multicellular eukaryote. Nucleic Acids Res *40*, 7247-7256.

Hsu, D.W., Gaudet, P., Hudson, J.J., Pears, C.J., and Lakin, N.D. (2006). DNA damage signaling and repair in Dictyostelium discoideum. Cell Cycle *5*, 702-708.

Hsu, D.W., Kiely, R., Couto, C.A., Wang, H.Y., Hudson, J.J., Borer, C., Pears, C.J., and Lakin, N.D. (2011). DNA double-strand break repair pathway choice in Dictyostelium. J Cell Sci *124*, 1655-1663.

Hu, Y., Petit, S.A., Ficarro, S.B., Toomire, K.J., Xie, A., Lim, E., Cao, S.A., Park, E., Eck, M.J., Scully, R., *et al.* (2014). PARP1-driven poly-ADP-ribosylation regulates BRCA1 function in homologous recombination-mediated DNA repair. Cancer Discov *4*, 1430-1447.

Hudson, J.J., Hsu, D.W., Guo, K., Zhukovskaya, N., Liu, P.H., Williams, J.G., Pears, C.J., and Lakin, N.D. (2005). DNA-PKcs-dependent signaling of DNA damage in Dictyostelium discoideum. Curr Biol *15*, 1880-1885.

Huletsky, A., de Murcia, G., Muller, S., Hengartner, M., Menard, L., Lamarre, D., and Poirier, G.G. (1989). The effect of poly(ADP-ribosyl)ation on native and H1-depleted chromatin. A role of poly(ADP-ribosyl)ation on core nucleosome structure. J Biol Chem *264*, 8878-8886.

Huletsky, A., Niedergang, C., Frechette, A., Aubin, R., Gaudreau, A., and Poirier, G.G. (1985). Sequential ADP-ribosylation pattern of nucleosomal histones. ADP-ribosylation of nucleosomal histones. Eur J Biochem *146*, 277-285.

Ikura, T., Ogryzko, V.V., Grigoriev, M., Groisman, R., Wang, J., Horikoshi, M., Scully, R., Qin, J., and Nakatani, Y. (2000). Involvement of the TIP60 histone acetylase complex in DNA repair and apoptosis. Cell *102*, 463-473.

Isabelle, M., Gagne, J.P., Gallouzi, I.E., and Poirier, G.G. (2012). Quantitative proteomics and dynamic imaging reveal that G3BP-mediated stress granule assembly is poly(ADP-ribose)-dependent following exposure to MNNG-induced DNA alkylation. J Cell Sci *125*, 4555-4566.

Izhar, L., Adamson, B., Ciccia, A., Lewis, J., Pontano-Vaites, L., Leng, Y., Liang, A.C., Westbrook, T.F., Harper, J.W., and Elledge, S.J. (2015). A Systematic Analysis of Factors Localized to Damaged Chromatin Reveals PARP-Dependent Recruitment of Transcription Factors. Cell Rep *11*, 1486-1500.

Jackson, S.P., and Bartek, J. (2009). The DNA-damage response in human biology and disease. Nature *461*, 1071-1078.

Jacobson, E.L., Antol, K.M., Juarez-Salinas, H., and Jacobson, M.K. (1983). Poly(ADP-ribose) metabolism in ultraviolet irradiated human fibroblasts. J Biol Chem *258*, 103-107.

Jakob, B., Splinter, J., Conrad, S., Voss, K.O., Zink, D., Durante, M., Lobrich, M., and Taucher-Scholz, G. (2011). DNA double-strand breaks in heterochromatin elicit fast repair protein recruitment, histone H2AX phosphorylation and relocation to euchromatin. Nucleic Acids Res *39*, 6489-6499.

Jankevicius, G., Hassler, M., Golia, B., Rybin, V., Zacharias, M., Timinszky, G., and Ladurner, A.G. (2013). A family of macrodomain proteins reverses cellular mono-ADP-ribosylation. Nat Struct Mol Biol *20*, 508-514.

Jasin, M., and Rothstein, R. (2013). Repair of strand breaks by homologous recombination. Cold Spring Harb Perspect Biol *5*, a012740.

Ji, Y., and Tulin, A.V. (2013). Post-transcriptional regulation by poly(ADP-ribosyl)ation of the RNA-binding proteins. Int J Mol Sci *14*, 16168-16183.

Jilani, A., Ramotar, D., Slack, C., Ong, C., Yang, X.M., Scherer, S.W., and Lasko, D.D. (1999). Molecular cloning of the human gene, PNKP, encoding a polynucleotide kinase 3'-phosphatase and evidence for its role in repair of DNA strand breaks caused by oxidative damage. J Biol Chem *274*, 24176-24186.

Jin, C., Zang, C., Wei, G., Cui, K., Peng, W., Zhao, K., and Felsenfeld, G. (2009). H3.3/H2A.Z double variant-containing nucleosomes mark 'nucleosome-free regions' of active promoters and other regulatory regions. Nat Genet *41*, 941-945.

Jump, D.B., Butt, T.R., and Smulson, M. (1979). Nuclear protein modification and chromatin substructure. 3. Relationship between poly(adenosine diphosphate) ribosylation and different functional forms of chromatin. Biochemistry *18*, 983-990.

Jungmichel, S., Rosenthal, F., Altmeyer, M., Lukas, J., Hottiger, M.O., and Nielsen, M.L. (2013). Proteome-wide identification of poly(ADP-Ribosyl)ation targets in different genotoxic stress responses. Mol Cell *52*, 272-285.

Jungmichel, S., and Stucki, M. (2010). MDC1: The art of keeping things in focus. Chromosoma *119*, 337-349.

Kaller, M., Euteneuer, U., and Nellen, W. (2006). Differential effects of heterochromatin protein 1 isoforms on mitotic chromosome distribution and growth in Dictyostelium discoideum. Eukaryot Cell *5*, 530-543.

Kanai, M., Hanashiro, K., Kim, S.H., Hanai, S., Boulares, A.H., Miwa, M., and Fukasawa, K. (2007). Inhibition of Crm1-p53 interaction and nuclear export of p53 by poly(ADP-ribosyl)ation. Nat Cell Biol *9*, 1175-1183.

Kang, H.C., Lee, Y.I., Shin, J.H., Andrabi, S.A., Chi, Z., Gagne, J.P., Lee, Y., Ko, H.S., Lee, B.D., Poirier, G.G., *et al.* (2011). Iduna is a poly(ADP-ribose) (PAR)-dependent E3 ubiquitin ligase that regulates DNA damage. Proc Natl Acad Sci U S A *108*, 14103-14108.

Karlberg, T., Hammarstrom, M., Schutz, P., Svensson, L., and Schuler, H. (2010). Crystal structure of the catalytic domain of human PARP2 in complex with PARP inhibitor ABT-888. Biochemistry *49*, 1056-1058.

Karow, J.K., Constantinou, A., Li, J.L., West, S.C., and Hickson, I.D. (2000). The Bloom's syndrome gene product promotes branch migration of holliday junctions. Proc Natl Acad Sci U S A *97*, 6504-6508.

Karras, G.I., Kustatscher, G., Buhecha, H.R., Allen, M.D., Pugieux, C., Sait, F., Bycroft, M., and Ladurner, A.G. (2005). The macro domain is an ADP-ribose binding module. Embo J *24*, 1911-1920.

Kasparek, T.R., and Humphrey, T.C. (2011). DNA double-strand break repair pathways, chromosomal rearrangements and cancer. Semin Cell Dev Biol *22*, 886-897.

Kass, E.M., and Jasin, M. (2010). Collaboration and competition between DNA double-strand break repair pathways. FEBS Lett *584*, 3703-3708.

Katoh, M., Curk, T., Xu, Q., Zupan, B., Kuspa, A., and Shaulsky, G. (2006). Developmentally regulated DNA methylation in Dictyostelium discoideum. Eukaryot Cell *5*, 18-25.

Kawaichi, M., Ueda, K., and Hayaishi, O. (1981). Multiple autopoly(ADP-ribosyl)ation of rat liver poly(ADP-ribose) synthetase. Mode of modification and properties of automodified synthetase. J Biol Chem *256*, 9483-9489.

Keith, G., Desgres, J., and de Murcia, G. (1990). Use of two-dimensional thin-layer chromatography for the components study of poly(adenosine diphosphate ribose). Anal Biochem *191*, 309-313.

Kickhoefer, V.A., Siva, A.C., Kedersha, N.L., Inman, E.M., Ruland, C., Streuli, M., and Rome, L.H. (1999). The 193-kD vault protein, VPARP, is a novel poly(ADP-ribose) polymerase. J Cell Biol *146*, 917-928.

Kim, H., Jacobson, M.K., Rolli, V., Menissier-de Murcia, J., Reinbolt, J., Simonin, F., Ruf, A., Schulz, G., and de Murcia, G. (1997). Photoaffinity labelling of human poly(ADP-ribose) polymerase catalytic domain. Biochem J *322 (Pt 2)*, 469-475.

Kim, M.Y., Mauro, S., Gevry, N., Lis, J.T., and Kraus, W.L. (2004). NAD+-dependent modulation of chromatin structure and transcription by nucleosome binding properties of PARP-1. Cell *119*, 803-814.

Kimura, H., and Cook, P.R. (2001). Kinetics of core histones in living human cells: little exchange of H3 and H4 and some rapid exchange of H2B. J Cell Biol *153*, 1341-1353.

Kleine, H., Poreba, E., Lesniewicz, K., Hassa, P.O., Hottiger, M.O., Litchfield, D.W., Shilton, B.H., and Luscher, B. (2008). Substrate-assisted catalysis by PARP10 limits its activity to mono-ADP-ribosylation. Mol Cell *32*, 57-69.

Kofler, B., Wallraff, E., Herzog, H., Schneider, R., Auer, B., and Schweiger, M. (1993). Purification and characterization of NAD+:ADP-ribosyltransferase (polymerizing) from Dictyostelium discoideum. Biochem J *293 (Pt 1)*, 275-281.

Koh, D.W., Lawler, A.M., Poitras, M.F., Sasaki, M., Wattler, S., Nehls, M.C., Stoger, T., Poirier, G.G., Dawson, V.L., and Dawson, T.M. (2004). Failure to degrade poly(ADP-ribose) causes increased sensitivity to cytotoxicity and early embryonic lethality. Proc Natl Acad Sci U S A *101*, 17699-17704.

Kolas, N.K., Chapman, J.R., Nakada, S., Ylanko, J., Chahwan, R., Sweeney, F.D., Panier, S., Mendez, M., Wildenhain, J., Thomson, T.M., *et al.* (2007). Orchestration of the DNA-damage response by the RNF8 ubiquitin ligase. Science *318*, 1637-1640.

Kornberg, R.D. (1977). Structure of chromatin. Annu Rev Biochem *46*, 931-954.

Kraus, W.L. (2008). Transcriptional control by PARP-1: chromatin modulation, enhancer-binding, coregulation, and insulation. Curr Opin Cell Biol *20*, 294-302.

Kreimeyer, A., Wielckens, K., Adamietz, P., and Hilz, H. (1984). DNA repair-associated ADP-ribosylation in vivo. Modification of histone H1 differs from that of the principal acceptor proteins. J Biol Chem *259*, 890-896.

Kriegs, M., Kasten-Pisula, U., Rieckmann, T., Holst, K., Saker, J., Dahm-Daphi, J., and Dikomey, E. (2010). The epidermal growth factor receptor modulates DNA double-strand break repair by regulating non-homologous end-joining. DNA Repair (Amst) *9*, 889-897.

Krishnakumar, R., Gamble, M.J., Frizzell, K.M., Berrocal, J.G., Kininis, M., and Kraus, W.L. (2008). Reciprocal binding of PARP-1 and histone H1 at promoters specifies transcriptional outcomes. Science *319*, 819-821.

Krupitza, G., and Cerutti, P. (1989). Poly(ADP-ribosylation) of histones in intact human keratinocytes. Biochemistry *28*, 4054-4060.

Kun, E., Kirsten, E., and Ordahl, C.P. (2002). Coenzymatic activity of randomly broken or intact double-stranded DNAs in auto and histone H1 trans-poly(ADP-ribosylation), catalyzed by poly(ADP-ribose) polymerase (PARP I). J Biol Chem *277*, 39066-39069.

Kuspa, A., and Loomis, W.F. (1992). Tagging developmental genes in Dictyostelium by restriction enzyme-mediated integration of plasmid DNA. Proc Natl Acad Sci U S A *89*, 8803-8807.

Lamarche, B.J., Orazio, N.I., and Weitzman, M.D. (2010). The MRN complex in double-strand break repair and telomere maintenance. FEBS Lett *584*, 3682-3695.

Langelier, M.F., Planck, J.L., Roy, S., and Pascal, J.M. (2011). Crystal structures of poly(ADP-ribose) polymerase-1 (PARP-1) zinc fingers bound to DNA: structural and functional insights into DNA-dependent PARP-1 activity. J Biol Chem *286*, 10690-10701.

Langelier, M.F., Planck, J.L., Roy, S., and Pascal, J.M. (2012). Structural basis for DNA damage-dependent poly(ADP-ribosyl)ation by human PARP-1. Science *336*, 728-732.

Langelier, M.F., Riccio, A.A., and Pascal, J.M. (2014). PARP-2 and PARP-3 are selectively activated by 5' phosphorylated DNA breaks through an allosteric regulatory mechanism shared with PARP-1. Nucleic Acids Res *42*, 7762-7775.

Langelier, M.F., Servent, K.M., Rogers, E.E., and Pascal, J.M. (2008). A third zinc-binding domain of human poly(ADP-ribose) polymerase-1 coordinates DNA-dependent enzyme activation. J Biol Chem *283*, 4105-4114.

Le Page, F., Schreiber, V., Dherin, C., De Murcia, G., and Boiteux, S. (2003). Poly(ADP-ribose) polymerase-1 (PARP-1) is required in murine cell lines for base excision repair of oxidative DNA damage in the absence of DNA polymerase beta. J Biol Chem *278*, 18471-18477.

Lehtio, L., Jemth, A.S., Collins, R., Loseva, O., Johansson, A., Markova, N., Hammarstrom, M., Flores, A., Holmberg-Schiavone, L., Weigelt, J., *et al.* (2009). Structural basis for inhibitor specificity in human poly(ADP-ribose) polymerase-3. J Med Chem *52*, 3108-3111.

Leung, A., Todorova, T., Ando, Y., and Chang, P. (2012). Poly(ADP-ribose) regulates post-transcriptional gene regulation in the cytoplasm. RNA Biol *9*, 542-548.

Li, B., and Comai, L. (2000). Functional interaction between Ku and the werner syndrome protein in DNA end processing. J Biol Chem *275*, 28349-28352.

Li, G.Y., McCulloch, R.D., Fenton, A.L., Cheung, M., Meng, L., Ikura, M., and Koch, C.A. (2010a). Structure and identification of ADP-ribose recognition motifs of APLF and role in the DNA damage response. Proc Natl Acad Sci U S A *107*, 9129-9134.

Li, M., Lu, L.Y., Yang, C.Y., Wang, S., and Yu, X. (2013). The FHA and BRCT domains recognize ADP-ribosylation during DNA damage response. Genes Dev *27*, 1752-1768.

Li, M., and Yu, X. (2013). Function of BRCA1 in the DNA damage response is mediated by ADP-ribosylation. Cancer Cell *23*, 693-704.

Li, S., Kanno, S., Watanabe, R., Ogiwara, H., Kohno, T., Watanabe, G., Yasui, A., and Lieber, M.R. (2011). Polynucleotide kinase and aprataxin-like forkhead-associated protein (PALF) acts as both a single-stranded DNA endonuclease and a single-stranded DNA 3' exonuclease and can participate in DNA end joining in a biochemical system. J Biol Chem *286*, 36368-36377.

Li, X., Corsa, C.A., Pan, P.W., Wu, L., Ferguson, D., Yu, X., Min, J., and Dou, Y. (2010b). MOF and H4 K16 acetylation play important roles in DNA damage repair by modulating recruitment of DNA damage repair protein Mdc1. Mol Cell Biol *30*, 5335-5347.

Liang, Y.C., Hsu, C.Y., Yao, Y.L., and Yang, W.M. (2013). PARP-2 regulates cell cycle-related genes through histone deacetylation and methylation independently of poly(ADP-ribosyl)ation. Biochem Biophys Res Commun *431*, 58-64.

Lieber, M.R. (2010). The mechanism of double-strand DNA break repair by the nonhomologous DNA end-joining pathway. Annu Rev Biochem *79*, 181-211.

Lin, W., Ame, J.C., Aboul-Ela, N., Jacobson, E.L., and Jacobson, M.K. (1997). Isolation and characterization of the cDNA encoding bovine poly(ADP-ribose) glycohydrolase. J Biol Chem *272*, 11895-11901.

Liu, J., Doty, T., Gibson, B., and Heyer, W.D. (2010). Human BRCA2 protein promotes RAD51 filament formation on RPA-covered single-stranded DNA. Nat Struct Mol Biol *17*, 1260-1262.

Loseva, O., Jemth, A.S., Bryant, H.E., Schuler, H., Lehtio, L., Karlberg, T., and Helleday, T. (2010). PARP-3 is a mono-ADP-ribosylase that activates PARP-1 in the absence of DNA. J Biol Chem *285*, 8054-8060.

Luger, K., Mader, A.W., Richmond, R.K., Sargent, D.F., and Richmond, T.J. (1997). Crystal structure of the nucleosome core particle at 2.8 A resolution. Nature *389*, 251-260.

Lukas, C., Melander, F., Stucki, M., Falck, J., Bekker-Jensen, S., Goldberg, M., Lerenthal, Y., Jackson, S.P., Bartek, J., and Lukas, J. (2004). Mdc1 couples DNA double-strand break recognition by Nbs1 with its H2AX-dependent chromatin retention. Embo J *23*, 2674-2683.

Ma, Y., Lu, H., Tippin, B., Goodman, M.F., Shimazaki, N., Koiwai, O., Hsieh, C.L., Schwarz, K., and Lieber, M.R. (2004). A biochemically defined system for mammalian nonhomologous DNA end joining. Mol Cell *16*, 701-713.

Mahajan, A., Yuan, C., Lee, H., Chen, E.S., Wu, P.Y., and Tsai, M.D. (2008). Structure and function of the phosphothreonine-specific FHA domain. Sci Signal *1*, re12.

Mailand, N., Bekker-Jensen, S., Faustrup, H., Melander, F., Bartek, J., Lukas, C., and Lukas, J. (2007). RNF8 ubiquitylates histones at DNA double-strand breaks and promotes assembly of repair proteins. Cell *131*, 887-900.

Maison, C., and Almouzni, G. (2004). HP1 and the dynamics of heterochromatin maintenance. Nat Rev Mol Cell Biol *5*, 296-304.

Malanga, M., Pleschke, J.M., Kleczkowska, H.E., and Althaus, F.R. (1998). Poly(ADP-ribose) binds to specific domains of p53 and alters its DNA binding functions. J Biol Chem *273*, 11839-11843.

Manke, I.A., Lowery, D.M., Nguyen, A., and Yaffe, M.B. (2003). BRCT repeats as phosphopeptide-binding modules involved in protein targeting. Science *302*, 636-639.

Marsischky, G.T., Wilson, B.A., and Collier, R.J. (1995). Role of glutamic acid 988 of human poly-ADP-ribose polymerase in polymer formation. Evidence for active site similarities to the ADP-ribosylating toxins. J Biol Chem *270*, 3247-3254.

Mathiasen, D.P., and Lisby, M. (2014). Cell cycle regulation of homologous recombination in Saccharomyces cerevisiae. FEMS Microbiol Rev *38*, 172-184.

Mattiussi, S., Tempera, I., Matusali, G., Mearini, G., Lenti, L., Fratarcangeli, S., Mosca, L., D'Erme, M., and Mattia, E. (2007). Inhibition of Poly(ADP-ribose)polymerase impairs Epstein Barr Virus lytic cycle progression. Infect Agent Cancer *2*, 18.

McKittrick, E., Gafken, P.R., Ahmad, K., and Henikoff, S. (2004). Histone H3.3 is enriched in covalent modifications associated with active chromatin. Proc Natl Acad Sci U S A *101*, 1525-1530.

Menissier de Murcia, J., Ricoul, M., Tartier, L., Niedergang, C., Huber, A., Dantzer, F., Schreiber, V., Ame, J.C., Dierich, A., LeMeur, M., *et al.* (2003). Functional interaction between PARP-1 and PARP-2 in chromosome stability and embryonic development in mouse. Embo J *22*, 2255-2263.

Messner, S., Altmeyer, M., Zhao, H., Pozivil, A., Roschitzki, B., Gehrig, P., Rutishauser, D., Huang, D., Caflisch, A., and Hottiger, M.O. (2010). PARP1 ADP-ribosylates lysine residues of the core histone tails. Nucleic Acids Res *38*, 6350-6362.

Miller, K.M., Tjeertes, J.V., Coates, J., Legube, G., Polo, S.E., Britton, S., and Jackson, S.P. (2010). Human HDAC1 and HDAC2 function in the DNA-damage response to promote DNA nonhomologous end-joining. Nat Struct Mol Biol *17*, 1144-1151.

Mimori, T., and Hardin, J.A. (1986). Mechanism of interaction between Ku protein and DNA. J Biol Chem *261*, 10375-10379.

Miwa, M., Saikawa, N., Yamaizumi, Z., Nishimura, S., and Sugimura, T. (1979). Structure of poly(adenosine diphosphate ribose): identification of 2'-[1''-ribosyl-2''-(or 3''-)(1'''-ribosyl)]adenosine-5',5'',5'''-tris(phosphate) as a branch linkage. Proc Natl Acad Sci U S A *76*, 595-599.

Morillo-Huesca, M., Clemente-Ruiz, M., Andujar, E., and Prado, F. (2010). The SWR1 histone replacement complex causes genetic instability and genome-wide transcription misregulation in the absence of H2A.Z. PLoS One *5*, e12143.

Morio, T., and Kim, H. (2008). Ku, Artemis, and ataxia-telangiectasia-mutated: signalling networks in DNA damage. Int J Biochem Cell Biol *40*, 598-603.

Morrison, C., Smith, G.C., Stingl, L., Jackson, S.P., Wagner, E.F., and Wang, Z.Q. (1997). Genetic interaction between PARP and DNA-PK in V(D)J recombination and tumorigenesis. Nat Genet *17*, 479-482.

Moyal, L., Lerenthal, Y., Gana-Weisz, M., Mass, G., So, S., Wang, S.Y., Eppink, B., Chung, Y.M., Shalev, G., Shema, E., *et al.* (2011). Requirement of ATM-dependent monoubiquitylation of histone H2B for timely repair of DNA double-strand breaks. Mol Cell *41*, 529-542.

Mueller-Dieckmann, C., Kernstock, S., Lisurek, M., von Kries, J.P., Haag, F., Weiss, M.S., and Koch-Nolte, F. (2006). The structure of human ADP-ribosylhydrolase 3 (ARH3) provides insights into the reversibility of protein ADP-ribosylation. Proc Natl Acad Sci U S A *103*, 15026-15031.

Muller-Taubenberger, A., Bonisch, C., Furbringer, M., Wittek, F., and Hake, S.B. (2011). The histone methyltransferase Dot1 is required for DNA damage repair and proper development in Dictyostelium. Biochem Biophys Res Commun *404*, 1016-1022.

Muramoto, T., and Chubb, J.R. (2008). Live imaging of the Dictyostelium cell cycle reveals widespread S phase during development, a G2 bias in spore differentiation and a premitotic checkpoint. Development *135*, 1647-1657.

Murr, R., Loizou, J.I., Yang, Y.G., Cuenin, C., Li, H., Wang, Z.Q., and Herceg, Z. (2006). Histone acetylation by Trrap-Tip60 modulates loading of repair proteins and repair of DNA double-strand breaks. Nat Cell Biol *8*, 91-99.

Nakamura, K., Kato, A., Kobayashi, J., Yanagihara, H., Sakamoto, S., Oliveira, D.V., Shimada, M., Tauchi, H., Suzuki, H., Tashiro, S., *et al.* (2011). Regulation of homologous recombination by RNF20-dependent H2B ubiquitination. Mol Cell *41*, 515-528.

Neale, M.J., Pan, J., and Keeney, S. (2005). Endonucleolytic processing of covalent protein-linked DNA double-strand breaks. Nature *436*, 1053-1057.

Nichols, J.M., Veltman, D., and Kay, R.R. (2015). Chemotaxis of a model organism: progress with Dictyostelium. Curr Opin Cell Biol *36*, 7-12.

Niedergang, C.P., de Murcia, G., Ittel, M.E., Pouyet, J., and Mandel, P. (1985). Time course of polynucleosome relaxation and ADP-ribosylation. Correlation between relaxation and histone H1 hyper-ADP-ribosylation. Eur J Biochem *146*, 185-191.

Nimonkar, A.V., Genschel, J., Kinoshita, E., Polaczek, P., Campbell, J.L., Wyman, C., Modrich, P., and Kowalczykowski, S.C. (2011). BLM-DNA2-RPA-MRN and EXO1-BLM-RPA-MRN constitute two DNA end resection machineries for human DNA break repair. Genes Dev *25*, 350-362.

Nishizuka, Y., Ueda, K., Nakazawa, K., and Hayaishi, O. (1967). Studies on the polymer of adenosine diphosphate ribose. I. Enzymic formation from nicotinamide adenine dinuclotide in mammalian nuclei. J Biol Chem *242*, 3164-3171.

O'Shaughnessy, A., and Hendrich, B. (2013). CHD4 in the DNA-damage response and cell cycle progression: not so NuRDy now. Biochem Soc Trans *41*, 777-782.

Oberoi, J., Richards, M.W., Crumpler, S., Brown, N., Blagg, J., and Bayliss, R. (2010). Structural basis of poly(ADP-ribose) recognition by the multizinc binding domain of checkpoint with forkhead-associated and RING Domains (CHFR). J Biol Chem *285*, 39348-39358.

Oda, H., Hubner, M.R., Beck, D.B., Vermeulen, M., Hurwitz, J., Spector, D.L., and Reinberg, D. (2010). Regulation of the histone H4 monomethylase PR-Set7 by CRL4(Cdt2)-mediated PCNA-dependent degradation during DNA damage. Mol Cell *40*, 364-376.

Ogata, N., Ueda, K., and Hayaishi, O. (1980a). ADP-ribosylation of histone H2B. Identification of glutamic acid residue 2 as the modification site. J Biol Chem *255*, 7610-7615.

Ogata, N., Ueda, K., Kagamiyama, H., and Hayaishi, O. (1980b). ADP-ribosylation of histone H1. Identification of glutamic acid residues 2, 14, and the COOH-terminal lysine residue as modification sites. J Biol Chem *255*, 7616-7620.

Ogata, N., Ueda, K., Kawaichi, M., and Hayaishi, O. (1981). Poly(ADP-ribose) synthetase, a main acceptor of poly(ADP-ribose) in isolated nuclei. J Biol Chem *256*, 4135-4137.

Ogiwara, H., Ui, A., Otsuka, A., Satoh, H., Yokomi, I., Nakajima, S., Yasui, A., Yokota, J., and Kohno, T. (2011). Histone acetylation by CBP and p300 at double-strand break sites facilitates SWI/SNF chromatin remodeling and the recruitment of non-homologous end joining factors. Oncogene *30*, 2135-2146.

Oka, S., Kato, J., and Moss, J. (2006). Identification and characterization of a mammalian 39-kDa poly(ADP-ribose) glycohydrolase. J Biol Chem *281*, 705-713.

Okano, S., Lan, L., Caldecott, K.W., Mori, T., and Yasui, A. (2003). Spatial and temporal cellular responses to single-strand breaks in human cells. Mol Cell Biol *23*, 3974-3981.

Ooi, S.L., Priess, J.R., and Henikoff, S. (2006). Histone H3.3 variant dynamics in the germline of Caenorhabditis elegans. PLoS Genet *2*, e97.

Otto, H., Reche, P.A., Bazan, F., Dittmar, K., Haag, F., and Koch-Nolte, F. (2005). In silico characterization of the family of PARP-like poly(ADP-ribosyl)transferases (pARTs). BMC Genomics *6*, 139.

Paddock, M.N., Bauman, A.T., Higdon, R., Kolker, E., Takeda, S., and Scharenberg, A.M. (2011). Competition between PARP-1 and Ku70 control the decision between high-fidelity and mutagenic DNA repair. DNA Repair (Amst) *10*, 338-343.

Palazzo, L., Thomas, B., Jemth, A.S., Colby, T., Leidecker, O., Feijs, K.L., Zaja, R., Loseva, O., Puigvert, J.C., Matic, I., *et al.* (2015). Processing of protein ADP-ribosylation by Nudix hydrolases. Biochem J *468*, 293-301.

Parrilla-Castellar, E.R., Arlander, S.J., and Karnitz, L. (2004). Dial 9-1-1 for DNA damage: the Rad9-Hus1-Rad1 (9-1-1) clamp complex. DNA Repair (Amst) *3*, 1009-1014.

Paul, K., Wang, M., Mladenov, E., Bencsik-Theilen, A., Bednar, T., Wu, W., Arakawa, H., and Iliakis, G. (2013). DNA ligases I and III cooperate in alternative non-homologous end-joining in vertebrates. PLoS One *8*, e59505.

Paull, T.T., Rogakou, E.P., Yamazaki, V., Kirchgessner, C.U., Gellert, M., and Bonner, W.M. (2000). A critical role for histone H2AX in recruitment of repair factors to nuclear foci after DNA damage. Curr Biol *10*, 886-895.

Pears, C.J., Couto, C.A., Wang, H.Y., Borer, C., Kiely, R., and Lakin, N.D. (2012). The role of ADP-ribosylation in regulating DNA double-strand break repair. Cell Cycle *11*, 48-56.

Pei, H., Zhang, L., Luo, K., Qin, Y., Chesi, M., Fei, F., Bergsagel, P.L., Wang, L., You, Z., and Lou, Z. (2011). MMSET regulates histone H4K20 methylation and 53BP1 accumulation at DNA damage sites. Nature *470*, 124-128.

Peng, J.C., and Karpen, G.H. (2008). Epigenetic regulation of heterochromatic DNA stability. Curr Opin Genet Dev *18*, 204-211.

Perina, D., Mikoc, A., Ahel, J., Cetkovic, H., Zaja, R., and Ahel, I. (2014). Distribution of protein poly(ADP-ribosyl)ation systems across all domains of life. DNA Repair (Amst) *23*, 4-16.

Perry, J.J., Yannone, S.M., Holden, L.G., Hitomi, C., Asaithamby, A., Han, S., Cooper, P.K., Chen, D.J., and Tainer, J.A. (2006). WRN exonuclease structure and molecular mechanism imply an editing role in DNA end processing. Nat Struct Mol Biol *13*, 414-422.

Phulwani, N.K., and Kielian, T. (2008). Poly (ADP-ribose) polymerases (PARPs) 1-3 regulate astrocyte activation. J Neurochem *106*, 578-590.

Pierce, A.J., Hu, P., Han, M., Ellis, N., and Jasin, M. (2001). Ku DNA end-binding protein modulates homologous repair of double-strand breaks in mammalian cells. Genes Dev *15*, 3237-3242.

Pleschke, J.M., Kleczkowska, H.E., Strohm, M., and Althaus, F.R. (2000). Poly(ADP-ribose) binds to specific domains in DNA damage checkpoint proteins. J Biol Chem *275*, 40974-40980.

Poirier, G.G., Brown, T.C., and Cerutti, P.A. (1985). Poly ADP-ribosylation and DNA strand breakage in SV40 minichromosomes. Carcinogenesis *6*, 283-287.

Poirier, G.G., de Murcia, G., Jongstra-Bilen, J., Niedergang, C., and Mandel, P. (1982). Poly(ADP-ribosyl)ation of polynucleosomes causes relaxation of chromatin structure. Proc Natl Acad Sci U S A *79*, 3423-3427.

Povirk, L.F., Zhou, T., Zhou, R., Cowan, M.J., and Yannone, S.M. (2007). Processing of 3'-phosphoglycolate-terminated DNA double strand breaks by Artemis nuclease. J Biol Chem *282*, 3547-3558.

Rajawat, J., Vohra, I., Mir, H.A., Gohel, D., and Begum, R. (2007). Effect of oxidative stress and involvement of poly(ADP-ribose) polymerase (PARP) in Dictyostelium discoideum development. Febs J *274*, 5611-5618.

Rass, U., Compton, S.A., Matos, J., Singleton, M.R., Ip, S.C., Blanco, M.G., Griffith, J.D., and West, S.C. (2010). Mechanism of Holliday junction resolution by the human GEN1 protein. Genes Dev *24*, 1559-1569.

Raynard, S., Niu, H., and Sung, P. (2008). DNA double-strand break processing: the beginning of the end. Genes Dev *22*, 2903-2907.

Redon, C., Pilch, D., Rogakou, E., Sedelnikova, O., Newrock, K., and Bonner, W. (2002). Histone H2A variants H2AX and H2AZ. Curr Opin Genet Dev *12*, 162-169.

Rickwood, D., and Osman, M.S. (1979). Characterisation of poly(ADP-Rib) polymerase activity in nuclei from the slime mould Dictyostelium discoideum. Mol Cell Biochem *27*, 79-84.

Rieckmann, T., Kriegs, M., Nitsch, L., Hoffer, K., Rohaly, G., Kocher, S., Petersen, C., Dikomey, E., Dornreiter, I., and Dahm-Daphi, J. (2013). p53 modulates homologous recombination at I-SceI-induced double-strand breaks through cell-cycle regulation. Oncogene *32*, 968-975.

Riley, J.P., Kulkarni, A., Mehrotra, P., Koh, B., Perumal, N.B., Kaplan, M.H., and Goenka, S. (2013). PARP-14 binds specific DNA sequences to promote Th2 cell gene expression. PLoS One *8*, e83127.

Rogakou, E.P., Pilch, D.R., Orr, A.H., Ivanova, V.S., and Bonner, W.M. (1998). DNA double-stranded breaks induce histone H2AX phosphorylation on serine 139. J Biol Chem *273*, 5858-5868.

Rosado, M.M., Bennici, E., Novelli, F., and Pioli, C. (2013). Beyond DNA repair, the immunological role of PARP-1 and its siblings. Immunology *139*, 428-437.

Rosenthal, F., Feijs, K.L., Frugier, E., Bonalli, M., Forst, A.H., Imhof, R., Winkler, H.C., Fischer, D., Caflisch, A., Hassa, P.O., *et al.* (2013). Macrodomain-containing proteins are new mono-ADP-ribosylhydrolases. Nat Struct Mol Biol *20*, 502-507.

Rothkamm, K., Kruger, I., Thompson, L.H., and Lobrich, M. (2003). Pathways of DNA double-strand break repair during the mammalian cell cycle. Mol Cell Biol *23*, 5706-5715.

Rouet, P., Smih, F., and Jasin, M. (1994). Introduction of double-strand breaks into the genome of mouse cells by expression of a rare-cutting endonuclease. Mol Cell Biol *14*, 8096-8106.

Rouleau, M., McDonald, D., Gagne, P., Ouellet, M.E., Droit, A., Hunter, J.M., Dutertre, S., Prigent, C., Hendzel, M.J., and Poirier, G.G. (2007). PARP-3 associates with polycomb group bodies and with components of the DNA damage repair machinery. J Cell Biochem *100*, 385-401.

Ruf, A., de Murcia, G., and Schulz, G.E. (1998). Inhibitor and NAD+ binding to poly(ADP-ribose) polymerase as derived from crystal structures and homology modeling. Biochemistry *37*, 3893-3900.

Ruf, A., Mennissier de Murcia, J., de Murcia, G., and Schulz, G.E. (1996). Structure of the catalytic fragment of poly(AD-ribose) polymerase from chicken. Proc Natl Acad Sci U S A *93*, 7481-7485.

Rulten, S.L., Cortes-Ledesma, F., Guo, L., Iles, N.J., and Caldecott, K.W. (2008). APLF (C2orf13) is a novel component of poly(ADP-ribose) signaling in mammalian cells. Mol Cell Biol *28*, 4620-4628.

Rulten, S.L., Fisher, A.E., Robert, I., Zuma, M.C., Rouleau, M., Ju, L., Poirier, G., Reina-San-Martin, B., and Caldecott, K.W. (2011). PARP-3 and APLF function together to accelerate nonhomologous end-joining. Mol Cell *41*, 33-45.

Ruscetti, T., Lehnert, B.E., Halbrook, J., Le Trong, H., Hoekstra, M.F., Chen, D.J., and Peterson, S.R. (1998). Stimulation of the DNA-dependent protein kinase by poly(ADP-ribose) polymerase. J Biol Chem *273*, 14461-14467.

Rybanska, I., Ishaq, O., Chou, J., Prakash, M., Bakhsheshian, J., Huso, D.L., and Franco, S. (2013). PARP1 and DNA-PKcs synergize to suppress p53 mutation and telomere fusions during T-lineage lymphomagenesis. Oncogene *32*, 1761-1771.

Santorelli, L.A., Thompson, C.R., Villegas, E., Svetz, J., Dinh, C., Parikh, A., Sucgang, R., Kuspa, A., Strassmann, J.E., Queller, D.C., *et al.* (2008). Facultative cheater mutants reveal the genetic complexity of cooperation in social amoebae. Nature *451*, 1107-1110.

Sartori, A.A., Lukas, C., Coates, J., Mistrik, M., Fu, S., Bartek, J., Baer, R., Lukas, J., and Jackson, S.P. (2007). Human CtIP promotes DNA end resection. Nature *450*, 509-514.

Schaniel, C., and Moore, K.A. (2009). Genetic models to study quiescent stem cells and their niches. Ann N Y Acad Sci *1176*, 26-35.

Schreiber, V., Ame, J.C., Dolle, P., Schultz, I., Rinaldi, B., Fraulob, V., Menissier-de Murcia, J., and de Murcia, G. (2002). Poly(ADP-ribose) polymerase-2 (PARP-2) is required for efficient base excision DNA repair in association with PARP-1 and XRCC1. J Biol Chem *277*, 23028-23036.

Sebesta, M., Burkovics, P., Juhasz, S., Zhang, S., Szabo, J.E., Lee, M.Y., Haracska, L., and Krejci, L. (2013). Role of PCNA and TLS polymerases in D-loop extension during homologous recombination in humans. DNA Repair (Amst) *12*, 691-698.

Seitz, E.M., and Kowalczykowski, S.C. (2006). Human Rad51 protein displays enhanced homologous pairing of DNA sequences resembling those at genetically unstable loci. Nucleic Acids Res *34*, 2847-2852.

Shanbhag, N.M., Rafalska-Metcalf, I.U., Balane-Bolivar, C., Janicki, S.M., and Greenberg, R.A. (2010). ATM-dependent chromatin changes silence transcription in cis to DNA double-strand breaks. Cell *141*, 970-981.

Sharma, G.G., So, S., Gupta, A., Kumar, R., Cayrou, C., Avvakumov, N., Bhadra, U., Pandita, R.K., Porteus, M.H., Chen, D.J., *et al.* (2010). MOF and histone H4 acetylation at lysine 16 are critical for DNA damage response and double-strand break repair. Mol Cell Biol *30*, 3582-3595.

Shibata, A., Moiani, D., Arvai, A.S., Perry, J., Harding, S.M., Genois, M.M., Maity, R., van Rossum-Fikkert, S., Kertokalio, A., Romoli, F., *et al.* (2014). DNA double-strand

break repair pathway choice is directed by distinct MRE11 nuclease activities. Mol Cell *53*, 7-18.

Shieh, W.M., Ame, J.C., Wilson, M.V., Wang, Z.Q., Koh, D.W., Jacobson, M.K., and Jacobson, E.L. (1998). Poly(ADP-ribose) polymerase null mouse cells synthesize ADP-ribose polymers. J Biol Chem *273*, 30069-30072.

Shimizu, Y., Hasegawa, S., Fujimura, S., and Sugimura, T. (1967). Solubilization of enzyme forming ADPR polymer from NAD. Biochem Biophys Res Commun *29*, 80-83.

Sigurdsson, S., Van Komen, S., Petukhova, G., and Sung, P. (2002). Homologous DNA pairing by human recombination factors Rad51 and Rad54. J Biol Chem *277*, 42790-42794.

Simpson, R.T. (1978). Structure of chromatin containing extensively acetylated H3 and H4. Cell *13*, 691-699.

Slade, D., Dunstan, M.S., Barkauskaite, E., Weston, R., Lafite, P., Dixon, N., Ahel, M., Leys, D., and Ahel, I. (2011). The structure and catalytic mechanism of a poly(ADP-ribose) glycohydrolase. Nature *477*, 616-620.

Smeenk, G., Wiegant, W.W., Marteijn, J.A., Luijsterburg, M.S., Sroczynski, N., Costelloe, T., Romeijn, R.J., Pastink, A., Mailand, N., Vermeulen, W., *et al.* (2013). Poly(ADP-ribosyl)ation links the chromatin remodeler SMARCA5/SNF2H to RNF168-dependent DNA damage signaling. J Cell Sci *126*, 889-903.

Smerdon, M.J., and Lieberman, M.W. (1978). Nucleosome rearrangement in human chromatin during UV-induced DNA- reapir synthesis. Proc Natl Acad Sci U S A *75*, 4238-4241.

Smith, S., Giriat, I., Schmitt, A., and de Lange, T. (1998). Tankyrase, a poly(ADP-ribose) polymerase at human telomeres. Science *282*, 1484-1487.

Spagnolo, L., Barbeau, J., Curtin, N.J., Morris, E.P., and Pearl, L.H. (2012). Visualization of a DNA-PK/PARP1 complex. Nucleic Acids Res *40*, 4168-4177.

Spagnolo, L., Rivera-Calzada, A., Pearl, L.H., and Llorca, O. (2006). Three-dimensional structure of the human DNA-PKcs/Ku70/Ku80 complex assembled on DNA and its implications for DNA DSB repair. Mol Cell *22*, 511-519.

Sprung, R., Chen, Y., Zhang, K., Cheng, D., Zhang, T., Peng, J., and Zhao, Y. (2008). Identification and validation of eukaryotic aspartate and glutamate methylation in proteins. J Proteome Res *7*, 1001-1006.

Stevense, M., Chubb, J.R., and Muramoto, T. (2011). Nuclear organization and transcriptional dynamics in Dictyostelium. Dev Growth Differ *53*, 576-586.

Stiff, T., O'Driscoll, M., Rief, N., Iwabuchi, K., Lobrich, M., and Jeggo, P.A. (2004). ATM and DNA-PK function redundantly to phosphorylate H2AX after exposure to ionizing radiation. Cancer Res *64*, 2390-2396.

Strmecki, L., Greene, D.M., and Pears, C.J. (2005). Developmental decisions in Dictyostelium discoideum. Dev Biol *284*, 25-36.

Sugimura, T., Fujimura, S., Hasegawa, S., and Kawamura, Y. (1967). Polymerization of the adenosine 5'-diphosphate ribose moiety of NAD by rat liver nuclear enzyme. Biochim Biophys Acta *138*, 438-441.

Sun, Y., Jiang, X., Xu, Y., Ayrapetov, M.K., Moreau, L.A., Whetstine, J.R., and Price, B.D. (2009). Histone H3 methylation links DNA damage detection to activation of the tumour suppressor Tip60. Nat Cell Biol *11*, 1376-1382.

Szanto, M., Brunyanszki, A., Kiss, B., Nagy, L., Gergely, P., Virag, L., and Bai, P. (2012). Poly(ADP-ribose) polymerase-2: emerging transcriptional roles of a DNA-repair protein. Cell Mol Life Sci *69*, 4079-4092.

Szenker, E., Ray-Gallet, D., and Almouzni, G. (2011). The double face of the histone variant H3.3. Cell Res *21*, 421-434.

Talbert, P.B., and Henikoff, S. (2010). Histone variants--ancient wrap artists of the epigenome. Nat Rev Mol Cell Biol *11*, 264-275.

Tamburini, B.A., and Tyler, J.K. (2005). Localized histone acetylation and deacetylation triggered by the homologous recombination pathway of double-strand DNA repair. Mol Cell Biol *25*, 4903-4913.

Tartier, L., Spenlehauer, C., Newman, H.C., Folkard, M., Prise, K.M., Michael, B.D., Menissier-de Murcia, J., and de Murcia, G. (2003). Local DNA damage by proton microbeam irradiation induces poly(ADP-ribose) synthesis in mammalian cells. Mutagenesis *18*, 411-416.

Timinszky, G., Till, S., Hassa, P.O., Hothorn, M., Kustatscher, G., Nijmeijer, B., Colombelli, J., Altmeyer, M., Stelzer, E.H., Scheffzek, K., *et al.* (2009). A macrodomain-containing histone rearranges chromatin upon sensing PARP1 activation. Nat Struct Mol Biol *16*, 923-929.

Tissenbaum, H.A. (2015). Using for aging research. Invertebr Reprod Dev *59*, 59-63.

Tjeertes, J.V., Miller, K.M., and Jackson, S.P. (2009). Screen for DNA-damage-responsive histone modifications identifies H3K9Ac and H3K56Ac in human cells. Embo J *28*, 1878-1889.

Tomimatsu, N., Mukherjee, B., Deland, K., Kurimasa, A., Bolderson, E., Khanna, K.K., and Burma, S. (2012). Exo1 plays a major role in DNA end resection in humans and influences double-strand break repair and damage signaling decisions. DNA Repair (Amst) *11*, 441-448.

Trucco, C., Oliver, F.J., de Murcia, G., and Menissier-de Murcia, J. (1998). DNA repair defect in poly(ADP-ribose) polymerase-deficient cell lines. Nucleic Acids Res *26*, 2644-2649.

Ueda, K., Oka, J., Naruniya, S., Miyakawa, N., and Hayaishi, O. (1972). Poly ADP-ribose glycohydrolase from rat liver nuclei, a novel enzyme degrading the polymer. Biochem Biophys Res Commun *46*, 516-523.

Ushiroyama, T., Tanigawa, Y., Tsuchiya, M., Matsuura, R., Ueki, M., Sugimoto, O., and Shimoyama, M. (1985). Amino acid sequence of histone H1 at the ADP-ribose-accepting

site and ADP-ribose X histone-H1 adduct as an inhibitor of cyclic-AMP-dependent phosphorylation. Eur J Biochem *151*, 173-177.

van Attikum, H., Fritsch, O., and Gasser, S.M. (2007). Distinct roles for SWR1 and INO80 chromatin remodeling complexes at chromosomal double-strand breaks. Embo J *26*, 4113-4125.

Vempati, R.K., Jayani, R.S., Notani, D., Sengupta, A., Galande, S., and Haldar, D. (2010). p300-mediated acetylation of histone H3 lysine 56 functions in DNA damage response in mammals. J Biol Chem *285*, 28553-28564.

Veuger, S.J., Curtin, N.J., Richardson, C.J., Smith, G.C., and Durkacz, B.W. (2003). Radiosensitization and DNA repair inhibition by the combined use of novel inhibitors of DNA-dependent protein kinase and poly(ADP-ribose) polymerase-1. Cancer Res *63*, 6008-6015.

Vyas, S., Matic, I., Uchima, L., Rood, J., Zaja, R., Hay, R.T., Ahel, I., and Chang, P. (2014). Family-wide analysis of poly(ADP-ribose) polymerase activity. Nat Commun *5*, 4426.

Walker, J.R., Corpina, R.A., and Goldberg, J. (2001). Structure of the Ku heterodimer bound to DNA and its implications for double-strand break repair. Nature *412*, 607-614.

Wang, B., Matsuoka, S., Carpenter, P.B., and Elledge, S.J. (2002). 53BP1, a mediator of the DNA damage checkpoint. Science *298*, 1435-1438.

Wang, M., Wu, W., Rosidi, B., Zhang, L., Wang, H., and Iliakis, G. (2006). PARP-1 and Ku compete for repair of DNA double strand breaks by distinct NHEJ pathways. Nucleic Acids Res *34*, 6170-6182.

Wang, Q., Goldstein, M., Alexander, P., Wakeman, T.P., Sun, T., Feng, J., Lou, Z., Kastan, M.B., and Wang, X.F. (2014). Rad17 recruits the MRE11-RAD50-NBS1 complex to regulate the cellular response to DNA double-strand breaks. Embo J *33*, 862-877.

Wang, Y., Kim, N.S., Haince, J.F., Kang, H.C., David, K.K., Andrabi, S.A., Poirier, G.G., Dawson, V.L., and Dawson, T.M. (2011). Poly(ADP-ribose) (PAR) binding to apoptosis-inducing factor is critical for PAR polymerase-1-dependent cell death (parthanatos). Sci Signal *4*, ra20.

Wang, Z., Michaud, G.A., Cheng, Z., Zhang, Y., Hinds, T.R., Fan, E., Cong, F., and Xu, W. (2012). Recognition of the iso-ADP-ribose moiety in poly(ADP-ribose) by WWE domains suggests a general mechanism for poly(ADP-ribosyl)ation-dependent ubiquitination. Genes Dev *26*, 235-240.

Wesierska-Gadek, J., Schmid, G., and Cerni, C. (1996). ADP-ribosylation of wild-type p53 in vitro: binding of p53 protein to specific p53 consensus sequence prevents its modification. Biochem Biophys Res Commun *224*, 96-102.

White, D., Rafalska-Metcalf, I.U., Ivanov, A.V., Corsinotti, A., Peng, H., Lee, S.C., Trono, D., Janicki, S.M., and Rauscher, F.J., 3rd (2012). The ATM substrate KAP1 controls DNA repair in heterochromatin: regulation by HP1 proteins and serine 473/824 phosphorylation. Mol Cancer Res *10*, 401-414.

Wielckens, K., George, E., Pless, T., and Hilz, H. (1983). Stimulation of poly(ADP-ribosyl)ation during Ehrlich ascites tumor cell "starvation" and suppression of concomitant DNA fragmentation by benzamide. J Biol Chem *258*, 4098-4104.

Wielckens, K., Schmidt, A., George, E., Bredehorst, R., and Hilz, H. (1982). DNA fragmentation and NAD depletion. Their relation to the turnover of endogenous mono(ADP-ribosyl) and poly(ADP-ribosyl) proteins. J Biol Chem *257*, 12872-12877.

Wong, N.C., Poirier, G.G., and Dixon, G.H. (1977). Adenosine diphosphoribosylation of certain basic chromosomal proteins in isolated trout testis nuclei. Eur J Biochem *77*, 11-21.

Wu, J., Huen, M.S., Lu, L.Y., Ye, L., Dou, Y., Ljungman, M., Chen, J., and Yu, X. (2009). Histone ubiquitination associates with BRCA1-dependent DNA damage response. Mol Cell Biol *29*, 849-860.

Xu, Y., Ayrapetov, M.K., Xu, C., Gursoy-Yuzugullu, O., Hu, Y., and Price, B.D. (2012). Histone H2A.Z controls a critical chromatin remodeling step required for DNA double-strand break repair. Mol Cell *48*, 723-733.

Yan, Q., Xu, R., Zhu, L., Cheng, X., Wang, Z., Manis, J., and Shipp, M.A. (2013). BAL1 and its partner E3 ligase, BBAP, link Poly(ADP-ribose) activation, ubiquitylation, and double-strand DNA repair independent of ATM, MDC1, and RNF8. Mol Cell Biol *33*, 845-857.

Ying, S., Hamdy, F.C., and Helleday, T. (2012). Mre11-dependent degradation of stalled DNA replication forks is prevented by BRCA2 and PARP1. Cancer Res *72*, 2814-2821.

Yun, M.H., and Hiom, K. (2009). CtIP-BRCA1 modulates the choice of DNA double-strand-break repair pathway throughout the cell cycle. Nature *459*, 460-463.

Zee, B.M., and Garcia, B.A. (2010). Electron transfer dissociation facilitates sequencing of adenosine diphosphate-ribosylated peptides. Anal Chem *82*, 28-31.

Zhang, F., Chen, Y., Li, M., and Yu, X. (2014). The oligonucleotide/oligosaccharide-binding fold motif is a poly(ADP-ribose)-binding domain that mediates DNA damage response. Proc Natl Acad Sci U S A *111*, 7278-7283.

Zhang, X.Y., Langenick, J., Traynor, D., Babu, M.M., Kay, R.R., and Patel, K.J. (2009). Xpf and not the Fanconi anaemia proteins or Rev3 accounts for the extreme resistance to cisplatin in Dictyostelium discoideum. PLoS Genet *5*, e1000645.

Zhang, Y., and Jasin, M. (2011). An essential role for CtIP in chromosomal translocation formation through an alternative end-joining pathway. Nat Struct Mol Biol *18*, 80-84.

Zhang, Y., Liu, S., Mickanin, C., Feng, Y., Charlat, O., Michaud, G.A., Schirle, M., Shi, X., Hild, M., Bauer, A., *et al.* (2011). RNF146 is a poly(ADP-ribose)-directed E3 ligase that regulates axin degradation and Wnt signalling. Nat Cell Biol *13*, 623-629.

Zhang, Y., Wang, J., Ding, M., and Yu, Y. (2013). Site-specific characterization of the Asp- and Glu-ADP-ribosylated proteome. Nat Methods *10*, 981-984.